

PHD DISSERTATION 3 | 2021

Helmholtz Centre for Environmental Research – UFZ  
Department of Soil System Science

Lisa Haselow

---

**Methods, potentials, and challenges in  
the determination of soil water balance  
parameters for dry steppe soils –  
Case studies from southwest Siberia and  
Kazakhstan**

Methods, potentials, and challenges in the determination of soil water balance parameters for  
dry steppe soils – Case studies from southwest Siberia and Kazakhstan

**Dissertation**  
**zur Erlangung des**  
**Doktorgrades der Naturwissenschaften (Dr. rer. nat.)**

der

Naturwissenschaftlichen Fakultät III  
Agrar- und Ernährungswissenschaften,  
Geowissenschaften und Informatik

der Martin-Luther-Universität Halle-Wittenberg

vorgelegt von

Frau Haselow, Lisa  
Geb. am 20.11.1990 in Berlin



## Table of contents

<b>Summary</b>	<b>v</b>
<b>Zusammenfassung</b>	<b>vii</b>
<b>List of Abbreviations</b>	<b>ix</b>
<b>List of Figures</b>	<b>xii</b>
<b>List of Tables</b>	<b>xiv</b>
<b>1 Introduction</b>	<b>1</b>
1.1 The significance of precipitation and evapotranspiration in semiarid environments ..	1
1.2 Determining soil water balance parameters .....	2
1.3 Objectives and outline.....	4
<b>2 Evaluation of precipitation measurements methods: A comparison of the standard rain gauge with a weighable lysimeter and a piezoelectric precipitation sensor</b>	<b>6</b>
2.1 Abstract .....	6
2.2 Introduction .....	6
2.3 Material and methods .....	8
2.3.1 Site description .....	8
2.3.2 The monitoring network .....	8
2.3.3 Data availability .....	11
2.3.4 Data preparation .....	12
2.3.5 Calculating precipitation from lysimeter data .....	12
2.3.6 Data analyses .....	13
2.4 Results and discussion .....	14
2.4.1 Comparison of precipitation measurements .....	14
2.4.2 Bias correction .....	18
2.5 Conclusions .....	21

<b>3</b>	<b>Measurement and estimation of evapotranspiration for semiarid grassland</b>	<b>22</b>
3.1	Abstract .....	22
3.2	Introduction .....	22
3.3	Material and methods .....	24
3.3.1	Data preparation and calculation of $ET_a$ .....	24
3.3.2	Estimation of $ET_0$ by using the PM FAO model .....	25
3.4	Results and discussion .....	26
<b>4</b>	<b>Determination of soil water balance parameters in the dry steppe of southwest Siberia</b>	<b>32</b>
4.1	Introduction .....	32
4.2	Material and methods .....	32
4.3	Results and discussion .....	33
4.3.1	Precipitation and actual evapotranspiration .....	33
4.3.2	Soil moisture .....	35
4.4	Conclusions .....	37
<b>5</b>	<b>Research study on the soil water balance in the steppe of Kazakhstan</b>	<b>38</b>
5.1	Abstract .....	38
5.2	Introduction .....	38
5.3	Material and methods .....	39
5.3.1	Site description .....	39
5.3.2	The monitoring network .....	40
5.3.3	Measuring strategy .....	42
5.4	Results and discussion .....	43

<b>6 A novel method for reliable lysimeter measurements under snow and ice conditions?</b>	<b>48</b>
6.1 Abstract .....	48
6.2 Introduction .....	48
6.3 Material and methods .....	50
6.3.1 Site description and experimental set-up .....	50
6.3.2 Data processing .....	50
6.3.3 Study preparatory to experimental development .....	51
6.3.4 Applied technology .....	51
6.4 Results .....	52
6.4.1 Precipitation and actual evapotranspiration .....	52
6.4.2 Soil parameters .....	54
6.5 Discussion .....	56
6.5.1 Lysimeter weighing, precipitation, and actual evapotranspiration .....	56
6.5.2 Soil parameters .....	58
6.5.3 Soil water balance .....	59
6.5.4 Technology to prevent freezing effects .....	60
6.6 Conclusions .....	60
<b>7 Measured and simulated water fluxes in dry steppe soils: A comparison between pristine grassland and agricultural land</b>	<b>62</b>
7.1 Abstract .....	62
7.2 Introduction .....	62
7.3 Material and methods .....	64
7.3.1 Study site and experimental set-up .....	64
7.3.2 Data availability .....	64
7.3.3 Model set-up .....	64
7.3.4 Analysis of model performance .....	67
7.4 Results .....	67

7.4.1 Lysimeter measurements .....	67
7.4.2 Hydrological simulations .....	69
7.5 Discussion .....	72
7.5.1 Impacts on field measurements.....	72
7.5.2 Impacts on model simulations .....	75
7.5.3 Model limitations .....	76
7.6 Conclusions .....	77
<b>8 Synthesis and conclusions</b> .....	<b>79</b>
8.1 Precipitation and evapotranspiration under semiarid conditions .....	79
8.2 Measuring methods for determining soil water balance parameters .....	79
8.3 Potential and challenges in the determination of soil water balance parameters .....	81
8.4 Outlook and recommendations .....	82
<b>Bibliography</b> .....	<b>84</b>
<b>Appendix</b> .....	<b>95</b>
Curriculum Vitae .....	95
List of Publications .....	96
Danksagung / Acknowledgement .....	97
Eidesstattliche Erklärung / Declaration under Oath .....	98

## Summary

The ongoing climate change characterised by increasing temperatures will pose a challenge for many nations. Especially agriculture as an often keystone of a system, both by the food security and also in the securing of economic livelihoods, is facing its effects since decreasing water resources lead to crop losses and contribute to the global food crisis. In particular semiarid regions, where water scarcity is already a reality, the issue will still increase in the future, and water in any form becomes essential. As a result, agriculture is forced to adapt to climate and sustainability by adjusting current land management practices to regional conditions.

Within the context, this study focus on the soil water balance of semiarid steppe soils whose optimisation may contribute to increasing yields. Through field studies conducted in the steppes of southwest Siberia and Kazakhstan, attempts were made to determine the regional soil water balance to derive recommendations for sustainable soil management. The aim is to store the available water that is naturally fed into the soil and provide it for plant production. For this purpose, pedo-hydrological information is needed to quantify the soil water balance. To fulfill these objectives, monitoring networks were established to enable long-term in situ measurements at the study sites. These networks relied on the use of weighable gravitation lysimeters that turned out as a suitable method to investigate pedo-hydrological processes. Through the high-resolution weighing technique, it is possible to detect minor mass changes, which are caused by water input (precipitation) or water output (evapotranspiration, outflow). Using two lysimeters comparative analyses were conducted to quantify the demand for soil water as a function of the land management. The monolithically extracted soil columns were characterised by different vegetation cover and soil management. They stemmed from fallow sites covered by pristine steppe grass and arable land, which was continuously cultivated by the regional dominating crop.

It was shown that the determination of individual soil water balance parameters was a scientific challenge. It emerged that weighable lysimeters provide high-resolution data at the determination of soil water balance parameters. A comparison of methods indicated that weighable lysimeters are an optimal instrument at precipitation measurements, contrary to the initial purpose. The record of actual evapotranspiration proved to be difficult under given conditions. During summer, edge effects accompanied by the vegetation on the lysimeter and in the surrounding area could distort the determination of the evapotranspiration, whereas snow and wind showed a considerable impact on its measurement. Although there are widely accepted and suitable models for the estimation of evapotranspiration, common approaches were not able to estimate reliable evapotranspiration rates due to the dryness and the properties of the steppe vegetation.

Furthermore, the often neglected sublimation of snow as part of evapotranspiration is also an essential aspect. The cold and snowy winter periods have made it impossible to get full-year measurements so far. Since in particular, the high snow volume is a considerable water reservoir, it is also necessary to determine the amount of evapotranspiration during winter. Having established that snow and ice affect the lysimeter weighing, a technique was developed to prevent the impairments and enable reliable measurements during winter periods for the first time for this climate. Unfortunately, the technique proved to be unsuitable. Although the frost effects could be minimised, a significant impact on the natural soil water balance could be observed.

Even though these studies did not produce long-term and continuous time series, an overview of the soil water balance could be nonetheless gained. According to the steppe climate, the evapotranspiration exceeded the precipitation. Thus, a negative water balance was identified at both study sites. It could be observed that the high snow amounts led to an increase of soil moisture in spring, but the soil was not able to store the water in the long-term under the current soil management.

Finally, it can be stated that there is a potential to use the steppe landscape as arable land with which an increase in yields could be achieved. However, a transformation from grassland to arable land is only possible by the consideration of the climate conditions and soil characteristics. Thus, adapted soil management should allow the securing of the areas as farmland in future.

## Zusammenfassung

Der voranschreitende Klimawandel, der durch zunehmende Temperaturen gekennzeichnet ist, stellt viele Nationen vor Herausforderungen. Insbesondere die Landwirtschaft kämpft mit den Folgen, die für viele einen Grundpfeiler darstellt, sowohl in der Ernährungssicherung als auch in der Sicherung der wirtschaftlichen Existenz. Schwindende Wasserressourcen führen nicht selten zu Ertragseinbußen und tragen somit zu der bereits verschärften Ernährungskrise bei. In semiariden Gebieten, die bereits durch Wasserknappheit gekennzeichnet sind, potenziert sich die Situation erheblich und macht Wasser in jeglicher Form unverzichtbar. Aufgrund dessen ist die Landwirtschaft gezwungen, sich klimatisch und nachhaltig anzupassen, in dem gegenwärtige Bewirtschaftungsmethoden optimiert und auf die regionalen Gegebenheiten abgestimmt werden sollten.

Diese Arbeit legt innerhalb dieses Kontextes den Fokus auf den Bodenwasserhaushalt von semiariden Steppenböden, dessen Optimierung dazu beitragen soll die landwirtschaftlichen Erträge zu steigern. Anhand von Feldstudien in den Steppen von Südwestsibirien und Kasachstan wurde der regionale Bodenwasserhaushalt bestimmt, um Empfehlungen für ein nachhaltiges Bodenmanagement abzuleiten. Ziel ist es, das verfügbare Wasser, das dem Boden natürlich zugeführt wird, zu halten und für die Pflanzenproduktion nutzbar zu machen. Hierfür braucht es jedoch pedo-hydrologische Informationen, um den Bodenwasserhaushalt quantitativ einzuordnen. Zur Erfüllung dieser Zielstellung wurden in den jeweiligen Untersuchungsgebieten Messnetzwerke errichtet, die langfristige In-situ-Messungen ermöglichen. Dabei wurde auf die Verwendung von wägbaren Gravitationslysimetern zurückgegriffen, die sich als eine geeignete Methode zur Erforschung von bodenhydrologischen Prozessen herausstellte. Durch die präzise Wägemesstechnik ist es möglich, kleinste Massenänderungen nachzuweisen, die durch eine Zufuhr von Wasser aufgrund von Niederschlag oder eine Abnahme von Bodenfeuchte durch Evapotranspiration und Abfluss herbeigeführt werden. Um den Bedarf an Bodenwasser in Abhängigkeit des Landmanagements quantitativ zu erfassen, wurden mithilfe von zwei Lysimetern Vergleichsanalysen durchgeführt. Die monolithisch extrahierten Bodensäulen wiesen unterschiedliche Vegetationsbedeckung und Bewirtschaftungsformen auf. Dabei repräsentierte stets ein Monolith den unbearbeiteten Boden mit natürlicher Steppenvegetation, während der zweite Bodenmonolith einem landwirtschaftlich genutzten Standort entnommen und regelmäßig mit der regional dominierenden Feldfrucht kultiviert wurde.

Innerhalb dieser Untersuchungen zeigte sich die wissenschaftliche Herausforderung in der Bestimmung einzelner Parameter. Es kristallisierte sich durch die Anwendung unterschiedlicher Methoden heraus, dass wägbare Lysimeter bei der Bestimmung von

Bodenwasserhaushaltsparametern hochaufgelöste Daten hervorbringen und im Vergleich zu anderen gängigen Methoden geringe systematische Fehlerquellen aufweisen. Ein Methodenvergleich machte deutlich, dass ein wägbares Lysimeter, entgegen des ursprünglichen Zwecks, das optimale Instrument bei der Niederschlagserfassung ist, jedoch die Messung der realen Evapotranspiration unter den klimatischen Bedingungen sich als problematisch herausstellte. Während im Sommer insbesondere Randeffekte, die mit dem Bewuchs auf dem Lysimeter als auch mit dem der unmittelbaren Umgebung einhergehen, die Ermittlung der Evapotranspiration verfälschen können, zeigte sich im Winter ein erheblicher Einfluss durch Schnee und Wind auf dessen Ermittlung. Obwohl bereits gängige und geeignete Modelle für die Abschätzung der Evapotranspiration existieren, hat sich gezeigt, dass sie bei gegebener Steppenvegetation und der geringen Wasserverfügbarkeit die Evapotranspirationsraten nicht zuverlässig wiedergeben.

Des Weiteren ist die oft vernachlässigte Sublimation von Schnee als Teil der Evapotranspiration ein nicht zu vernachlässigender Aspekt. Die kalten und schneereichen Winterperioden machten es bisher unmöglich, ganzjährige Messungen durchzuführen. Da insbesondere das hohe Schneevolumen ein erhebliches Wasserreservoir darstellt, ist es auch hier notwendig, den winterlichen Evapotranspirationsanteil zu bestimmen. Nachdem festgestellt wurde, dass Schnee und Eis die Wägung der Lysimeter beeinflusste, wurde eine Technik entwickelt, die die Beeinträchtigungen vermeiden und erstmals zuverlässige Messungen über den Winter für diesen Klimaraum ermöglichen sollte. Leider erwies sich diese Technik als nicht optimal. Obwohl sie die Frosteffekte minimierte, wurde ein erheblicher Einfluss auf den natürlichen Bodenwasserhaushalt festgestellt.

Wenngleich die Studien keine durchgehenden Messzeitreihen hervorbrachten, konnte trotz dessen ein Überblick über den Bodenwasserhaushalt gewonnen werden. Dem Steppenklima entsprechend, übersteigt der Anteil der Evapotranspiration den des Niederschlags, womit in beiden Untersuchungsgebieten ein negativer Wasserhaushalt vorherrscht. Es konnte beobachtet werden, dass die hohen Schneemengen die Bodenwasservorräte im Frühling wieder auffüllen, der Boden unter der aktuellen Bewirtschaftungsform jedoch nicht in der Lage war, das Wasser langfristig zu speichern.

Letztendlich kann festgehalten werden, dass das Potential, diese Steppenlandschaft als landwirtschaftliche Fläche zu nutzen, besteht und somit eine Ertragssteigerung zu erzielen wäre. Jedoch müssen bei der Betrachtung einer Transformation die klimatischen Bedingungen sowie die Ansprüche an den Boden vorrangig beachtet werden. Mit einem angepassten Bodenmanagement können die hiesigen Flächen zukünftig als Agrarstandort langfristig gesichert werden.

## List of Abbreviations

a.m.	ante meridiem
Apr	April
a.s.l.	above sea level
Aug	August
AWAT	adaptive window and adaptive threshold
BMBF	German Federal Ministry of Education and Research
cf.	confer
D	drainage
DWD	German Meteorological Service (Deutscher Wetterdienst)
e.g.	exempli gratia
Eq.	Equation
ET	evapotranspiration
ET <sub>0</sub>	reference evapotranspiration
ET <sub>a</sub>	actual evapotranspiration
ET <sub>a</sub> -LYS 1	actual evapotranspiration of lysimeter 1
ET <sub>a</sub> -LYS 2	actual evapotranspiration of lysimeter 2
ET <sub>p</sub>	potential evapotranspiration
FAO	Food and Agriculture Organization of the United Nations
FDR	frequency-domain reflectometry
Fig.	Figure
ha	hectare
i.e.	id est

Jul	July
Jun	June
LYS	lysimeter
LYS 1	lysimeter 1 – arable land
LYS 2	lysimeter 2 – covered by pristine steppe vegetation
LYS-H	lysimeter equipped with a heating fence
LYS-N	non-equipped lysimeter
MAE	mean absolute error
n	number of observation days
NSE	Nash-Sutcliffe efficiency
Oct	October
P	precipitation
p	level of significance
PE-HD	polyethylene
p.m.	post meridiem
PM FAO	Penman-Monteith FAO-56
Prec. Sensor	piezoelectric precipitation sensor
R	surface runoff
r	Pearson correlation coefficient
rbias	relative bias
RMSE	root mean squared error
Sep	September
SMT	soil-moisture-temperature
Tab.	Table

TB	Tipping bucket rain gauge
TDR	time domain reflectometry
UFZ	Helmholtz Centre of Environmental Research
UGT	Umwelt-Geraete-Technik GmbH
UTC	Coordinated Universal Time
Vol.-%	percentage by volume
WMO	World Meteorological Organization
WRB	World reference base for soil resources

Variables and constants in equations are explained below the equations. Abbreviations for physical units are declared by the International System of Units.

## List of Figures

Figure 1	Experimental set-up of the monitoring network consisting of multisensor 'Vaisala', tipping bucket rain gauge and two weighable gravitation lysimeters .....	9
Figure 2	Cumulative precipitation (P) of Prec. Sensor, the tipping bucket rain gauge (TB) and the lysimeter (LYS) from 09/06/2016 to 31/09/2016 .....	14
Figure 3	The relationship between the rainfall data obtained by the rain gauges and lysimeter (LYS) on a daily basis .....	16
Figure 4	Comparison of rainfall data measured by the lysimeter (LYS), the tipping bucket (TB), and Prec. Sensor .....	16
Figure 5	Frequency distribution of daily precipitation rates in different intensity ranges and their contribution to the total rainfall .....	17
Figure 6	The daily precipitation (P) of the lysimeter (LYS) compared to the raw and corrected rainfall of the tipping bucket (TB) and Prec. Sensor .....	19
Figure 7	Comparison of $ET_a$ measured by lysimeters and $ET_0$ computed by the PM FAO model .....	27
Figure 8	Daily differences of ET between 08 June and 30 September 2016 .....	28
Figure 9	The relationship between $ET_a$ and $ET_0$ on a daily basis (n=115), and the respective error values .....	29
Figure 10	Illustration of the daily water availability between June and September 2016 .....	31
Figure 11	The lysimeter mass between 01 July and 31 August 2015 .....	34
Figure 12	The lysimeter mass and precipitation during 11 July 2015 .....	35
Figure 13	Soil moisture, P, and $ET_a$ measured by the lysimeters .....	36
Figure 14	Study area with lysimeter station and extraction sites .....	40
Figure 15	Illustration of the containerised lysimeter station including instrumentation ..	41
Figure 16	Lysimeter mass and precipitation (P) measurements from 26/10/2018 to 26/10/2019 .....	44

Figure 17	The soil moisture for LYS 1 and LYS 2 from 26/10/2018 to 26/10/2019 .....	45
Figure 18	The daily course of lysimeter mass and air temperature, air humidity, and solar radiation for 26/10/2018 .....	46
Figure 19	Lysimeter mass, air temperatures, and air humidity during the first snowfall between 07/11/2018 and 10/11/2018 .....	47
Figure 20	Photo of the top view of the installed double lysimeter station in winter season 2019/2020 in Pervomayka, Kazakhstan, and an illustration of the non-equipped lysimeter collar (LYS-N) as well as the lysimeter collar equipped with a heating wire system (LYS-H) .....	52
Figure 21	Mass of the lysimeter with a heating fence (LYS-H) and the non-equipped lysimeter (LYS-N) from 01/11/2019 to 31/03/2020 .....	53
Figure 22	Daily minima and maxima of air temperature and wind speed from 01/11/2019 to 31/03/2020 .....	54
Figure 23	Soil temperatures in the depths of 30, 50, and 120 cm within the lysimeter with a heating fence (LYS-H) and the non-equipped lysimeter (LYS-N) from 01/11/2019 to 31/03/2020 .....	55
Figure 24	Soil moisture in the depths of 30, 50, and 120 cm within the lysimeter with heating fence (LYS-H) and the non-equipped lysimeter (LYS-N) from 01/11/2019 to 31/03/2020 .....	56
Figure 25	Mass of the lysimeters with an arable soil (LYS 1) and pristine steppe soil (LYS 2) between 01/01/2019 and 31/12/2019 .....	65
Figure 26	Soil moisture in the depths of 30, 50, and 120 cm inside of LYS 1 and LYS 2 between 01/04/2019 and 31/10/2019 .....	69
Figure 27	The surface pressure head and surface fluxes of LYS 1 and LYS 2 .....	70
Figure 28	Cumulative surface fluxes simulated by HYDRUS-1D and calculated by mass changes of LYS 1 and LYS 2 for the 153 observation days .....	70
Figure 29	Soil moisture measured by LYS 1 and LYS 2, and simulated by HYDRUS-1D for the depths 30, 50, and 120 cm .....	72

## List of Tables

Table 1	Properties of precipitation measurements by Prec. Sensor, tipping bucket rain gauge, and lysimeter .....	11
Table 2	Monthly precipitation (P) of the lysimeter (LYS) and rain gauges .....	15
Table 3	The error indices MAE and RMSE as a function of rainfall intensity .....	18
Table 4	Monthly correction factors for Prec. Sensor and tipping bucket (TB) to reduce bias in the raw data .....	19
Table 5	Comparison of the error indices for Prec. Sensor and tipping bucket (TB) before and after bias correction .....	20
Table 6	Monthly $ET_a$ records of the lysimeters and $ET_0$ estimates calculated by PM FAO model .....	26
Table 7	Pearson correlation coefficients (r) between $ET_a$ of the lysimeters and meteorological parameters .....	27
Table 8	Properties of the extracted soils for lysimeter usage .....	33
Table 9	Properties of the soil moisture probe SMT-100 and tipping buckets according to manufacturer's information .....	42
Table 10	Particle size distribution and bulk density of the lysimeter soil layers .....	66
Table 11	The soil hydraulic van Genuchten parameters and saturated hydraulic conductivity (Ks) optimised for each layer of the soil profile by HYDRUS-1D .....	66
Table 12	Monthly $ET_a$ and P rates for the lysimeters, monthly mean temperatures, and mean maximum temperatures measured by the weather station .....	68
Table 13	Values of the model performance indices RMSE and NSE for the soil moisture .....	71

# 1 Introduction

## 1.1 The significance of precipitation and evapotranspiration in semiarid environments

In semiarid environments water resources are essential for the ecosystem and social economy. Due to the climate change it is to be assumed that its impact on the hydrological cycle will transform these regions to more vulnerable systems. The climate change will often be characterised by shifts of climatic pattern such as an increase in temperature, but it is also linked to changes in the frequency, intensity, spatial extent, and duration of weather and climate extremes (Field et al., 2012). Studies in Siberia indicated an increase of the mean temperature by more than 1 °C and an increase in winter precipitation over the last 15 years (Frey and Smith, 2003). In the neighbouring Kazakhstan an increase of drought risk are expected, which may spread towards to southwest Siberia (Pilifosova et al., 1997). Both regions are of global importance due to the large grain production. If the tendency becomes reality the impact could potentially change the regional climate and cause a northward shift of the current grain belt, which will negatively affected its ecosystem and natural resources (Degefie et al., 2014). As these environments are characterised by semiarid climate and therefore by high summer temperatures and low precipitation, water scarcity is an important issue. The dry climate has a significant impact on crop growth, yields, and its quality since the crops are often exposed to water stress. Thus, the evaluation of water resources is necessary for its management, particularly for agricultural purposes.

Precipitation and evapotranspiration are key components of the hydrological cycle. The latter is defined as the water loss in vapour form by a vegetative unsaturated surface. This water is transferred into the atmosphere by evaporation from soil and transpiration from plants (Lhomme, 1997). Occurrence and amount of evapotranspiration and precipitation can vary widely under drought or moist conditions. This variability is an important aspect in hydrological and meteorological investigations. In general, evapotranspiration and precipitation are equal in magnitude in the long-term in semiarid environments (Sala et al., 1992; Phillips, 1994; Reynolds et al., 2000). The variability of evapotranspiration, however, is high on shorter timescales and plays a crucial role in moisture-energy exchanges. The amount of precipitation divided in runoff and recharge, the impact of soil-atmosphere interactions on weather and climate as well as processes such as plant productivity will be affected by the variability of evapotranspiration (Kurc and Small, 2004). As precipitation is usually much less than evapotranspiration on timescales of seasons, evapotranspiration is often used as principal factor in regional water resource management purposes. It is assumed that evapotranspiration will be mainly limited by soil moisture in dry ecosystems

(Noy-Meir, 1973; Rodriguez-Iturbe, 2000), probably since about 99% of water is lost by transpiration (Lambers et al., 2008). If the soil moisture increases due to the snowmelt in spring – which is usually the case in southwest Siberia and Kazakhstan – evapotranspiration subsequently increases. Conversely, higher evapotranspiration rates lead to a decrease in soil moisture. These low soil moisture contents in turn control evapotranspiration, vegetation productivity, and water budget. Unless the soil water content is settled by precipitation, water balances will be increasingly negative. If soil moisture is not limiting due to sufficient water supply, evapotranspiration is driven by meteorological and vegetation conditions. In this case, the water budget is balanced when precipitation is relatively equal to evapotranspiration or positive when precipitation exceeds evapotranspiration (Shuttleworth, 1991; Park et al., 2008).

In order to get an understanding of the controlling factors and the interaction between these processes in semiarid ecosystems, it requires long-term data of evapotranspiration, precipitation, soil moisture, radiation, and other related components. As there is a high spatial variability, it is also necessary to investigate these variables under numerous soil and vegetation types (Wever et al., 2002; Kurc and Small, 2004).

## 1.2 Determining soil water balance parameters

There are several methods to determine the components of the soil water balance. The accuracy depends on the application of direct or indirect methods. In general, a physical value of a parameter is directly measured by an instrument for its quantification, whereas a determination of a value by means of a relationship among parameters is an indirect measurement. If a parameter, however, is calculated by a model, the value can be considered as estimation. The application of a respective method depends on factors such as availability of financial resources or suitability for given spatial and temporal scales. In order to determine the soil water balance, direct and indirect methods can be used. The water balance equation based on in- and outgoing water fluxes as well as changes in water storage in a one-dimensional, vertical soil. It can be described as follow:

$$P - ET - R - D = \pm\Delta S, \quad (1)$$

where P is precipitation, ET is evapotranspiration, R is surface runoff, D is drainage, and  $\Delta S$  is the change in soil water storage. All terms are in millimetres per unit time. These parameters can be measured or have to be estimated at least. In semiarid environments, R is often neglected for coarse soils (Jensen et al., 1990), but has to be

considered at extreme P events (high amount, duration, and intensity). Drainage (D) will also be neglected in dry regions, but it is advisable to make it dependent on soil depth, slope, and permeability (Jensen et al., 1990). The rest of the terms can be easily determined. Through rain gauges P will be directly quantified. It is important for an accurate determination to measure the soil water content (S) over an adequate depth. The gravimetric method, the technique of Time-Domain-Reflectometry (TDR) or Frequency-Domain-Reflectometry (FDR) is often used for soil moisture records (Topp et al., 1980; Lukanu and Savage, 2006). TDR and FDR are indirect methods, which measured the soil water content by the relative permittivity of the soil, whereas the gravimetric method directly determines the moisture by soil samples in the laboratory. The determination of ET is more complex. There are numerous methods for its quantification. In general, they can be divided in measurements and modelling aspects. Depending on the objective, the methods can be separated into the main approaches hydrology, micrometeorology, and plant physiology. The following methods can be assigned (Rana and Katerji, 2000):

1. Hydrological approaches
  - Soil water balance
  - Weighable lysimeter
2. Micrometeorological approaches
  - Energy balance and Bowen ratio
  - Aerodynamic method
  - Eddy covariance
3. Plant physiology approaches
  - Sap flow method
  - Chambers system

Should be referred to modelling approaches for developing management tools, understanding of a system or assessing experimental results, empirical or statistical approaches are commonly used due to the availability of data. These ET models can also be divided as follows:

4. Analytical approaches
  - Penman-Monteith model
5. Empirical approaches
  - Methods based on crop coefficient
  - Methods based on soil water balance modelling

A detailed overview of the methods is given by Rana and Katerji (2000).

Meanwhile, a preferred approach is the use of weighable lysimeters (Bethge-Steffens et al., 2004; Meissner et al., 2010; Nolz et al., 2014; Hagenau et al., 2015; Moorhead et al., 2019) since this tool enables to determine as many water balance components as possible by high-resolution in situ measurements, i.e. directly on site. A lysimeter, as tank or container, is a device that allows the detection of water movement through a soil by gravitation. Non-weighable lysimeters are originally used for the investigation of quantity and quality of seepage water. Their further development has been done particularly for the determination of ET. They measure directly the ET by the mass balance of water. In the last years, the additional measurement of P by weighable lysimeters became popular (Schrader et al., 2013; Hannes et al., 2015; Gebler et al., 2015; Hoffmann et al., 2016). Furthermore, besides ET and P the most unknown parameter D will also be directly measured (Meissner et al., 2000; Duncan et al., 2016; Kohfahl et al., 2019). With additional technical equipment pedo-hydrological measurements are possible (Meissner et al., 2008; Dijkema et al., 2017; Isch et al., 2019). If TDR or FDR probes, for instance, are distributed over the depth, detailed information of  $\Delta S$  will be gained. Taken together, this device is a suitable instrument that is often applied to determine the main components of the soil water balance in the field.

### **1.3 Objectives and outline**

The previous section pointed out how water resources are essential for semiarid environments. There are many regions which are highly vulnerable to the impacts of the climate change. Therefore, the determination of the soil water balance is crucial for many purposes within this context. In order to reduce the effects on the ecosystem, agriculture or socio-economy, it requires investigation regarding present water budgets and potential future changes within the hydrological cycle. For many regions, however, there is a lack of data, the base for all further steps towards a planning process. The knowledge of soil hydrology is particularly an important issue within the agriculture, which is usually confronted by low precipitation and droughts. The region around southwest Siberia and Kazakhstan is predestined for its occurrence. The area stands as a part of the grain belt for large land reserves and high grain production, but concentrated and advanced networks known from Europe or North America to monitoring hydro-meteorological parameters are virtually non-existent. Nevertheless, there is a special interest in such information, particularly by farmers. As yield losses occur more frequently, it becomes necessary to address this concern by providing information about local conditions. In order to narrow this gap, monitoring networks were established to investigate meteorological and pedo-hydrological parameters at selected sites in the dry steppes of southwest Siberia and Kazakhstan. The overall objective is the optimisation of the soil water regime by innovative soil management. The knowledge about

the water budget and the year-round ET process may be the basis for recommendations for the use of agricultural land and its sustainable land management. The achievement of this major objective is determining the soil water balance and all its components.

With this background the objectives of this thesis are:

- I. to evaluate different methods to determine the soil water balance parameters P and ET,
- II. to assess the measurement of ET by weighable lysimeters during cold and snowy conditions,
- III. to quantify the soil water balance in the steppes of southwest Siberia and Kazakhstan.

As mentioned above, there are numerous methods to determine individual parameters of the soil water balance. Although in the detection of P the use of standard rain gauges is widely common, now there are alternative methods that promise a higher accuracy. A comparison of three approaches and an evaluation in measuring accuracy are treated in **Chapter 2**.

The determination of ET is likely the most complex aspect within the water balancing. The range of methods makes it difficult to decide which approach is the most suitable. As the monitoring networks enable a record of high-resolution data, **Chapter 3** illustrates a comparison of a direct method by using weighable lysimeters and a modelling approach widely used for the estimation of ET.

After the comparison of methods, **Chapter 4** focuses on the lysimetry method to determine soil water balance parameters. Using the weighable lysimeters described in the chapters before, the components ET, P, and  $\Delta S$  will be quantified for a summer season in southwest Siberia.

In **Chapter 5**, a full-year lysimeter experiment is presented, which enabled the first quantification of the soil water balance for the study site in Kazakhstan.

**Chapter 6** deals with the challenge of the measurement of soil water balance parameters under winter conditions. As weighable lysimeters often show impairments by snow and frost effects, an attempt was made to reduce these effects by the development of a novel technology.

In **Chapter 7**, the measured water fluxes in the Kazakh steppe will be compared with those estimated by a process-based soil physical model. By means of the available lysimeter data, it will be tested whether the model is able to reflect the water regime under dry conditions.

## **2 Evaluation of precipitation measurements methods: A comparison of the standard rain gauge with a weighable lysimeter and a piezoelectric precipitation sensor**

This chapter based on the published paper: *Haselow, L., Meissner, R., Rupp, H., Miegel, K., 2019. Evaluation of precipitation measurements methods under field conditions during a summer season: A comparison of the standard rain gauge with a weighable lysimeter and a piezoelectric precipitation sensor. J. Hydrol. 575, 537-543.*

### **2.1 Abstract**

Current precipitation measurements are conducted largely by simple automatic rain gauges. Despite being error-prone and sometimes of questionable accuracy, the procedure is still widely used. In recent years new possibilities have emerged, which are based on different measuring principles. Although the application of alternative devices is increasing, its use in research is limited. In this study, precipitation measurements by different devices were compared, and systematic errors caused by individual characteristics were corrected. Data was collected by means of a monitoring network, which included a piezoelectric precipitation sensor mounted at 2.3 m, a standard tipping bucket at 1 m, and a weighable gravitation lysimeter at ground level. As measurements at ground level are considered as optimum, the records of the lysimeter were thereby determined as a reference. The results showed that precipitation measured by elevated rain gauges differed in total between -6.8% and +35% compared to rainfall measured by the lysimeter. The records correlated well, but the analyses indicated a strong influence of the precipitation intensity on the recorded amount of precipitation. The deviations between values of the rain gauges and those of the lysimeter increased with rainfall intensity. In general, the tipping bucket demonstrated negative error values and indicated an underestimation of precipitation compared to records at ground level, whereas the piezoelectric precipitation sensor showed an overestimation by highly positive error values. A subsequent precipitation correction through the linear scaling method improved significantly the raw data of the rain gauges.

### **2.2 Introduction**

Quantification of precipitation is important for many reasons. Information about rainfall, obtained from accurate point measurements, is widely used in climatology, hydrology or

agrometeorology. However, this method of precipitation measurement is associated with systematic underestimation (Sevruk, 1982; Richter, 1995; Førland et al., 1996; Goodison et al., 1998), which may strongly impair the accuracy. The effects of systematic errors on the quality of measurements depend on gauge design and their installation specifics, the surrounding area, meteorological parameters, and type of precipitation (Sevruk, 1982; Legates and DeLiberty, 1993). The well-known error sources, particularly caused by wind, wetting and evaporation loss, have affected all types of rain gauges for a long time. Especially, the installation of rain gauges at heights between 0.5 and 1.5 m above ground level (World Meteorological Organization; WMO, 2014) often result in erroneous recorded values up to 75% of single precipitation events (Neff, 1978).

According to WMO, there are three types of automatic precipitation recorders, which are deemed to be standard rain gauges: the weighing-recording type, the tipping bucket type, and the float type. All these devices are susceptible to error sources as mentioned above (WMO, 2014). Meanwhile, there are other new automatic recording gauges that are based on the optical or acoustical detection. Despite the advances, precipitation measurements at ground level are optimal, because the conditions are identical to the surrounding area and the wind-induced error is negligible (Mekonnen et al., 2015). Furthermore, measurements at ground level are the true reference since they show more precipitation than any elevated rain gauge (WMO, 2014).

Lysimetry is originally a method for the investigation of soil hydrology and soil chemistry. In the last few years, however, lysimeters will be increasingly used for precipitation measurements due to the high precision weighing system (von Unold and Fank, 2008; Meissner et al., 2010; Schrader et al., 2013; Peters et al., 2014; Gebler et al., 2015; Herbrich and Gerke, 2016; Hoffmann et al., 2016). The advantage of lysimeters in rainfall recording lies in the recognition that they do not exhibit the commonly occurring errors associated with the standard rain gauges. However, vibrations caused by wind, maintenance, fieldwork or due to animals entering the lysimeter vessel are sources of errors.

In this study, a monitoring network enables comparable analyses of precipitation measurements by three different types of rain gauges. These are an automatic tipping bucket, which corresponds to the standard device according to the WMO, a weighable gravitation lysimeter whose mass changes provide an estimation of precipitation, and a piezoelectric precipitation sensor, which is based on acoustic detection of raindrop impacts. All devices were part of the monitoring network that was established in southwest Siberia. The main objective of this study is to evaluate precipitation measurements of rain gauges in comparison with lysimeter data at ground level. Based on the results, this study also applies

a bias correction method to decrease systematic errors such as, in this case, different gauge designs.

## **2.3 Material and methods**

### **2.3.1 Site description**

The study area is part of the southwest Siberian Kulunda steppe lowland and located between the Central Asian steppe and the North Asian forest-steppe (Balikyn et al., 2016). North of Kulunda steppe is the Baraba forest steppe, and the eastern part of the Irtysh valley in Kazakhstan is situated in the west. The site is located at altitudes of 100-140 m a.s.l. and it is covered by a 50 to 60 cm thick layer of Pleistocene alluvial and 0.5-10 m of eolian sediments. Typical soils of the area are chestnut, meadow–chestnut, meadow, solonetz, and solonchak.

The Kulunda steppe is characterised by a continental climate with long, cold and snowy winters and short, hot and dry summers (Meissner et al., 2017). The steppe is often affected by cold air masses from the Kara Sea and warm and dry ones from Kazakh and Middle Asian steppes and deserts. Thus, dry winds are common and the temperatures are highly variable throughout the year. In spring, very dry periods are characteristic. The mean annual temperature is about 0 °C, the absolute minimum -47 °C, and the absolute maximum +40 °C. The mean temperature of the coldest month (January) is -19 °C, whereas the warmest month (July) has a mean temperature of +19 °C. The annual precipitation is about 250-450 mm. From April to October, the precipitation is about 200 mm. The frostless period lasts between 112 to 120 days per year from late May to early September. In late snow-free autumn periods, the temperature drops down to -20 °C or lower. From November to April a constant snow cover lasts for a period of 140-150 days with a mean depth of 15 cm (absolute maximum 35-38 cm). Furthermore, in winter, the soils freeze down to 2 m deep (and even more). The global radiation is 2-3 times higher than the energy that is required to evaporate the precipitation.

### **2.3.2 The monitoring network**

The monitoring network consisted of a weather station and a weighable gravitation lysimeter station (Fig. 1) (Meissner et al., 2017). The weather station was established in September 2012 and included a multisensor at a height of 2.3 m (recording wind speed, wind direction, air temperature, air humidity, barometric pressure, rainfall), a pyranometer at a height of 2 m

(recording solar radiation), and a tipping bucket rain gauge at the standard height of 1 m (recording liquid and solid precipitation).

The first precipitation measuring device used in this study was the precipitation sensor of the multisensor (Weather Transmitter WXT520; manufacturer 'Vaisala Inc.', Finland). It consisted of a steel cover and a piezoelectric sensor (Vaisala, 2012), capable of detecting individual raindrops, which are subsequently converted to cumulative rainfall. This is possible since the signal strength is proportional to the volume of all the drops. Interferences originating from other sources were filtered by using advanced noise filtering techniques. Further information about precipitation measuring properties is given in Table 1, whereby the piezoelectric precipitation sensor will be denoted hereafter as 'Prec. Sensor'.

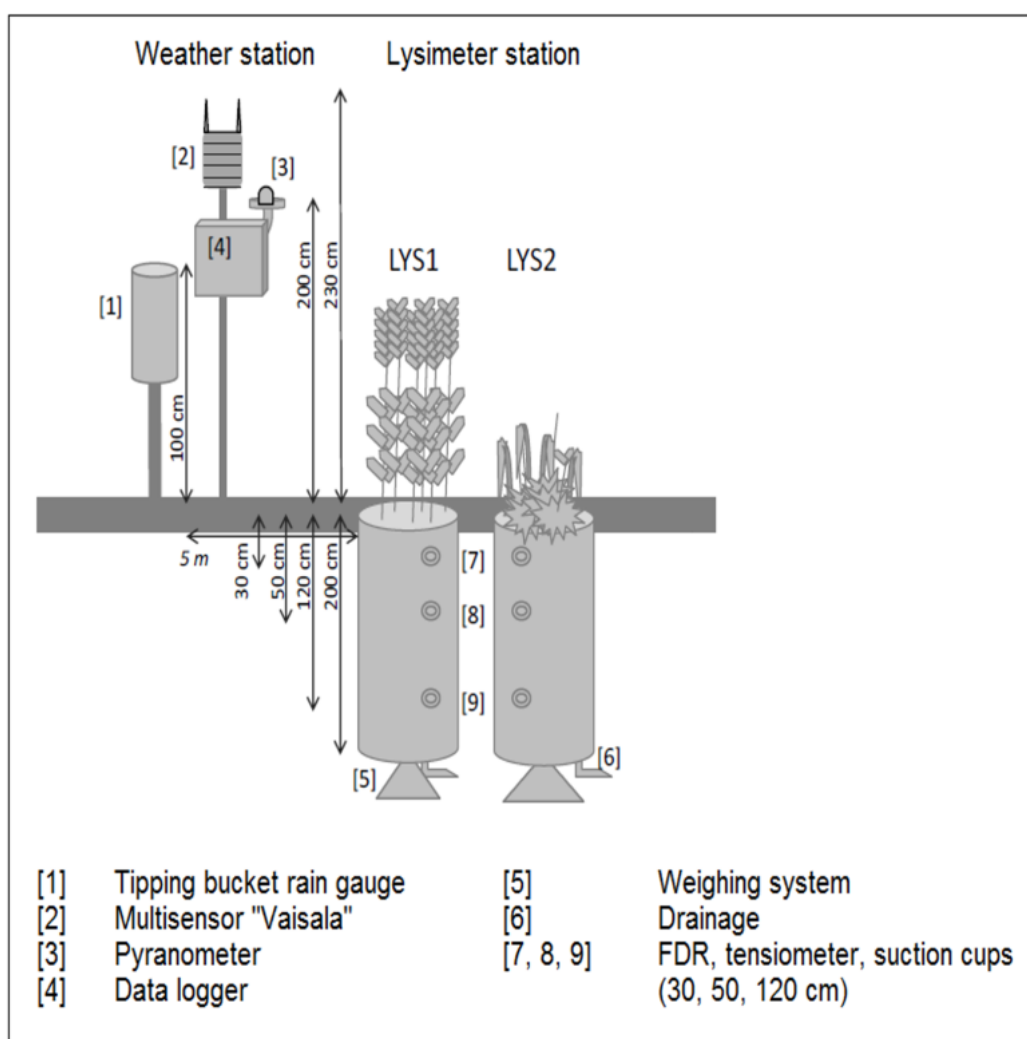


**Figure 1:** Experimental set-up of the monitoring network consisting of multisensor 'Vaisala', tipping bucket rain gauge and two weighable gravitation lysimeters (according to Meissner et al., 2017; modified).

The tipping bucket rain gauge (manufacturer 'ecoTech', Germany), which was also used in the study was based on the 'Guide to Meteorological Instruments No. 8' (WMO, 2008). The instrument was appropriate to measure the amount of rainfall and rainfall intensity (Thies Clima, 2008). A receiving surface of 200 cm<sup>2</sup> collected the rain, which was conducted through an inflow-sieve into a tipping bucket. An amount of 2 cm<sup>3</sup> led tipped the bucket that was equivalent to 0.1 mm precipitation. This tipping procedure produced an electrical signal which was recorded by a data logger. Since the number of tipping was not linearly related to the precipitation intensity, an intensity-dependent linearisation was carried out by a data logger, based on an intensity-dependent pulse-number-correction for the precipitation intensity range of approximately 0.5 to 11 mm min<sup>-1</sup>.

During June-August 2013 a containerised (Polyethylene PE-HD) lysimeter station with two weighable lysimeters (manufacturer 'UGT-Muencheberg', Germany and Helmholtz Centre for Environmental Research – UFZ, Germany) was installed at a test farm in Poluyamki (N52° 03.959' E79° 42.786'; approximately 700 km southwest of Novosibirsk). The soil monoliths were monolithically extracted from an arable land and from a fallow site, which had been covered with natural steppe vegetation since the 1950s. The lysimeters had a surface area of 1 m<sup>2</sup> and a depth of 2 m. A detailed description of the lysimeters is given by Meissner et al. (2017). The soils were identified as Calcic Chernozems according to the FAO guidelines. The vessels were positioned into the lysimeter station on load cells by using a three-legged steel frame (Meissner et al., 2007). The lysimeter mass was measured with a high precision of ±20 g (Xiao et al., 2009). The total mass of each lysimeter vessel was approximately 4000 kg and the mass changed by water input (precipitation, dew, rime, and the water equivalent of snow) and water output (actual evapotranspiration, outflow). Both lysimeters were equipped with FDR probes for the measurements of the soil moisture and the soil temperature, watermark-sensors for matrix potential measurements, and suction cups to extract soil solution. All sensors were installed at depths of 30, 50, and 120 cm, respectively. The amount of seepage water was collected in a storage container upon measuring by tipping bucket. The surface runoff was measured by a fixed drain at the container wall, which channelled the water to an additional tipping bucket.

All data were consolidated and stored in the respective data logger with a recording interval of one hour (Tab. 1).

**Table 1:** Properties of precipitation measurements by Prec. Sensor, tipping bucket rain gauge, and lysimeter.

Property	Prec. Sensor	Tipping bucket	Lysimeter
<b>Rainfall</b>	cumulative accumulation after the latest auto or manual reset		
Measuring height (above ground level)	2.3 m	1.0 m	0.0 m
Temporal resolution	60 min	60 min	60 min
Collecting area	60 cm <sup>2</sup>	200 cm <sup>2</sup>	10 000 cm <sup>2</sup>
Output resolution	0.01 mm	0.1 mm	0.02 mm
Accuracy	± 5 %	± 3 %	± 0.0005 %
Measuring range	0 ... 200 mm h <sup>-1</sup>	0.5 ... 11 mm min <sup>-1</sup>	
<b>Notice</b>	No information regarding calibration	Calibrated with a precipitation of 10 mm	

### 2.3.3 Data availability

To compare precipitation measured by the different systems identical time series were required. Due to the different time of installation synchronous measurements were only available from August 2013 to September 2016. The major challenge of precipitation measurements by lysimeters was the malfunction during winter in Siberia. Sub-zero temperatures and snow led to an inexplicable increase of the lysimeter mass. The failure-free operation was restarted in spring. Rising temperatures and frostless nights were necessary to stabilise the system at the initial time periods. Therefore, all periods between October and May were non-applicable for data analysis. Sufficient data was available during summer. The longest time series without data gaps was between 09 June and 30 September 2016 which was appropriated as investigation period. The two lysimeters were originally used for reference analyses between arable land and unconverted grassland. Thus, there was an ascertained crop rotation at the arable lysimeter (lysimeter – LYS 1): wheat (2013), peas (2014), wheat (2015), and fallow (2016). In contrast, the pristine lysimeter (lysimeter 2 – LYS 2) was dominated by natural feather grass (*Stípa pennáta*) between 2013 and 2016. Considering the purpose of the study only the data of the arable lysimeter in 2016 are

suitable for an unrestricted comparability to the rain gauges. The absence of vegetation represents the ideal condition to measure precipitation at ground level because there are no external factors that have a direct effect on the measurements. Although the development of ruderal vegetation was observed, the percentage of the canopy was still small during the investigated period so that the interception of vegetation, which is part of the precipitation term, is negligible.

#### 2.3.4 Data preparation

The processing of precipitation data of Prec. Sensor and tipping bucket rain gauge was followed the same procedure. First, the cumulative data were converted into absolute values per hour. In step two, the raw data was manually filtered, and all data during system error or noticeable outliers was removed. When the resulting gaps did not exceed a period of four hours, the values were estimated by linear interpolation. The processing of lysimeter data was done according to the principle of the adaptive window and adaptive threshold filter (AWAT), developed by Peters et al. (2014). The AWAT filter is an approach to filter and smooth noisy lysimeter data.

#### 2.3.5 Calculating precipitation from lysimeter data

Meissner et al. (2000, 2007, 2010) have shown that weighable lysimeters were able to measure water fluxes with high precision. The total mass of the system ( $M$ ) was the sum of the mass of lysimeter ( $M_{lys}$ ) and of drainage ( $M_{drain}$ ). It is assumed that a mass increase corresponds to precipitation ( $P$ ) and a mass decrease was actual evapotranspiration ( $ET_a$ ). With this assumption,  $P$  and  $ET_a$  cannot take place within the same time interval.  $ET_a$  is equal to zero when  $P$  occurs, and vice versa. Therefore,  $P$  was calculated from the mass changes of lysimeter by Schrader et al. (2013):

$$M = M_{lys} + M_{drain}$$

$$P = \begin{cases} \Delta M & \text{for } \Delta M > 0 \\ 0 & \text{for } \Delta M \leq 0 \end{cases} \quad (2)$$

$$ET_a = \begin{cases} \Delta M & \text{for } \Delta M < 0 \\ 0 & \text{for } \Delta M \geq 0 \end{cases}$$

In Eq. 2,  $M_{lys}$  [kg] is the mass of lysimeter vessel,  $M_{drain}$  [kg] is the amount of seepage water, and  $\Delta M$  [kg] is the total mass change of lysimeter vessel in the according time interval. Due to the geometry of the lysimeter vessel mentioned above, a change of mass is equal to a

water storage change in millimetres ( $1 \text{ kg} \approx 1 \text{ l/m}^2 = 1 \text{ mm}$ ). Therefore, all changes of mass are given in millimetres henceforward.

### 2.3.6 Data analyses

After data had been converted to hourly P values the study considered only rainfall data at at least one measurement station. Time steps without rainfall at all three stations and data lower than  $0.1 \text{ mm hour}^{-1}$  were removed. The latter is justified by the output resolution of the tipping bucket. Furthermore, the impact of dewfall at the lysimeter which may misinterpret as P is thereby avoided. Depending on the aims of data use, P can be expressed at different time scales. Where daily values are required, the hourly values are summed-up for one day, starting from 0.00 UTC and follows to 24 hours.

The evaluation of data is carried out by means of statistical indices. The correlation of Pearson ( $r$ ), bias (Eq. 3), relative bias (rbias, Eq. 4), mean absolute error (MAE, Eq. 5), and the root mean squared error (RMSE, Eq. 6) were calculated. Let the variables  $X_i$  and  $Y_i$  be the  $i$ th value from the particular rain gauge and the lysimeter, respectively;  $n$  is the total number of data for the observation period.

$$\text{bias} = \frac{\sum_{i=1}^n (X_i - Y_i)}{n} \quad (3)$$

$$\text{rbias} = \left( \frac{\sum_{i=1}^n (X_i - Y_i)}{\sum_{i=1}^n Y_i} \right) \times 100 \quad (4)$$

$$\text{MAE} = \frac{\sum_{i=1}^n |X_i - Y_i|}{n} \quad (5)$$

$$\text{RMSE} = \sqrt{\frac{\sum_{i=1}^n (X_i - Y_i)^2}{n}} \quad (6)$$

The error indices indicate how well the data of the rain gauges agree with the observed data of the lysimeter. Positive bias and rbias indicate an overestimation and negative values show an underestimation, while MAE and RMSE values of 0.0 show a perfect match between the measurements.

In order to correct bias in the rain gauge data and defining correction factors the linear scaling of P was conducted. The method aims to decrease the bias between observed and raw data by calculating monthly correction factors on a daily basis and multiplying them with the raw value (Fang et al., 2015):

$$P_{cor,m,d} = P_{raw,m,d} \times \frac{\mu(P_{obs,m})}{\mu(P_{raw,m})}, \quad (7)$$

where  $P_{cor,m,d}$  is the corrected  $P$  on the  $d$ th day of the  $m$ th month,  $P_{raw,m,d}$  is the raw  $P$  on the  $d$ th day of the  $m$ th month, and  $\mu$  is the mean value of observed and raw  $P$  at given month  $m$ . The observed and raw  $P$  corresponds to the lysimeter and the rain gauges, respectively.

## 2.4 Results and discussion

### 2.4.1 Comparison of precipitation measurements

The cumulative  $P$  of the lysimeter (LYS), Prec. Sensor and tipping bucket (TB) were compared during 44 days of rainfall (Fig. 2). Most of  $P$  was recorded by Prec. Sensor with a total of 229.4 mm, whereas TB measured the lowest sum of 158.4 mm. Values of LYS with a sum of 169.9 mm ranged between Prec. Sensor and TB. The cumulative  $P$  from rain gauges showed relative differences ranging from +35% (Prec. Sensor) to -6.8% (TB) in comparison to LYS. Results of the monthly analysis are given in Table 2. In a month by month comparison, the maximum and minimum of  $P$  were measured by Prec. Sensor and by TB, except for September where LYS presented the lowest  $P$  value. The smallest relative deviations were between LYS and TB which varied in -5.5% and -5.8% in June and August, whereas the deviations with -8.9% and +33.3% were increased in July and September, respectively. In contrast,  $P$  records of Prec. Sensor are totally unconnected with those by LYS because a continuous increase in deviations (up to +88.3% in September) was stated.

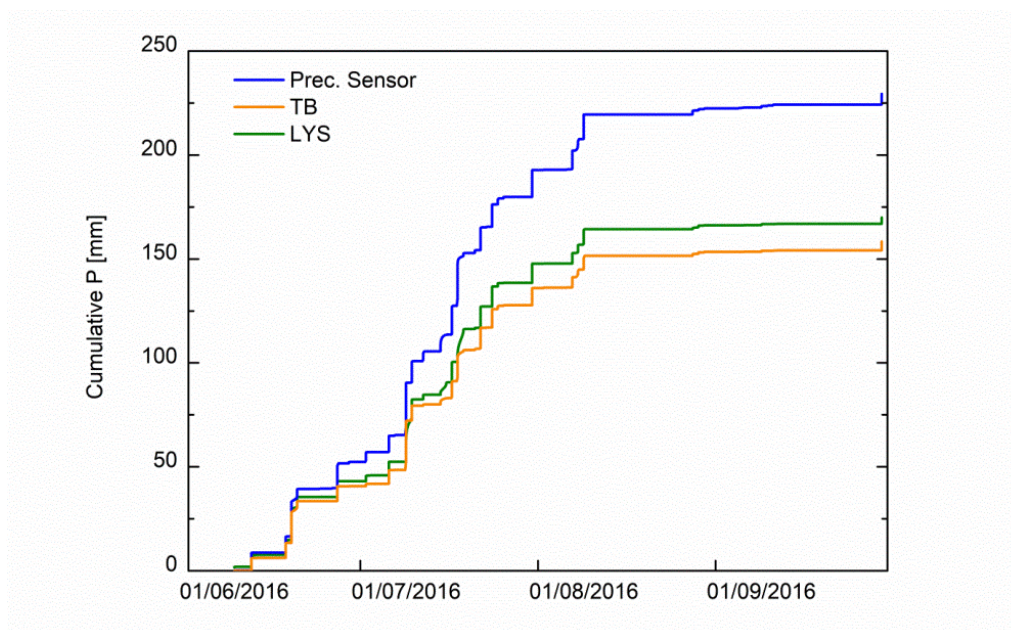


**Figure 2:** Cumulative precipitation ( $P$ ) of Prec. Sensor, the tipping bucket rain gauge (TB), and the lysimeter (LYS) from 09/06/2016 to 31/09/2016.

**Table 2:** Monthly precipitation (P) of the lysimeter (LYS) and rain gauges.

Period	Number of observation days (n)	P		
		Prec. Sensor	TB	LYS
Jun	22	52.3	40.7	43.1
Jul	31	140.4	95.3	104.6
Aug	31	29.6	17.4	18.5
Sep	30	7.1	5.0	3.7

Daily precipitation measurements correlated well with those of the rain gauges with  $r$  varying between 0.87 and 0.91 (Fig. 3). Daily P values of LYS, TB and Prec. Sensor ranged from 0 to 16.4 mm day<sup>-1</sup>, from 0 to 23.7 mm day<sup>-1</sup>, and from 0 to 25.1 mm day<sup>-1</sup>, respectively (Fig. 4). Data of Prec. Sensor showed a median of 2.2 mm day<sup>-1</sup> and they covered the widest range of values, whereas P measured by TB yielded the lowest values and a median of 0.8 mm day<sup>-1</sup>. Usually, P rate decreased with increasing measuring height (Sevruk, 1981; Fank and Klammler, 2013; Gebler et al., 2015; Hoffmann et al., 2016). Therefore, the installation height of TB justified the lower P rates compared to those measured at ground level. In addition, the smaller receiving surface, wind-field deformation, evaporation, splashing or wetting loss at the internal wall of the collector may also have reduced the measuring results. On the other hand, Prec. Sensor should show lower values than TB and LYS due to the measuring height of 2.3 m. According to the manufacturer, Prec. Sensor has to measure up to 30% less P than rain gauges at ground level (Vaisala, 2012). The disagreement cannot be explained without additional investigations. It is not due to systematic measurement errors of standard rain gauges. The measuring principle is based on the detection of individual raindrop impacts. Therefore, variation in the shape and velocity of raindrops caused by air movements was the major error factor. A further malfunction source could be the sensitivity variations over the sensor area due to surface wetness (Salmi and Ikonen, 2005).

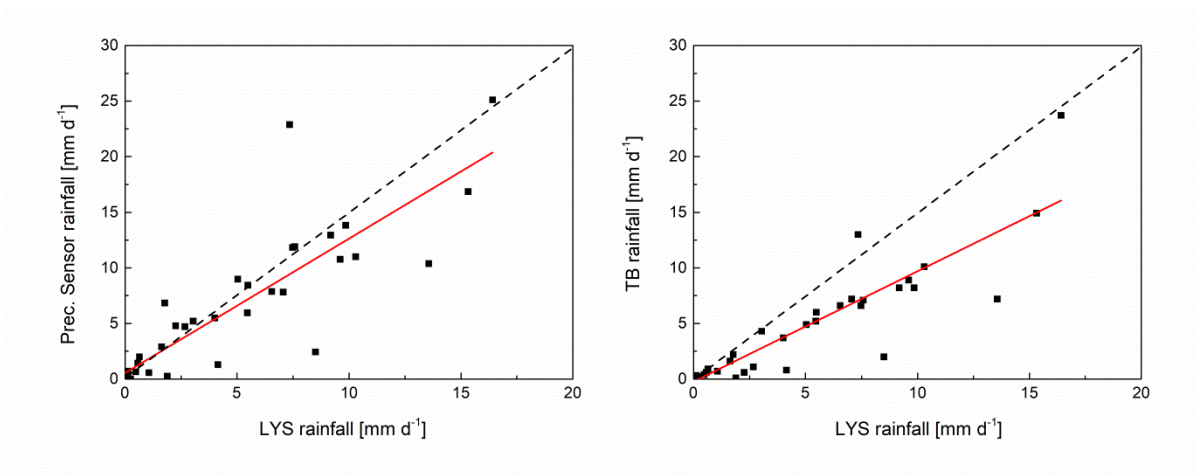


**Figure 3:** The relationship between the rainfall data obtained by the rain gauges and lysimeter (LYS) on a daily basis.

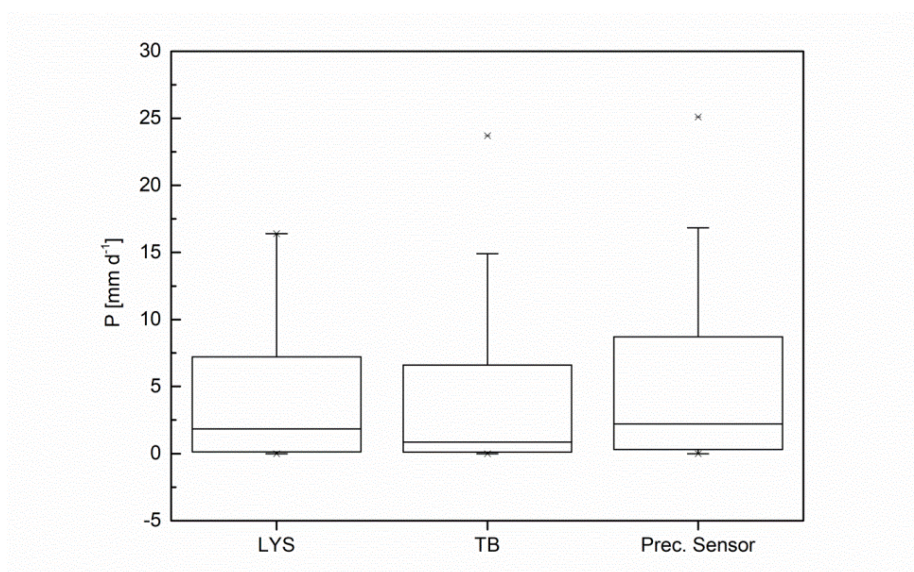


**Figure 4:** Comparison of rainfall data measured by the lysimeter (LYS), the tipping bucket (TB), and Prec. Sensor. The box plots are based on daily data. The box boundaries represent the 25th and 75th percentiles, the inner lines indicate the medians, the whiskers extend to 1.5 times the interquartile range, the crosses mark the 1st and 99th percentiles, and the strokes show the minimum and maximum values.

According to the German Meteorological Service (Deutscher Wetterdienst - DWD) rainfall intensity can be classified as light rain ( $<2.5 \text{ mm hour}^{-1}$ ), moderate rain ( $2.5\text{-}10 \text{ mm hour}^{-1}$ ) and heavy rain ( $>10 \text{ mm hour}^{-1}$ ). Within the studied time period, the absolute frequency of occurrence (i.e., the number of rainfall events that occur under a certain condition) decreased with increased rainfall intensity. Precipitation with light intensity predominated with

a contribution of 78 to 88% to the total rainfall (Fig. 5). LYS demonstrated a higher frequency of light rainfall than the rain gauges, but the absolute frequency of Prec. Sensor exceeded TB and LYS at moderate rainfall. Overall, moderate rainfall occurred with an absolute frequency of <21 and a percentage of 11% in the rain gauges. Events with rainfall intensity >10 mm hour<sup>-1</sup> did not occur at LYS, but it was measured twice at TB and four times at Prec. Sensor which accounted for a share of around 3%.

It has been observed that the differences in P between LYS and rain gauges are dependent on rainfall intensity. The higher the rainfall intensity the larger the errors to P measured by LYS became (Tab. 3). Prec. Sensor, as well as TB, demonstrated mostly similar differences. At light rainfall, they showed error values up to 2.9 mm hour<sup>-1</sup>. When LYS recorded moderate rainfall MAE and RMSE increased to approximately 4 mm hour<sup>-1</sup>. As LYS had measured no heavy rainfall, the calculation of MAE and RMSE were based on the rainfall events >10 mm recorded by Prec. Sensor. It should be mentioned that in the case of light or moderate rainfall detected by LYS and a simultaneous heavy rainfall detected by the rain gauges, the rainfall at the rain gauges should be regarded as an error of light or moderate rainfall. Nevertheless, MAE and RMSE have reached a maximum of 14.9 mm hour<sup>-1</sup> and 16.2 mm hour<sup>-1</sup>, respectively.

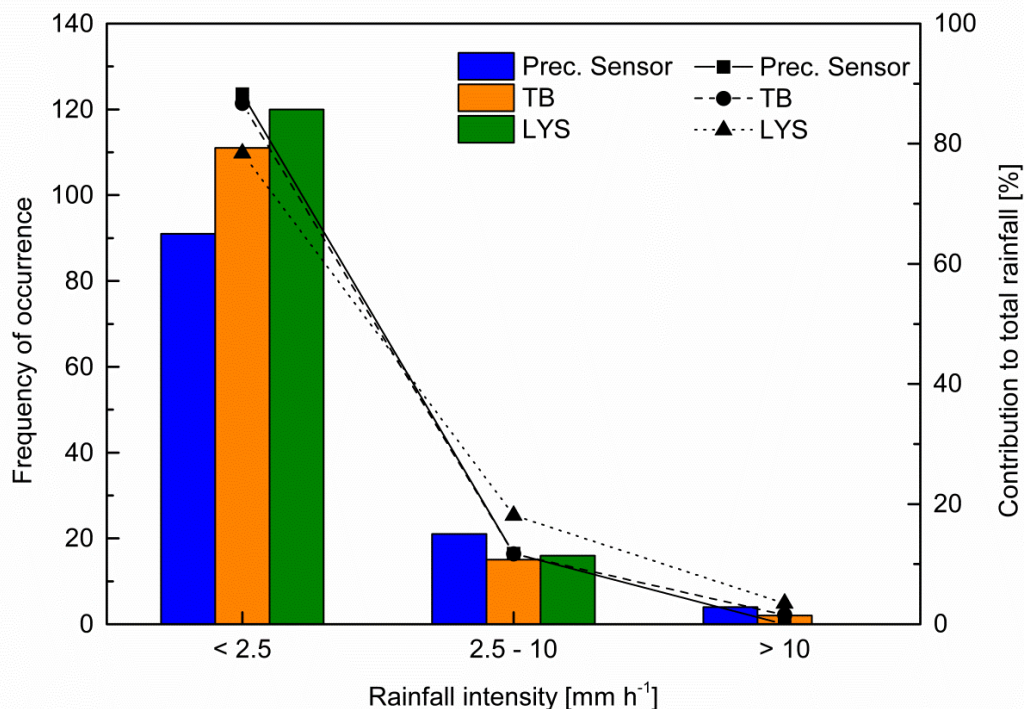


**Figure 5:** Frequency distribution of daily precipitation rates in different intensity ranges and their contribution to the total rainfall. The vertical bars are related to the left axis; the symbols and lines are related to the right axis.

These significant deviations could possibly demonstrate an overestimation of P by Prec. Sensor due to the high velocity of raindrops. This assumption may be confirmed by the more frequent measurements of P which were classified as moderate and heavy rainfall. However, on 09 July 2016, a phenomenon was observed which could be the reason for higher differences. The rain gauges measured up to 52% more P than LYS. If high P amount falls in a short time, water runs off across the LYS collar because the infiltration capacity of the previous dried-up soil becomes exceeded. This water was not recorded as P but rather as surface runoff. The lysimeter recorded a daily surface runoff of 4.3 mm. If this amount will be assumed as P, the deviation to P measured by the rain gauges becomes lower up to 30%.

**Table 3:** The error indices MAE and RMSE as a function of rainfall intensity. Note that the heavy rainfall events are based on P values of Prec. Sensor.

rainfall intensity	MAE		RMSE	
	Prec. Sensor [mm h <sup>-1</sup> ]	TB [mm h <sup>-1</sup> ]	Prec. Sensor [mm h <sup>-1</sup> ]	TB [mm h <sup>-1</sup> ]
light	1.2	0.9	2.9	2.1
moderate	3.7	3.8	4.1	4.2
heavy	14.9	9.9	16.2	12.3

#### 2.4.2 Bias correction

There are several reasons for the correction of rainfall data. Usually, it will be used for model calibration and validation since the simulations are often far different from observations. On the other hand, rainfall data can also be obtained from novel gauges or remote sensing which show other systematic errors and uncertainties. As rainfall data may vary considerably in their accuracy due to different measuring principles, data correction is necessary to decrease bias between the measurement devices. For this purpose, there are a lot of methods to correct bias (Teutschbein and Seibert, 2012; Fang et. al., 2015, Sungmin et al., 2018). In this study, the linear scaling method was chosen due to the exclusive use of wet days ( $P > 0.1$  mm) and derivation of correction factors. According to Eq. 7, correction factors and results are shown in Table 4 and Figure 6. The method significantly improved the raw data of the rain gauges. However, there were remained mismatches between LYS and corrected data where the rain gauges, for instance, did not follow the temporal pattern of LYS. This state of affairs was the result of the fact that the temporal record of devices

occasionally differed. Precipitation rates were cumulated and were provided as an absolute value at rain gauges, whereas LYS sometimes recorded the same rate distributed over hours. Thus, LYS showed a delayed response to rainfall. This phenomenon was noticeable during the analysis of daily P rates. This was peculiar with night rainfall. The amount of rainfall measured by rain gauges was summed-up for one day. Due to the delayed record of LYS, the P amount was distributed over two days. Therefore, the daily P rates were lower or higher compared to measurements by rain gauges for the respective day.

**Table 4:** Monthly correction factors for Prec. Sensor and tipping bucket (TB) to reduce bias in the raw data.

Month	Prec. Sensor	TB
Jun	0.82	1.06
Jul	0.75	1.10
Aug	0.62	1.06
Sep	0.53	0.75

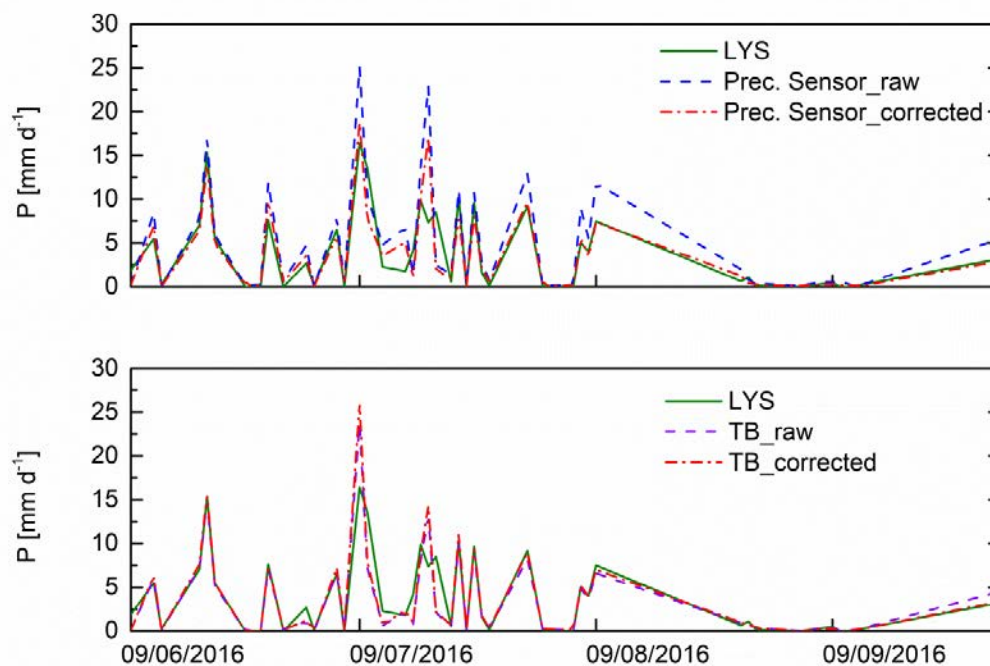


**Figure 6:** The daily precipitation (P) of the lysimeter (LYS) compared to the raw and corrected rainfall of the tipping bucket (TB) and Prec. Sensor.

Table 5 presents bias, rbias, MAE, and RMSE before and after the correction. The raw data of Prec. Sensor and TB had a total bias of  $1.3 \text{ mm day}^{-1}$  and  $-0.3 \text{ mm day}^{-1}$ , respectively. Bias and rbias of TB are negative, except for September. MAE and RMSE indicate relatively large total values with 2 and  $3.4 \text{ mm day}^{-1}$  for Prec. Sensor as well as 1 and  $2.1 \text{ mm day}^{-1}$  for TB, respectively. These values can result from convective P which is accompanied by high rainfall intensity. Convective systems occur usually during summer. In the investigated period heavy rainfall was particularly measured in July, which led to higher MAE and RMSE. After the correction, the monthly rbias range from 0.01 to  $-0.09\%$ . MAE and RMSE of Prec. Sensor decreased by 40 and 33%, whereas the error values of TB increased by 1 and 9%, respectively. In general, the corrected data are in good agreement with observed P measured by LYS. Shrestha et al. (2017) have proved that the linear scaling method delivers good results despite the simple technique. Recent studies are strongly in favour of the superiority of complex bias correction methods, but the simple implementation and similar performance compared to complex methods are arguments for their application. The big drawback is, however, the inability to correct the rainfall intensity as it could be observed in the data of July. The approach overcorrected rbias, MAE, and RMSE of TB and underestimated those of Prec. Sensor. Similar results were also found by Fang et al. (2015). In order to correct rainfall intensity, an alternative technique such as quantile mapping is more appropriate because it modifies the P distribution in expectation of changes due to more frequent extreme rainfall events.

**Table 5:** Comparison of the error indices for Prec. Sensor and tipping bucket (TB) before (b) and after (a) bias correction.

		<b>bias</b>		<b>rbias</b>		<b>MAE</b>		<b>RMSE</b>	
		Prec. Sensor [ $\text{mm d}^{-1}$ ]	TB [ $\text{mm d}^{-1}$ ]	Prec. Sensor [%]	TB [%]	Prec. Sensor [ $\text{mm d}^{-1}$ ]	TB [ $\text{mm d}^{-1}$ ]	Prec. Sensor [ $\text{mm d}^{-1}$ ]	TB [ $\text{mm d}^{-1}$ ]
Jun	b	0.9	-0.2	21.5	-5.5	1.3	0.4	1.8	0.6
	a	0.0	0.0	0.0	0.0	0.9	0.4	1.1	0.6
Jul	b	1.9	-0.5	34.2	-8.9	3.2	1.9	4.8	3.1
	a	0.0	0.0	-0.01	0.01	2.1	2.0	3.3	3.5
Aug	b	1.4	-0.1	60.5	-5.8	1.5	0.3	2.2	0.4
	a	0.0	0.0	-0.03	-0.03	0.3	0.2	0.4	0.2
Sep	b	0.5	0.2	88.3	33.3	0.5	0.2	0.8	0.5
	a	0.0	0.0	-0.08	-0.09	0.1	0.1	0.2	0.1

## 2.5 Conclusions

This study compared rainfall data of rain gauges with lysimeter data, and reduced effects of systematic errors resulting from their individual characteristics by P correction. As rainfall measured at ground level is the true reference, it can be assumed that the detection of rainfall by LYS provides precise and reliable rainfall data. However, the inability to account correctly for the effects of surface runoff at high rainfall intensity can lead to an underestimation of P. Furthermore, big drawbacks of the lysimetry and their use in P measurement are the high costs and effort for maintenance. In contrast, P measurements by rain gauges are convenient and inexpensive. Though, this study demonstrated the reduced accuracy compared to measurements at ground level. The application of TB is widely distributed for standard measurements, but TB underestimated significantly the amount of P due to the elevated installation. The application of Prec. Sensor as a new rain gauge is effective due to the maintenance-free and multi-disciplinary ability, but contrary to the statement made by the manufacturer, Prec. Sensor underestimate P up to 30% compared to ground level, the measuring results indicated an overestimation of P. It seems that the shape and velocity of raindrops have some influence on P detection.

Based on different conditions in measuring principle, a bias correction in the data of TB and Prec. Sensor was necessary. There are several P correction methods whose application is case dependent. The aim was to adjust the rain gauges data to the LYS data at ground level. Therefore, the linear scaling method was an appropriate approach to define correction values which will finally be applied to the raw data. After correction, TB and Prec. Sensor delivered improved rainfall data with decreased error values. Nevertheless, the method has failed for periods with high rainfall intensity. Raw data of TB were overcorrected, whereas the values of Prec. Sensor were underestimated.

Finally, it is not proven whether the calibration of Prec. Sensor is appropriate to other climate zones. Rainfall intensity, raindrop size, shape and rate of fall differ at the regional level, and they potentially require different calibrations. Due to the lack of scientific studies of piezoelectric precipitation sensors, further investigations are necessary, particularly with regard to their calibration and accuracy under different rainfall conditions.

### **3 Measurement and estimation of evapotranspiration for semiarid grassland**

This chapter based on the published paper: *Haselow, L., Rupp, H., Bondarovich, A., Meissner, R., 2019. Measurement and estimation of evapotranspiration in semi-arid grassland during the summer season in southwest Siberia. Eurasian J. Soil Sci. 8, 257-266.*

#### **3.1 Abstract**

This study quantifies actual evapotranspiration ( $ET_a$ ) for a period from June to September 2016 measured by two weighable gravitation lysimeters in semiarid grassland in southwest Siberia. As part of a crop rotation system, the first lysimeter was fallow but covered with ruderal vegetation. The second lysimeter is permanently characterised by pristine steppe vegetation. In addition to  $ET_a$  measurements, the reference evapotranspiration ( $ET_0$ ) is computed by a Penman-Monteith model. The estimates are related to the  $ET_a$  records and the model is evaluated with regard to its performance in a semiarid environment. The results indicated an  $ET_a$  driven by energy but limited by water. Within 115 days the total amounts of  $ET_a$  ranged from 205 mm to 374.1 mm, and daily values varied from 0.1 to 6.9 mm day<sup>-1</sup>. The large differences are caused by the different vegetation cover of the lysimeters. Due to the high and dense canopy of the pristine steppe vegetation, the transpiration term was considerably higher compared to the ruderal vegetation where soil evaporation took the major part. The daily  $ET_a$  records differed on average by -91.1% to the  $ET_0$  estimates. The statistical analyses yielded a low correlation between  $ET_a$  of the ruderal vegetation and  $ET_0$  but an acceptable model performance for the pristine steppe. However, it was observed that  $ET_a$  occasionally exceeds  $ET_0$ , particularly after precipitation. Due to the high water availability and the subsequent rise of  $ET_a$ ,  $ET_0$  was underestimated, whereas it was overestimated during dry periods. Finally, the performance of the Penman-Monteith model varied substantially with the water supply at the study site.

#### **3.2 Introduction**

As already mentioned, the availability of water is of particular importance in semiarid areas. These environments are characterised by low precipitation and water is a limited resource, which influences vegetation density, cover, and biomass. Knowledge of soil-atmosphere exchange of energy and moisture, as well as crop water requirement, is important for the management of regional water resources. For this purpose, processes have to be identified

that exhibit influence on the hydrological cycle. Actual evapotranspiration ( $ET_a$ ) is often used to determine the water loss from the soil surface (evaporation) and from the growth and temperature regulation process of plants (transpiration). However, measurement of  $ET_a$  is a challenge (Wohlfahrt et al., 2010; Allen et al., 2011; Amatya et al., 2016). There are different possibilities for obtaining accurate estimates of  $ET_a$ ; indirect methods such as residual energy balance, Bowen ratio energy balance, soil water balance (Shi et al., 2008; Wegehenkel et al., 2008; Meissner et al., 2016; Martel et al., 2018), and those that include lysimetry and eddy covariance methods for direct measurements (Wohlfahrt et al., 2010; Fleischer et al., 2015; Gebler et al., 2015). Weighable lysimeters are widely used for  $ET_a$  measurements (Von Unold and Fank, 2008; Schrader et al., 2013; Wegehenkel and Gerke, 2013; Mauder et al., 2017; Oberholzer et al., 2017). Though, for lysimeter measurements a lot of requirements have to be considered (Allen et al., 2011). In summary, soil properties and vegetation cover of the lysimeter must be very similar to the surrounding area. It is usually difficult to reconstruct the original soil profile and to maintain the field conditions of soil and vegetation. Eventually, lysimeter measurements represent only point measurements that will be transferred to large areas. Nevertheless, they remain effective due to the weighing system that enables the derivation of evapotranspiration (ET) from mass records with the highest accuracy compared to the methods mentioned above (Allen et al., 2011).

Furthermore, lysimeter measurements will also be used for calibration and validation of ET models (Makkink, 1957; DehghaniSanij et al., 2004; López-Urrea et al., 2006; Wegehenkel and Gerke, 2013). As water stress become more and more of an important issue, baseline information is required for water resource planning, particularly in arid and semiarid regions. Therefore, the estimation of ET by deterministic models has exponentially increased in recent years. These models built around climate and land surface data, provide reliable ET rates for a reference crop. From the several existing models, the Penman-Monteith FAO-56 (PM FAO) equation is the most used for estimating reference evapotranspiration ( $ET_0$ ). Due to the high demand of data, the PM FAO model proved to be highly accurate (DehghaniSanij et al., 2004; López-Urrea et al., 2006; Sabziparvar and Tabari, 2010; Martel et al., 2018). Nevertheless, the data demand is also a major drawback of the model. For calculation of  $ET_0$  high-resolution, the data that is required is limited in many regions. Large parts of Siberia, for instance, are not covered by meteorological measurement stations. Yet, water resources and ET estimations are relevant for these large areas; especially with regard to climate change, which has a direct impact on the regional hydrological cycle and agriculture (Fraser et al., 2013; Degefi et al., 2014). Moreover, they belong to the region which has the potential to become the 'bread basket' of the world due to the large land and yield reserves (Bagley et al., 2012; Swinnen et al., 2017).

Previous studies conducted in Siberia (Yamazaki et al., 2004; Park et al., 2008; Fleischer et al., 2015), have used land surface models to investigate water and energy exchanges at forests and transition zones. The estimation of ET refers solely to the Bowen ratio method, eddy covariance, and models based on Penman formulations. However, there is an absence of studies based on ET estimation by weighable lysimeter measurements.

An established monitoring network enabled the measurement of  $ET_a$  by weighable gravitation lysimeters in the Kulunda grass steppe of southwest Siberia. On this basis, the study quantifies  $ET_a$  of two lysimeters with different vegetation cover under semiarid conditions. In addition,  $ET_0$  is calculated by using the PM FAO equation (Allen et al., 1998), which was selected due to the crop reference of grass and the independence to the climate type.

The objectives of the study are:

- i. to assess  $ET_a$  as a function of vegetation cover and climatic conditions,
- ii. to compare  $ET_0$  estimates with  $ET_a$  records,
- iii. to assess the PM FAO model for a semiarid environment.

### 3.3 Material and methods

#### 3.3.1 Data preparation and calculation of $ET_a$

The data for the following analysis was collected between 09 June and 30 September 2016 by the monitoring network in the Kulunda steppe described in Chapter 2.3.2.

The processing of the lysimeter data was executed in several steps according to the principle of the adaptive window and adaptive threshold filter (AWAT) developed by Peters et al. (2014) (cf. chapter 2.3.4). The data was smoothed by using an adapted window width. The *Savitzky-Golay* filter (Savitzky and Golay, 1964) was proven as an eligible smoothing routine for the data set. The window width ( $\omega$ ) was set at 5 hours and a polynomial of 3<sup>rd</sup> order was used. The window width was adapted to increasing noises. Third, an adaptive threshold ( $\delta$ ) was applied to obtain  $ET_a$  out of mass data. The setting of threshold was optimised for lysimeter separately. For the arable lysimeter the lower limit for threshold ( $\delta_{min}$ ) was set to 0.04 mm, whereas the upper limit ( $\delta_{max}$ ) was set to 0.7 mm. The threshold values of the pristine steppe lysimeter were increased with  $\delta_{min} = 0.05$  mm and  $\delta_{max} = 0.8$  mm. Inconsistent values of the filter output were corrected manually. Finally,  $ET_a$  was calculated according to Eq. 2.

For lysimeter readings of  $ET_a$ , the pristine steppe lysimeter was considered as a reference since the canopy of the lysimeter corresponded to the surrounding field.

### 3.3.2 Estimation of $ET_0$ by using the PM FAO model

The measurements of  $ET_a$  by lysimeters were compared with  $ET_0$  calculated by the PM FAO equation according to Allen et al. (1998). The Penman-based models are widely used in virtually any climate type. The recommended FAO version has proven as a highly accurate model for calculating  $ET_0$  if the required meteorological input parameters are available. The approach assumes a surface of a uniform and actively growing grass vegetation without water stress, an approximate height of 0.12 m, a daily surface resistance of  $70 \text{ s m}^{-1}$ , and an albedo of 0.23. In connection with the original Penman-Monteith equation (Monteith, 1965) the final form is as follows:

$$ET_0 = \frac{408\Delta(R_n - G) + \gamma \frac{900}{T + 273} u_2 (e_s - e_a)}{\Delta + \gamma(1 + 0.34 u_2)}, \quad (8)$$

where  $ET_0$  is the reference evapotranspiration [ $\text{mm d}^{-1}$ ],  $R_n$  the net radiation [ $\text{MJ m}^{-2} \text{ d}^{-1}$ ],  $G$  the soil heat flux density [ $\text{MJ m}^{-2} \text{ d}^{-1}$ ],  $T$  the mean daily air temperature [ $^{\circ}\text{C}$ ],  $u_2$  the mean daily wind speed at 2 m height [ $\text{m s}^{-1}$ ],  $e_s$  the saturation vapour pressure [ $\text{kPa}$ ],  $e_a$  the actual vapour pressure [ $\text{kPa}$ ],  $\Delta$  the slope vapour pressure curve [ $\text{kPa } ^{\circ}\text{C}^{-1}$ ], and  $\gamma$  the psychrometric constant [ $\text{kPa } ^{\circ}\text{C}^{-1}$ ] (Allen et al. 1998).

The calculation of daily  $ET_0$  values was conducted by using R software. The R software package '*Evapotranspiration*' included different models to estimate  $ET_a$ ,  $ET_0$  and potential evapotranspiration ( $ET_p$ ) (Guo et al., 2016). For the modelling, PM FAO required information about daily minimum and maximum temperature, incoming solar radiation, and wind speed as well as minimum and maximum relative humidity. The data was taken from the weather station of the monitoring network. Hourly data was manually calculated according to Eq. 8. In order to assess the model results related to the  $ET_a$  records the correlation of Pearson ( $r$ ), the root mean square error (RMSE, Eq. 6), and the mean absolute error (MAE, Eq. 5) were used. In addition, the ratio of  $ET_a$  to  $ET_0$  delivers information about the water supply of the soil for a grass vegetation with an height of 0.12 m. The daily  $ET_a$  record divided by  $ET_0$  estimate resulted in an index varying between 0 and 1. The water availability is high (moist) by an index of 1, i.e. there is no climatic risk of non-water supply (Louzada et al., 2018). Optimal water availability goes along with an index between 0.8 and 1. An index of  $<0.8$  indicates a water deficit where only  $<80\%$  of  $ET_0$  will be satisfied (Roth et al., 2005).

### 3.4 Results and discussion

Within the measuring period of 115 days, the total sum of  $ET_0$  was considerably higher than  $ET_a$  of the lysimeters, +157.8% for ruderal vegetation (LYS 1) and +41.3% for pristine steppe (LYS 2). The minimum of  $ET_a$  was 205 mm measured by LYS 1, which was 45.2% less than  $ET_a$  measured by LYS 2 (374.1 mm). A maximum of  $ET_0$  was calculated by 528.6 mm. As the theoretical maximum estimate by  $ET_0$  was not reached, it is assumed that  $ET_a$  was limited by water and not by energy. Table 6 lists the monthly  $ET_a$  and  $ET_0$  records of June – September 2016. The maximum  $ET_a$  was achieved in July as well as the slightest deviation (-31%) between both lysimeters. The largest deviation was in June with -66.4%.  $ET_0$  differs on average +235.5% (ruderal vegetation) and +163% (pristine steppe) per month, respectively.

**Table 6:** Monthly  $ET_a$  records of the lysimeters and  $ET_0$  estimates calculated by PM FAO model. The data are based on daily mean values.

Month	$ET_a$		$ET_0$
	LYS 1 - ruderal vegetation	LYS 2 - pristine steppe	PM FAO
	[mm month <sup>-1</sup> ]	[mm month <sup>-1</sup> ]	[mm month <sup>-1</sup> ]
Jun <sup>1</sup>	34.8	103.7	125.8
Jul	88.5	128.3	145.2
Aug	56.4	100.2	142.4
Sep	25.3	41.8	115.4

<sup>1</sup>No data from 01 June to 07 June 2016

The daily  $ET_a$  values were within the range of 0.1 to 6.9 mm day<sup>-1</sup>, whereas  $ET_0$  calculated by PM FAO model varied from 2 to 8.3 mm day<sup>-1</sup> (Fig. 7). The medians lay between 1.4 and 4.5 mm day<sup>-1</sup>. The difference between mean  $ET_a$  of the lysimeters and  $ET_0$  is -91.1%. The  $ET_a$  of the ruderal vegetation had the smallest median and yielded the lowest values as well as variation. The median of the  $ET_a$  of the pristine steppe was at 3.3 mm day<sup>-1</sup> and it covered the widest range of values. The minimum and maximum values of  $ET_a$  of the lysimeters were very similar.  $ET_0$  had a maximum value of 8.3 mm day<sup>-1</sup> with a maximum difference of +24.5% (to  $ET_a$  of the ruderal vegetation), and a mean difference of +20.7% (to maximum  $ET_a$  of both lysimeters). The absolute deviation was greatest with 7 mm day<sup>-1</sup> between  $ET_a$  of the ruderal vegetation and  $ET_0$ , which corresponds to a difference of -556.3%.

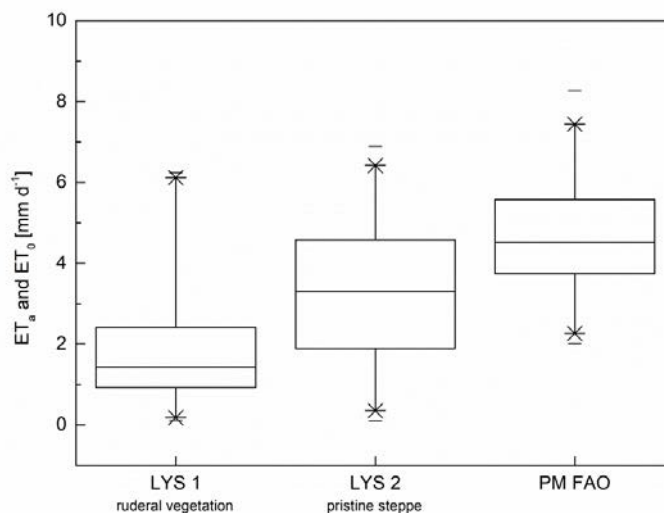


**Figure 7:** Comparison of  $ET_a$  measured by lysimeters and  $ET_0$  computed by the PM FAO model. The box plots are based on daily data. The box boundaries represent the 25th and 75th percentiles, the inner lines indicate the medians, the whiskers extend to 1.5 times the interquartile range, the crosses mark the 1st and 99th percentiles, and the strokes show the minimum and maximum values.

In general, daily  $ET_a$  and daily values of solar radiation and air temperature were positively correlated (Tab. 7). Therefore, the energy was the leading factor for  $ET_a$  at the study site. In contrast to observations of other studies in which factors such as relative humidity and wind speed removed water vapour from the vegetation surface (Priestley and Taylor, 1972; Shi et al., 2008; Yang et al., 2014) their low correlation indicated no relationship. The negative correlation with wind speed was noticeable, but similar results were found in previous studies with arid and semiarid site conditions (El Bably, 2003; Martel et al., 2018)

**Table 7:** Pearson correlation coefficients ( $r$ ) between  $ET_a$  of the lysimeters and meteorological parameters.

Lysimeter	Meteorological parameter			
	Solar radiation	Air temperature	Relative humidity	Wind speed
LYS 1	0.41**	0.45**	0.46**	-0.17
LYS 2	0.80**	0.69**	0.18*	-0.13

\* $p < 0.05$

\*\* $p < 0.01$

Daily  $ET_a$  rates between lysimeters and  $ET_0$  illustrated largely negative differences (Fig. 8). LYS 1 recorded up to  $5.2 \text{ mm day}^{-1}$  (14/06/2016) less than LYS 2 (Fig. 8a). The fluctuations were high in June and became lower from August. This may have been caused by the diversity of vegetation. LYS 2 exhibited a high and dense layer of grass, which has induced  $ET_a$  and interception. On the other hand, LYS 1 was fallow in June. Hence, evaporation was the exclusive process at LYS 1, as a result of the lack of vegetation. From July a convergence of  $ET_a$  of LYS 1 to  $ET_a$  of LYS 2 was observed based on the development of ruderal vegetation and the additional transpiration term at LYS 1. The conditions of LYS 1 were also reflected in the high fluctuation between  $ET_a$  of the ruderal vegetation and  $ET_0$  during the whole period (Fig. 8b). The discrepancies between observed and calculated data were high with an average of  $-3.2 \text{ mm day}^{-1}$ , except for July where the deviations became lower with a mean of  $-1.8 \text{ mm day}^{-1}$ .  $ET_a$  of the pristine steppe demonstrated minor deviations to  $ET_0$  between June and August, and account for several days where  $ET_a = ET_0$  (Fig. 8c). It was found that  $ET_a$  repeatedly exceeded  $ET_0$  with amounts up to  $+0.8 \text{ mm day}^{-1}$  (13/07/2016), in which  $ET_a$  of the pristine steppe tended more frequently to exceed  $ET_0$ .

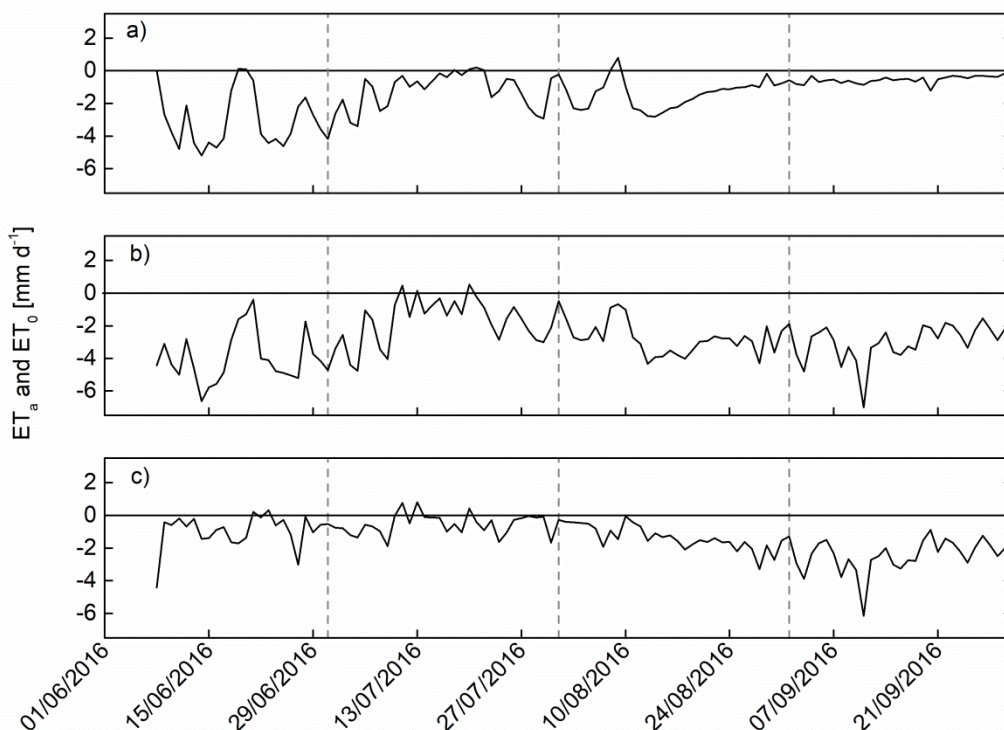


**Figure 8:** Daily differences of ET between 08 June and 30 September 2016; a)  $ET_a$  of ruderal vegetation –  $ET_a$  of pristine steppe, b)  $ET_a$  of ruderal vegetation –  $ET_0$ , c)  $ET_a$  of pristine steppe -  $ET_0$ .

The results of the statistical analyses showed a low correlation between  $ET_a$  of the ruderal vegetation and  $ET_0$  (Fig. 9). In addition to the high values of RMSE and MAE, the model can be assessed with poor quality for LYS 1. The PM FAO assumes an extensive surface canopy that completely covers the ground. However, the ruderal vegetation at LYS 1 did not comply with these conditions over the investigated period.  $ET_a$  of the pristine steppe and  $ET_0$  were strongly correlated. The RMSE with 1.7 mm and MAE with 1.4 mm presented a significant performance, with a tendency to overestimation. Nevertheless, due to the dense and high steppe grass at LYS 2, the transpiration term may be larger than the model assumed. This assumption is justified by Roth et al. (2005) who pointed that the water consumption of a full developed vegetation cover may lead to an underestimation of  $ET_0$ . Similar results were also found by other studies (Wegehenkel and Gerke, 2013; Gebler et al., 2015). Indeed, a further and more widespread explanation for  $ET_a > ET_0$  is the oasis effect. It occurs if conditions of vegetation and atmosphere of the lysimeters differ to those of the surrounding area. In actual fact, LYS 2 had to be preventing the oasis effect by reason of the same vegetation cover. Yet, LYS 1 was fallow; therefore, different soil water availability between the surrounding area and LYS 1 has to be considered. On the other hand, there is also the possibility that  $ET_a$  was overestimated by the pristine steppe vegetation. If the canopy of the lysimeter exceeds the rim, the effective area of the lysimeter can be larger than the original lysimeter extent. This bloom effect leads to higher radiation absorption of the vegetation, which eventually results in increased  $ET_a$  (Allen et al., 2011). The bloom condition can be excluded at LYS 1 because the vegetation is not tall and dense enough to exceed the lysimeter. There is a low likelihood that the oasis effect, as well as the bloom effect, occurs at both lysimeters at the same time. Thus, they cannot be responsible for  $ET_a > ET_0$  in this case.

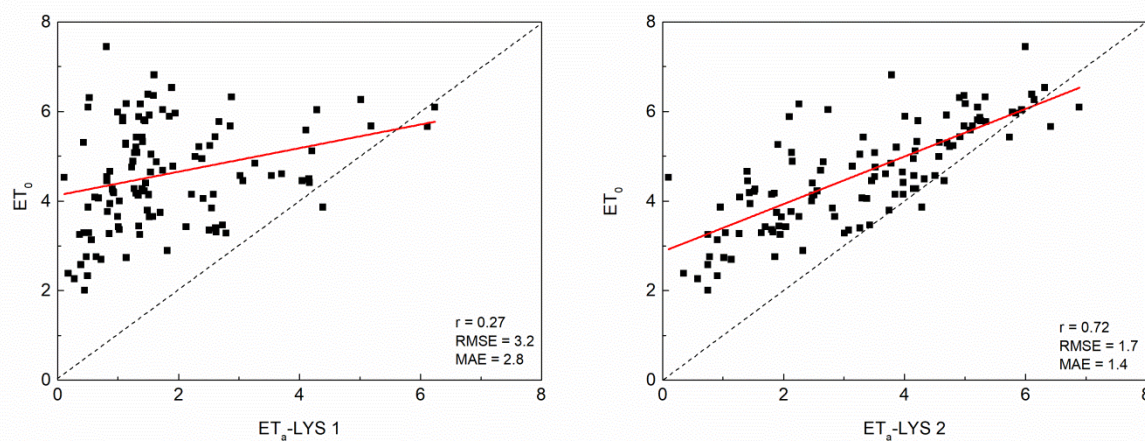


**Figure 9:** The relationship between  $ET_a$  and  $ET_0$  on a daily basis ( $n=115$ ), and the respective error values.

Figure 10 illustrates the daily water availability for the lysimeters. In June, the mean soil water availability index was at 0.3 for LYS 1 and at 0.8 for LYS 2. Thus, the pristine steppe showed an optimal water supply, whereas only 30% of the potential water demand was available for soil and the ruderal vegetation of LYS 1. However, the values for the ruderal vegetation should be treated with caution since it has already been demonstrated that the model quality was poor for LYS 1. Thus, the lower index of the ruderal vegetation in June was less related to the soil water availability. Frequent P caused a rise in water availability in July; consequently,  $ET_a$  is increased (Wever et al., 2002; Armstrong et al., 2008). On some days the water availability crossed the 100% threshold ( $ET_a/ET_0 = 1$ ), which follows from  $ET_a > ET_0$  (cf. Fig. 8b, 8c). A connection was found between  $ET_a > ET_0$  and P events with cumulative amounts of  $>20$  mm occurring a few days before. Between 09 and 11 July, for instance, a total rainfall of 30.9 mm was measured by TB. Within two days the water availability indices rose from 0.3 (ruderal vegetation) and 0.7 (pristine steppe) to 1.1, respectively. However, the virtual absence of P led to a decrease of  $ET_a$  from August to September. During this period only 30 to 50% of  $ET_0$  could be covered by  $ET_a$ . Due to the water stress, the deviations from observed data have increased. Hence, the PM FAO model overestimated  $ET_0$  and indicated that the quality is strongly influenced by water availability. The PM FAO model is more suitable for short vegetation with permanent high water supply. As the growth stage constitutes an essential part within the  $ET_a$  process, the crop evapotranspiration may be a more appropriate approach because the crop canopy and aerodynamic resistance will be adapted to the reference crop. Though, the response to water stress cannot be reproduced since the method does not process information about soil water content. The issue of  $ET_a > ET_0$  suggests that the calculated  $ET_0$  reflects insufficiently the real water consumption of the vegetation (Roth et al., 2005). In such a case, plant-specific correction factors are necessary to derive  $ET_a$  from  $ET_0$ . In this circumstance it again proves that lysimeter measurements are qualified to improve model estimations (irrespective of model assumptions) because they provide reliable field data.

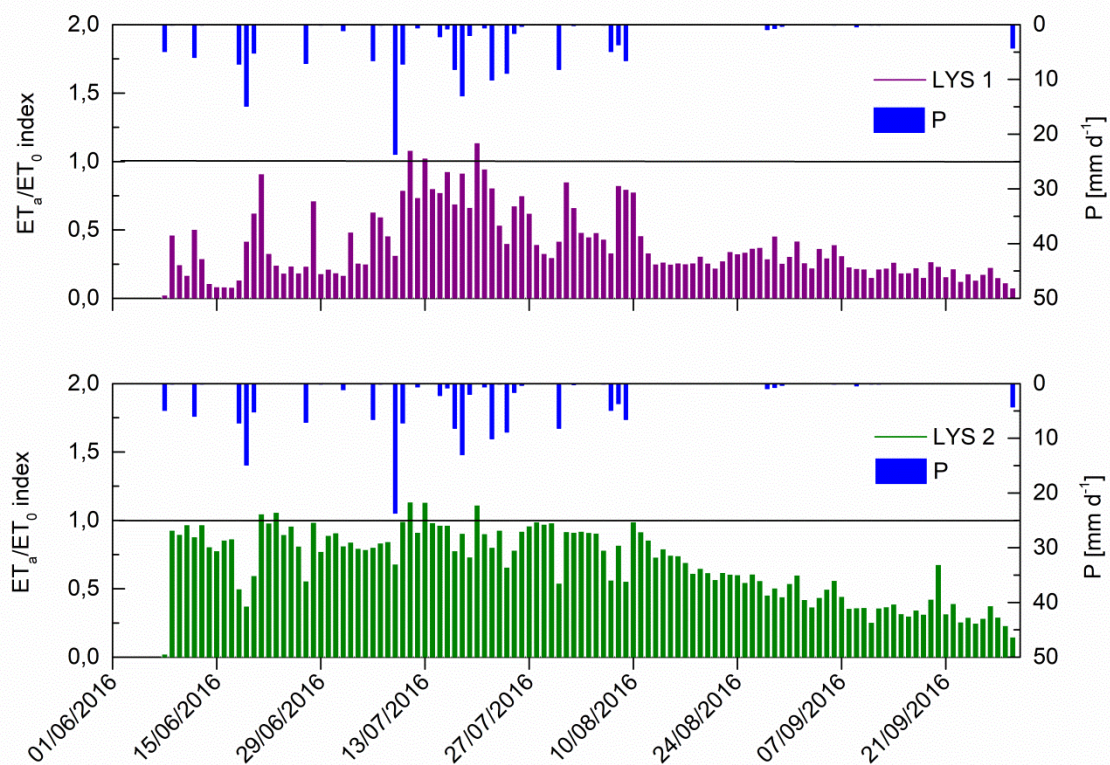


**Figure 10:** Illustration of the daily water availability between June and September 2016. The  $ET_a/ET_0$  indices are related to the left axis; the upper bars are related to the right axis and show the daily sum of  $P$  measured by a tipping bucket rain gauge.

## **4 Determination of soil water balance parameters in the dry steppe of southwest Siberia**

This chapter based on the published text book chapter: *Meissner, R., Rupp, H., Haselow, L., 2020. Use of lysimeters for monitoring soil water balance parameters and nutrient leaching. In: Prasad, M.N.V., Pietrzykowski, M. (Eds.), Climate Change and Soil Interactions. Elsevier, Amsterdam, pp. 171-205.*

### **4.1 Introduction**

As stated above, precise quantification of soil water balance parameters is a challenge. Its determination is beside scientific question and a practical issue, e.g. for sustainable management of water, agriculture, and forestry (Meissner et al., 2010). A selection of methods is already presented. However, no standard method is available for measuring the soil water balance. The decision finally depends on scientific objective, effort, accuracy, maintenance time, and financial budget.

In recent years, the use of lysimetry as direct method to quantify water fluxes has increased (cf. Chapter 1.2). The range of lysimeter types provides numerous opportunities to get environmental data at different scales and with high resolution. In general, the lysimeter types could be distinguished in the following ways:

- soil filling procedure (disturbed-undisturbed)
- weighability (weighable or non-weighable)
- lysimeter size (depends on scientific question and scale of observation)
- lower boundary conditions (free drainage or tension-controlled drainage)

The application of lysimeters is already popular in Europe, but this study used the method to determine the soil water balance parameters in southwest Siberia for the first time. For this purpose, free drainage weighable lysimeters were used which were filled by undisturbed soils. As measurements by lysimeters are under the influence of soil, vegetation and local climate, a comparative analysis was conducted where the two available lysimeters were filled by soil columns with different properties. This enabled a comparison between the land management practices and its impact on the soil water balance components.

### **4.2 Material and methods**

On the basis of the monitoring network in the Kulunda steppe (cf. Chapter 2.3.2) the collected data of the period 01 July to 31 August 2015 are used for this study. Within the

period, the lysimeter filled by an arable soil (LYS 1) was cultivated by summer wheat, whereas the lysimeter that contained the untreated soil (LYS 2) was characterised by pristine steppe grass (cf. Chapter 2.3.3). The properties of the lysimeters can be gathered from Table 8.

**Table 8:** Properties of the extracted soils for lysimeter usage (modified according to Meissner et al., 2017).

	LYS 1				LYS 2			
Usage	Field/Summer wheat				Natural steppe vegetation			
Tillage	Conventional tillage				No tillage for decades			
Soil type	Calcic Chernozem				Calcic Chernozem			
Lower boundary (cm)	25	50	70	120+	30	45	70	110+
Grain size fraction	Uls	Uls	Lu	SI4	Uls	Lu	SI4	SI4

## 4.3 Results and discussion

### 4.3.1 Precipitation and actual evapotranspiration

Using the lysimeter mass of July and August 2015 (Fig. 11),  $P$  and  $ET_a$  could be calculated according to Eq. 2. Within 62 observation days, total  $P$  of 114.6 mm and 125.7 mm was measured by the lysimeters. LYS 1 detected 9.7% less than LYS 2. This is caused by different vegetation cover. The summer wheat favours interception which is part of the precipitation term. Although it can be assumed that  $ET_a$  and  $P$  cannot take place within the same time interval, the large leaf surface of the crop intercepts a part of the  $P$  amount before it is evaporated from the leaf. Though, interception is a process that could not be determined which may lead to a reduction of the daily amount of rainfall. Another influencing parameter is dew which however caused an overestimation of  $P$ . Chapter 2 pointed out the high precision of  $P$  measurements by lysimeters, but it has also been shown that dew can be detected by weighable lysimeters (Meissner et al., 2007; Xiao et al., 2009; Groh et al., 2018). As dew formation is accompanied by a mass increase, it is regarded as  $P$ . Its formation is dependent on leaf shape and, in particular, predestined for grass. Thus, it can be assumed that a higher dew amount has contributed to the  $P$  measured by LYS 2.

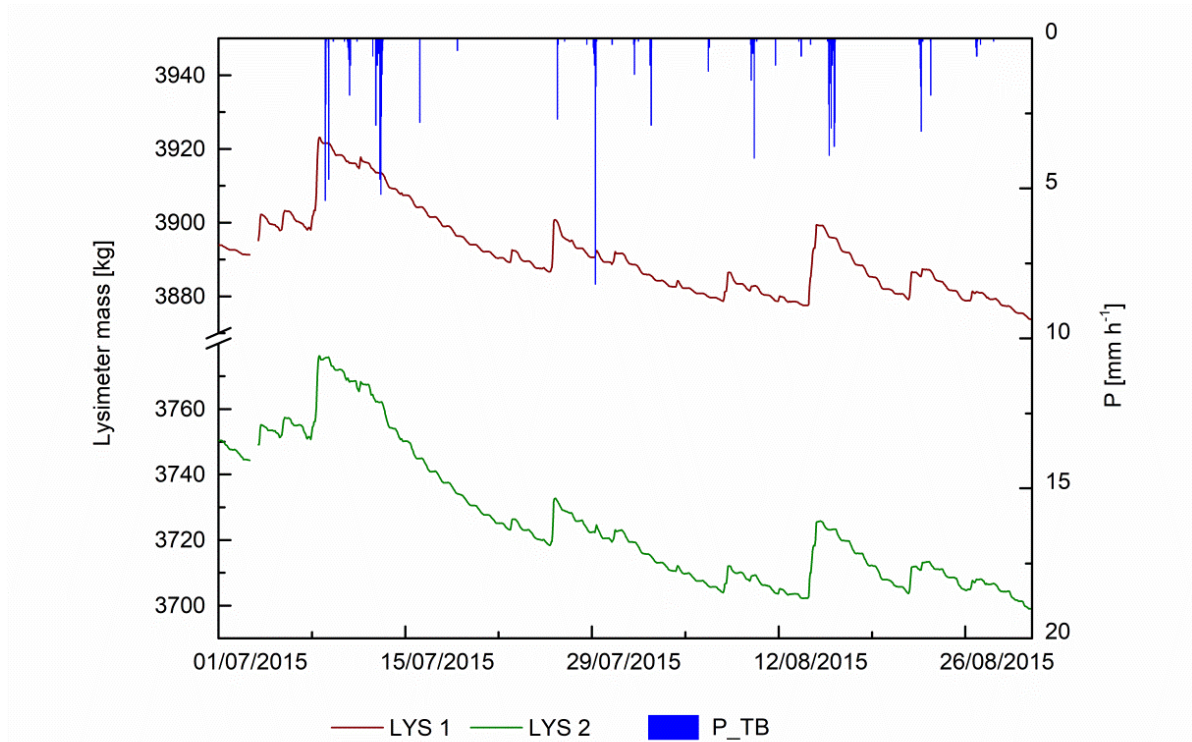


**Figure 11:** The lysimeter mass between 01 July and 31 August 2015. P was measured by a tipping bucket (TB) mounted next to the lysimeters. Note that there are no data measurements for 03 July 2015.

As no seepage water was recorded, the decreases in lysimeter mass were solely caused by  $ET_a$ . Therefore, its amount could be quantified to 140.3 mm and 184.4 mm, respectively. This means that 22.4% and 62.1% more water evaporated than provided by P. The mean  $ET_a$  was  $2.3 \text{ mm day}^{-1}$  (LYS 1) and  $3 \text{ mm day}^{-1}$  (LYS 2), and amounted to a maximum of  $4.9 \text{ mm day}^{-1}$  and  $8.1 \text{ mm day}^{-1}$ , respectively. The lower  $ET_a$  rates of LYS 1 were also caused by the wheat which is able to regulate its transpiration process to reduce  $ET_a$ . The transpiration rate is controlled by stomatal factors. Under water stress, stomatal density, stomatal length, and stomatal aperture will be affected. The low soil moisture leads to a low stomatal conductance, which in turn decreases the transpiration rate (Changhei et al., 2010).

For a more detailed view, Figure 12 illustrates the processes during the course of the day 11 July 2015. There was a slight increase in the lysimeter mass between 02:00 a.m. and 07:00 a.m. There was no P, the temperature was close to the dew point temperature, and the air humidity was 76% on average. Although the meteorological parameters were measured at a height of 2.3 m it can be assumed that the temperature reached the dew point temperature and the high air humidity led to a condensation of the water vapour at ground level. Therefore, there was dew formation which was measured by the lysimeters with an amount of 0.03 mm (LYS 1) and 0.2 mm (LYS 2), respectively. The lysimeter mass began to

drop two hours after sunrise at 07:00 a.m. The solar radiation, increasing temperatures, and decreasing humidity have led to  $ET_a$ . The daily values were by 2.8 mm at LYS 1 and by 4.1 mm at LYS 2. In the afternoon, P occurred with an amount of 2.8 mm measured by TB and with 3.1 mm measured by the lysimeters. The reasons for the differences were already discussed (cf. Chapter 2.4.1). From 09:00 p.m. the reoccurred  $ET_a$  stagnated due to the missing radiation. The increasing air humidity induced a low dew formation at both lysimeters directly after sunset at 10:00 p.m. From then the lysimeter mass remained steady.

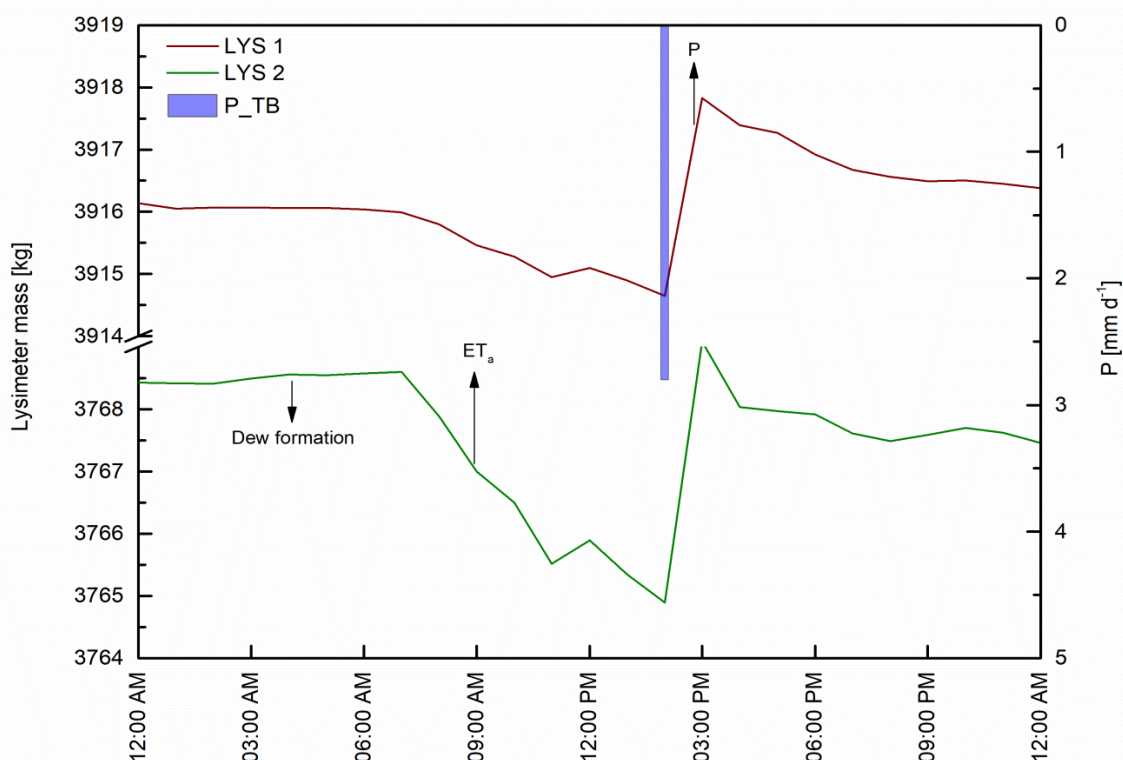


**Figure 12:** The lysimeter mass and precipitation during 11 July 2015.

#### 4.3.2 Soil moisture

Analysis of the soil moisture showed a high fluctuation dependent on P in the topsoil of LYS 1 (Fig. 13). An increase in soil moisture was mostly detected at the beginning of July. As the sowing usually takes place in May, it is assumed that the crop was not yet fully developed at that time. Thus, more rainfall reached the ground and seeped in the soil. The high P event mid-August showed no significant impact on soil moisture because the part of the interception was considerably higher due to the current fully developed vegetation cover.

Furthermore,  $ET_a$  rates were relatively high for the next days as the temperatures rose to over 30 °C. Nevertheless, the soil moisture decreased with increasing depth. The mean moisture content was by 21.8 Vol.-% in 30 cm depth and dropped to 12.9 Vol.-% in 120 cm depth. This circumstance resulted essentially from the agricultural use. Due to the larger and better-branched root system of the summer wheat, there was a high percentage of macropores which contributing to an increased infiltration capacity. However, the soil is not able to retain water for an extended period of time. In contrast, LYS 2 showed no significant effects on soil moisture after P. As an increase of  $ET_a$  could be observed after rainfall, the water has been directly available for evaporation without percolating to the soil. The mean soil moisture content of the topsoil was by 18.3 Vol.-% which increased to 23.8 Vol.-% in the subsoil. The low fluctuation and soil moisture in the topsoil indicated a dry and densely packed soil with a low infiltration capacity. The higher soil moisture content in the depth of 120 cm is probably caused by the water reserves of the snow during the winter. This instance proves that the soil has stored more water that however was continuously reduced by  $ET_a$  during summer. Finally, it can be assumed that the soil is more resistant to droughts because the water is available for the vegetation during dry periods.

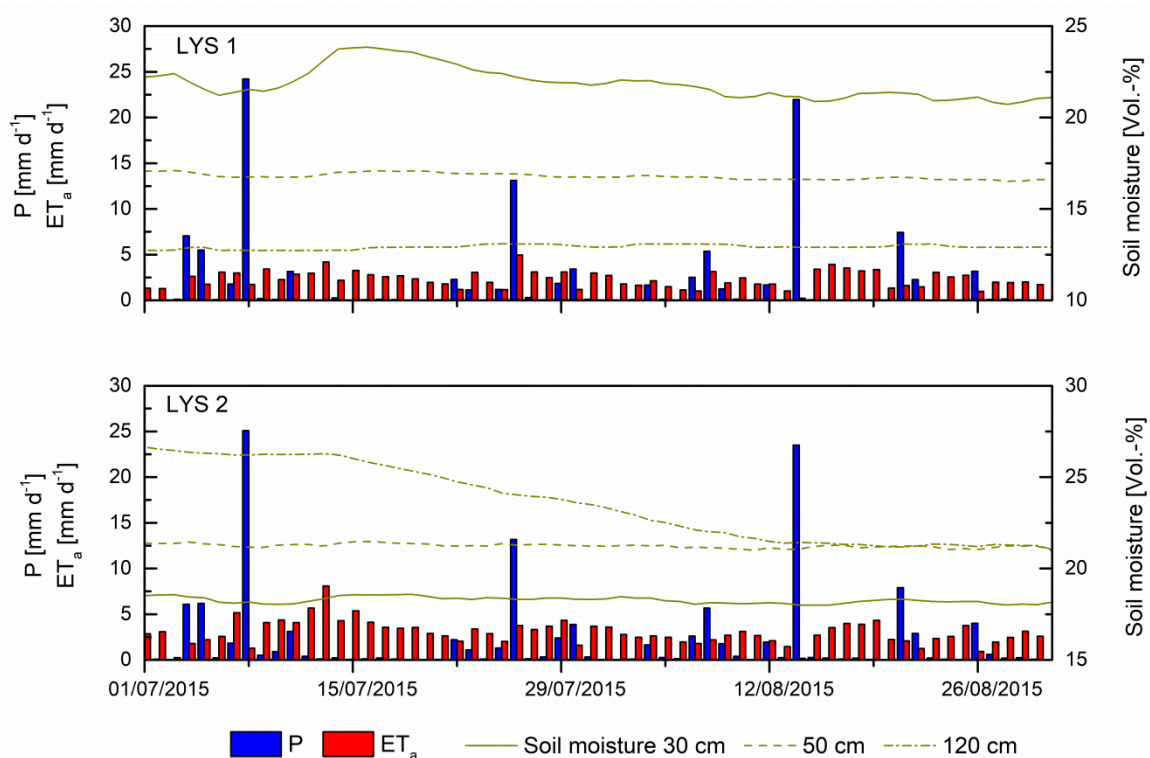


**Figure 13:** Soil moisture, P, and  $ET_a$  measured by the lysimeters.

#### 4.4 Conclusions

The application of weighable gravitation lysimeters has proven successful to determine components of the soil water balance. Due to the high precision weighing system and its property reflecting natural conditions, lysimeters enable reliable records of water input and output. However, the vegetation showed significant influence on measurements of P and  $ET_a$ . While interception leads to an underestimation of P,  $ET_a$  was affected by physiological processes of the crop. In addition to atmospheric conditions and soil water content,  $ET_a$  is also dependent on the leaf surface. As the summer wheat has a large leaf surface,  $ET_a$  rates have to be higher compared to those of grass. Though, wheat is able to prevent high water loss by  $ET_a$  due to plant physiological reasons. Nevertheless, the water balance of both soils was negative and the soil moisture decreased with advanced dry period.

## **5 Research study on the soil water balance in the steppe of Kazakhstan**

This chapter based on the published paper: *Haselow, L., Rupp, H., Akshalov, K., Meißner, R., 2020. Research study on the soil water balance in the steppe of Kazakhstan. WasserWirtschaft 110, 34-40. (in German)*

### **5.1 Abstract**

The following study presents the implementation of a monitoring network in the steppe of Kazakhstan. The objective is to improve the effectiveness of water usage of the dry steppe soils by adapted soil management. The focus will be on the soil water balance determined by meteorological and pedo-hydrological in situ measurements. Moreover,  $ET_a$  will be investigated for the first time by weighable gravitation lysimeters over the whole year for this climate. For comparative analysis, there are two lysimeters whose soils stem from different sites. While the first lysimeter vessel was monolithically filled with an arable soil, the second lysimeter vessel contains a pristine steppe soil. The measurements started immediately after installation. Results of  $ET_a$ , P, and soil moisture will be presented for the first year from October 2018 to October 2019. As the measurements during winter are of particular importance, lysimeter data, as well as meteorological data, will be illustrated during the first snowfall.

### **5.2 Introduction**

The arable land of Kazakhstan reaches sizes of 208 million hectares, which has the potential to get to be part of the bread basket of the world. With a share of 89% of grassland (steppe), Kazakhstan is worldwide ranked sixth place. However, agricultural production is low with a dry matter of 0.1-0.4 t ha<sup>-1</sup>. The previous 23 million hectares of arable land is mainly used for the cultivation of summer wheat that has still originated from an initiative of the former Soviet Union of the 1950s. The approximately 42 million hectares of steppe soils were converted to arable land. Today, more than half of the area is part of Kazakhstan. The cultivation of summer wheat in the form of monocropping is predominantly applied intermitting by fallow periods. Nevertheless, the yields are low and unstable (Mueller et al., 2014). Furthermore, the landscape is currently confronted by challenges such as climate change, soil degradation, land-use changes, and rural exodus.

Despite the aforementioned obstacles, the region shows the potential to contribute to the global food crisis due to its natural conditions. The challenge is to create forward-looking strategies that will be finally a gain for ecosystem regeneration as well as sustainable agriculture. On the basis of the results of the studies conducted in the Siberian Kulunda steppe (Fruehauf et al., 2020a), the highly dry and extensive steppes of Kazakhstan will be included into the research context. The focus is also on the development of innovative, sustainable climate-adaptive land use concepts. The previous studies showed the importance of the factor water in the establishment of sustainable management activities. As the region is characterised by the ongoing process of climate change, the sustainable use of the naturally available water resources represents a new priority. There is a current tendency of slightly increased precipitation accompanied by a simultaneous increase in temperature. The impact would be the rapid drying of the soil water as well as yield losses. The effects of adaptive soil management on the availability of soil water and therefore the development of crops have been stated by Meissner et al. (2017). This knowledge based mainly on information about the regional soil water balance. Particularly important is the actual evapotranspiration ( $ET_a$ ), where its amount and course should provide information about the water demand for crops. Direct measurements over a whole year could not be conducted so far for the steppes of southwest Siberia and Kazakhstan. Thus, the major challenge is still the realisation of lysimeter measurements for this climate. Although the winter conditions are the most demanding on the measuring technique, the high snow amounts provide additional water resources. If it will be able to store this water into the soil and to make it available for crop growth, it would contribute considerably to ensuring this site as arable land.

## **5.3 Material and methods**

### **5.3.1 Site description**

The study was conducted in the Kazakh steppe approximately 100 km west of Nur-Sultan (Fig. 14), the capital of Kazakhstan. The lowlands are part of the dry grass steppe at an altitude of 322 m a.s.l. The basis of the local soils is loess, which stems from deposited loam or eolian fine sand. Typical soils are Kastanozems and Chernozems. The continental climate is characterised by hot summers and cold, snowy winters. The mean annual temperature is 2.7 °C. The mean temperature of the coldest month of January is -15.9 °C, whereas the warmest month of July has a mean temperature of +21 °C. Usually, the period without night frost lasts from May to September. From November to March a constant snow cover lasts for 120-150 days with a mean depth of 11-15 cm. The annual precipitation varies between

200 and 400 mm. The potential evapotranspiration is  $600 \text{ mm a}^{-1}$  and up to 3 times higher than the precipitation (Mueller et al., 2014; Mashtayeva et al., 2016).



**Figure 14:** Study area with lysimeter station and extraction sites; the distance between them is around 15 km.

### 5.3.2 The monitoring network

In October 2018, a monitoring network was established at Pervomayka, Kazakhstan ( $51^{\circ}14'13.2''\text{N}$ ,  $70^{\circ}04'12.0''\text{E}$ ). This network consisted of a lysimeter and weather station (manufacturer 'UGT-Muencheberg', Germany). For the lysimeter station (Fig. 15), two soil columns consisting of silty clay and determined as Chernozems (according to the World reference base for soil resources - WRB) were monolithically extracted. The first one stemmed from arable land, which was used for the cultivation of summer wheat at the time of extraction. The second monolith was part of a fallow site, which was covered by pristine steppe vegetation. After filling the lysimeter vessel, a filter layer consisting of quartz sand, coarse sand, and gravel was added at the bottom of the soil columns. The lysimeters were subsequently equipped by measuring sensors and were positioned on three load cells,

respectively, inside the lysimeter station. An exemplary description of the extraction and set-up is given by Balykin et al. (2016).

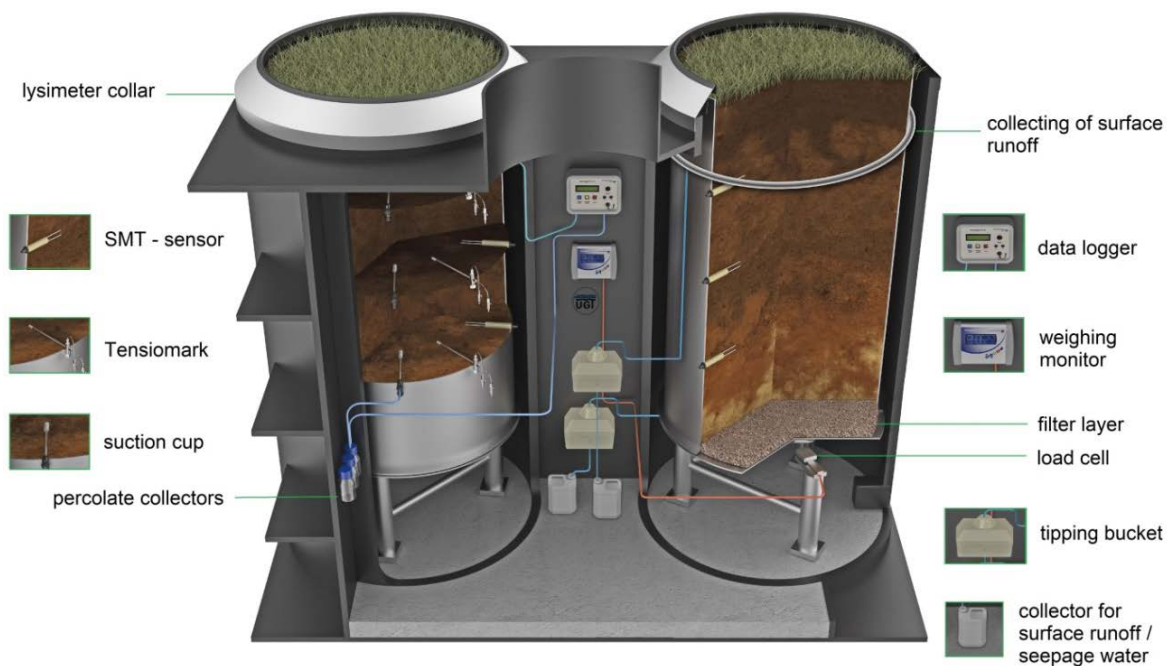


**Figure 15:** Illustration of the containerised lysimeter station including instrumentation.

The lysimeter vessels had a surface of 1 m<sup>2</sup> and a depth of 2 m. The total mass of each lysimeter vessel including the soil was approximately 3900 kg and was measured with an accuracy of  $\pm 20$  g (Xiao et al., 2009). Additional to the mass, which changed by water input (precipitation, dew, rime, and the water equivalent of snow) and water output (actual evapotranspiration, outflow), pedo-hydrological parameters were determined inside the soil monolith. In the depths of 30, 50, and 120 cm soil moisture and soil temperature were measured by SMT-100 probes (Tab. 9). The SMT-100 is a combination of a FDR and a TDR sensor system. Like a TDR, it measures the travel time of an electromagnetic wave signal to determine the dielectric constant of the soil, and like a FDR, it converts this dielectric constant into a measure frequency. It utilises a ring oscillator to transform the signals travel time into the measured frequency. The resulting frequency (>100 MHz) is high enough to operate well in sandy and clayey soils alike. Moreover, the probes are frost resistant and show low disturbance to salinity. The matrix potential was measured by Tensiomark sensors (manufacturer 'ecoTech', Germany), and soil solution was extracted by ceramic suction cups. In the case of outflow, the water was discharged through drainage at the lysimeter bottom, quantified by a tipping bucket, and collected in a storage container. The surface runoff was

measured by a drain fixed between the lysimeter collar and container wall, which channelled the water to an additional tipping bucket (Tab. 9).

**Table 9:** Properties of the soil moisture probe SMT-100 and tipping buckets according to manufacturer's information.

Properties	Lysimeter	SMT-100		Tipping bucket	Tipping bucket	
		Soil moisture	Soil temperature	Surface runoff, outflow	Ground level	1 m height
Measuring range		0 to 60 Vol.-%	-40 to +80 °C		0 ... 11 mm min <sup>-1</sup>	0 ... 1.6 mm min <sup>-1</sup>
Accuracy	±0.0005%	±3 Vol.-%	±0.2 °C	±1%		
Resolution	0.02 mm	0.1 Vol.-%	0.01 °C		0.1 mm	0.2 mm
Collecting area	10,000 cm <sup>2</sup>				200 cm <sup>2</sup>	200 cm <sup>2</sup>
Flow				5 mm min <sup>-1</sup>		
Volume of tipping tray				0.1 mm		

With a distance of 1.5 m, respectively, three tipping bucket rain gauges were mounted around the lysimeter station to measure the precipitation at ground level. With a distance of 3 m, a weather station and an additional tipping bucket rain gauge at the standard height of 1 m were installed. Besides the precipitation meteorological parameters such as air temperature, air humidity, air pressure, wind direction, wind speed, and global radiation were measured at a height of 2 m. A camera mounted opposite enabled visual access to the network. Finally, all data of the lysimeter and weather station was measured with a temporal resolution of 10 min and was consolidated and stored in the respective data logger.

### 5.3.3 Measuring strategy

As has been demonstrated earlier, the lysimeter studies conducted in the Kulunda steppe in southwest Siberia were only able to generate reliable and plausible weighing data during summer periods. The measurements during winter were the biggest challenge until now. If the temperature dropped down to the freezing point and snowfall occurred, the values became implausible. Although both lysimeters of the previous network were equipped by a snow cutting system powered by threaded rods, no reliable operation of the lysimeters could

be observed. Due to the development of snow bridges between the lysimeter container and the lysimeter collar, the free alignment of the lysimeter above the load cells were influenced. In order to simulate the climatic conditions, a lysimeter model was established in an indoor ski hall. Therefore, it could be investigated how snow and frost lead to scab and icing which finally affect the weighing. The results should be the basis for experiments with different technical opportunities to prevent the freezing of the lysimeter collar and the development of snow bridges.

#### **5.4 Results and discussion**

The measurement campaign started with the installation of the measuring network on 23 October 2018. Figure 16 shows the lysimeter mass from 26 October 2018 to 26 October 2019. As no seepage water was recorded during the observation period, it is assumed that a mass increase is precipitation ( $P$ ) and a mass decrease is actual evapotranspiration ( $ET_a$ ). In consequence of unreliable winter measurements, the period between 12 November 2018 and 27 March 2019 was excluded whereby the calculation of the annual soil water balance was again unfeasible. For 229 days, a total  $ET_a$  of 278.5 mm at the arable lysimeter (LYS 1) and 288.7 mm at the pristine steppe lysimeter (LYS 2) was measured, respectively. The difference was caused by the vegetation cover. The steppe lysimeter was covered by grass the whole year. The arable lysimeter, however, was fallow until 18 May 2019. The seeding of summer wheat followed afterward. Thus, LYS 1 was mainly characterised by evaporation until the beginning of summer, whereas the part of transpiration predominated at LYS 2. The precipitation was recorded from the lysimeters as well as the surrounding TB at ground level. The total of the rain gauges was by 167.4 mm, whereas the lysimeters measured 256.2 mm (LYS 1) and 239.9 mm (LYS 2). The difference between the rain gauges and the lysimeters was caused by the different technical resolution (tipping bucket 0.1 mm, lysimeter 0.02 mm), of the one part, and the unavoidable influence of the surrounding farm activities (husks transported by the wind at grain drying) of the other part. The difference of around 16 mm between the lysimeters was only resulted by the infiltrated meltwater during the melting period mid-March 2019. Using the data of soil moisture and surface runoff, the amount of snow was determined and added to the total  $P$  which contributed to the water balance of the lysimeters. In this case, the lacking vegetation cover at LYS 1 led to an increased infiltration rate.

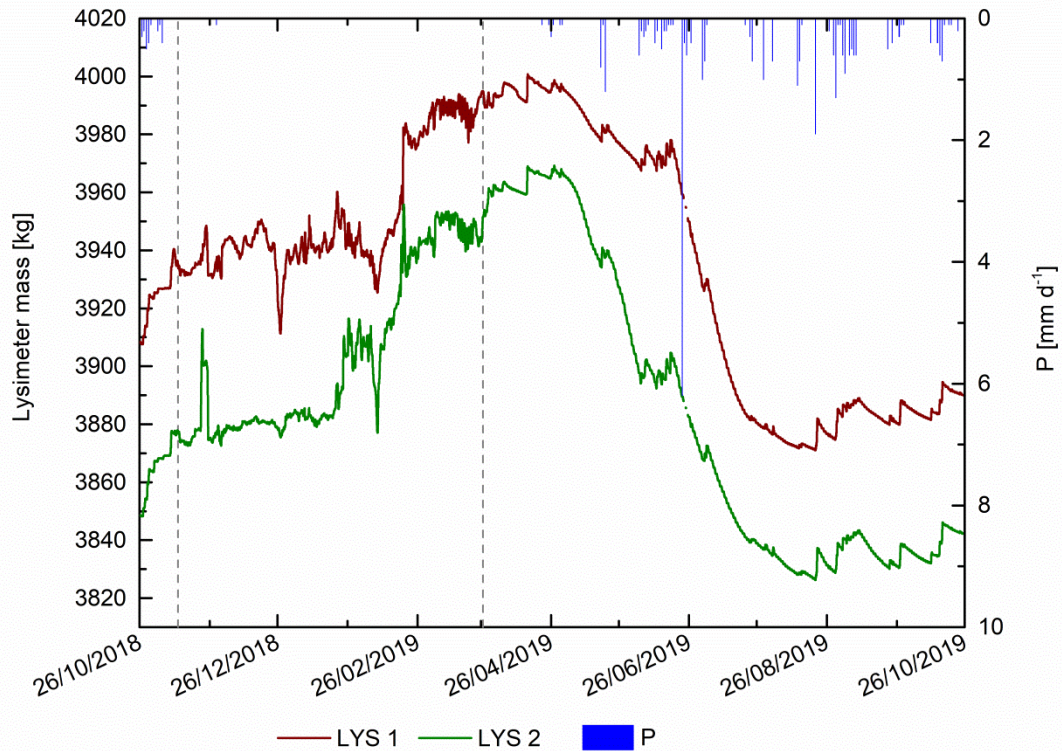


**Figure 16:** Lysimeter mass and precipitation (P) measurements from 26/10/2018 to 26/10/2019. The dashed lines represent the time period excluded from calculations.

The impact of P was also reflected in the soil moisture (Fig. 17). From 30 October 2018, an increase in soil moisture at topsoil (30 cm) was observed at both lysimeters accompanied by the occurrence of snowfall at the beginning of winter. From Mid-November 2018, there was soil frost which led to no registration of reliable soil moisture data. With the thawing of the soil and the opportunity to measure plausible values again, another increase in soil moisture content was recorded caused by the meltwater at the end of March 2019. Due to an identical value of 30 Vol.-% water content at both lysimeters at the beginning of April 2019, the course of soil moisture could be observed depending on lysimeter cover during the vegetation period. An impact of the different soil management became apparent. From April, a rapid decrease in soil moisture was recorded in 30 cm depth at LYS 2, whereas the soil moisture at LYS 1 remained relatively stable over a longer period. With increased height and density of the summer wheat, the  $ET_a$  rate increased from June. Thus, soil moisture decreased. At the topsoil of both lysimeters, a decrease of soil moisture was already observed for July from 30 Vol.-% to 15 Vol.-% (LYS 1) and 13 Vol.-% (LYS 2), respectively. However, the soil moisture simultaneously increased in the depth of 120 cm. At the beginning of April, soil moisture of 15 Vol.-% was measured at LYS 1 and increased to 22 Vol.-% in July. On the other hand, LYS 2 indicated only an increase of 2 Vol.-% (from 12 Vol.-% to 14 Vol.-%).

This was a result of the increased infiltration capacity of the arable soil caused by its soil management and the root system of the summer wheat. The resulting macropores led to faster and higher absorption of water. In contrast, the pristine steppe soil was dry and dense. Thus, less water infiltrated over a longer period.

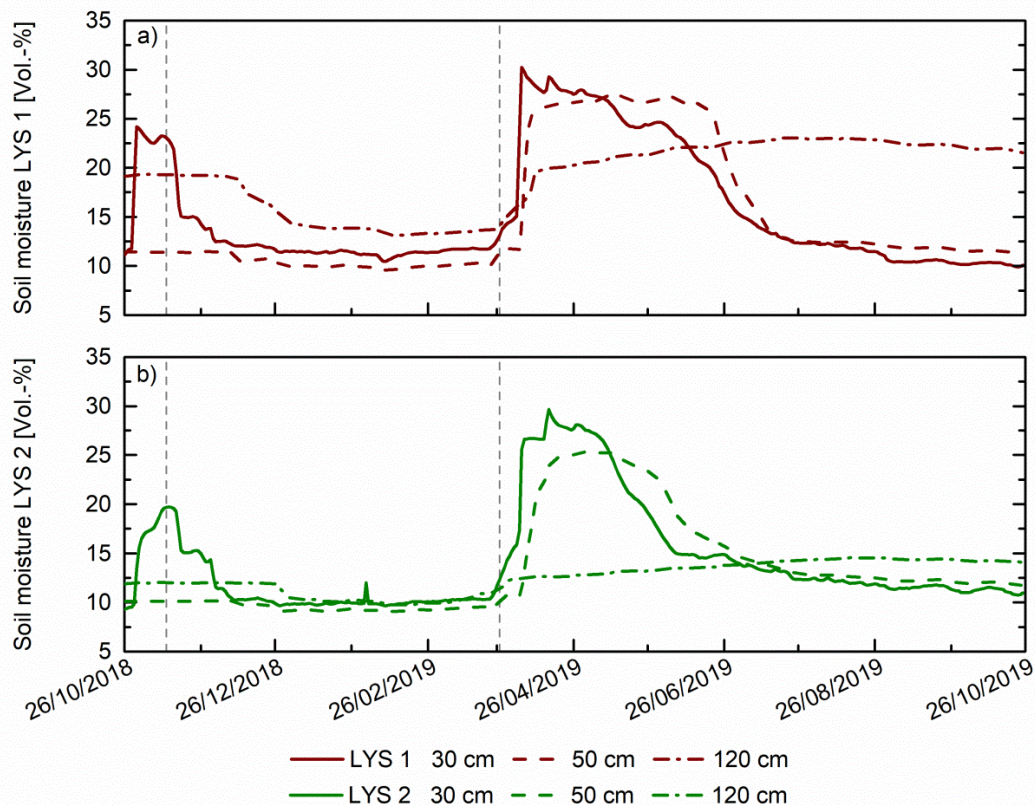


**Figure 17:** The soil moisture for a) LYS 1 and b) LYS 2 from 26/10/2018 to 26/10/2019.

Figure 18 shows the course of the day of 26 October 2018. Both lysimeters exhibited the same development in mass (Fig. 18a). Between midnight and 9:30 a.m., there was a slight mass increase of 0.14 mm, respectively. The rain gauges did not record P, the temperature was around the dew point temperature, and the air humidity showed a mean of 85% (Fig. 18b). It must be noted that the meteorological parameters were measured at a height of 2 m. Therefore, it can be assumed that the temperature at the ground level reached the dew point which led to the condensation of water vapour above the ground surface. As the temperature was below the freezing point, there was soil frost instead of dew formation (Groh et al., 2018), which was confirmed by the camera. With sunrise and the increase in radiation and temperature as well as the decrease in air humidity, the lysimeter mass decreased due to  $ET_a$ . Values of 0.76 mm (LYS 1) and 0.45 mm (LYS 2) were measured between 9:30 a.m. and 7:00 p.m. At sunset around 7:00 p.m., the process of  $ET_a$  stopped due to the missing radiation and the lysimeter mass remained thereafter stable.

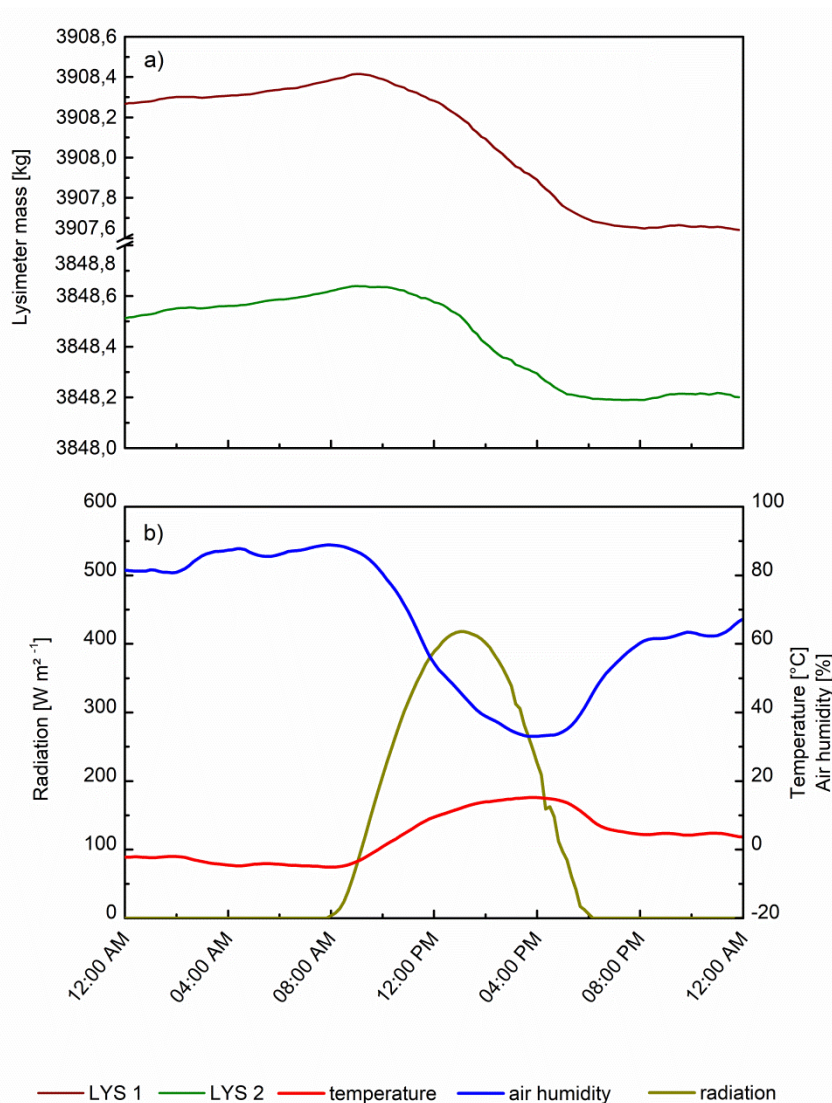


**Figure 18:** The daily course of a) lysimeter mass and b) air temperature, air humidity, and solar radiation for 26/10/2018.

As no current winter measurements exist, the data of lysimeter mass, temperature, and air humidity from 07-10 November 2018 were included for this analysis (Fig. 19). For this period, the rain gauges have recorded no P. However, the lysimeters showed a mass increase of 14 mm (LYS 1) and 7 mm (LYS 2), respectively. Through the camera, snowfall could be confirmed from 08 November. One day later, both lysimeters were already covered by a layer of snow. Despite lacking P data (due to an absent heat function of TB), the temperature and air humidity provided information about potential snowfall. At the time of the mass increase, the temperature was below the freezing point and the air humidity increased above 98%. Within the scope of a study, the probability of snowfall in dependence of temperature and air humidity was investigated for numerous locations of the northern hemisphere (Jennings et al., 2018). A rain-snow threshold was determined which stated that a rainfall

event occurs with a probability of 50% of snow or rainfall at a given temperature. This value is  $>1.2$  °C for Kazakhstan. If the air humidity will be included, the threshold is by  $0.7$  °C at given air humidity between 90 and 100%. Therefore, at temperatures below this threshold P occurs as snow with a probability of  $>75\%$ . On 08 November, the mean temperature was at  $-1$  °C. Thus, the probability of snowfall was at  $>90\%$ . On 09 November, the temperature dropped to  $-20$  °C and the air humidity decreased. It is assumed that the snowfall stopped and the increase in lysimeter mass was caused by the increase in snow density, already collected on the lysimeters. From 09 November, the mass of LYS 2 remained relatively stable, whereas the mass of LYS 1 increased during the course of the day. Using the images of the camera and the meteorological data, there is the presumption of snowdrifts. As LYS 1 lay downwind (wind speeds with up to  $10 \text{ m s}^{-1}$ ), there was an accumulation of snow on the lysimeter.

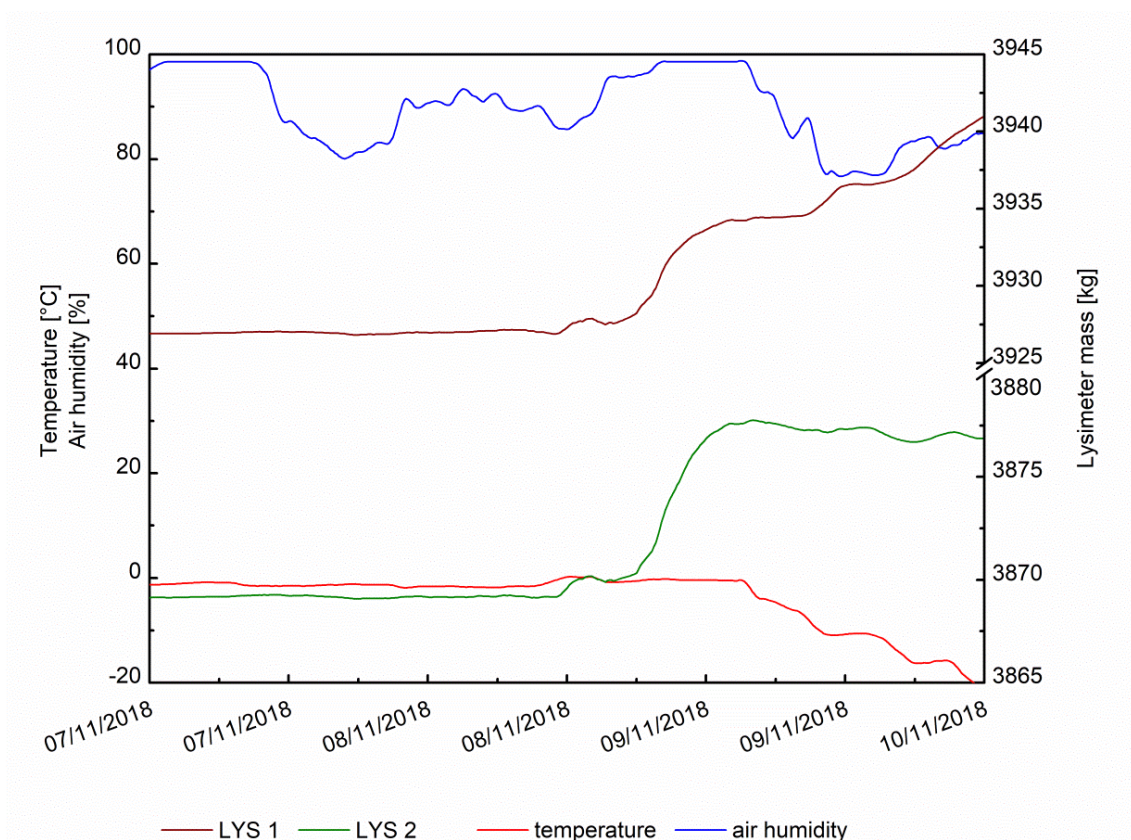


**Figure 19:** Lysimeter mass, air temperatures, and air humidity during the first snowfall between 07/11/2018 and 10/11/2018.

During the first year of the measuring campaign in Kazakhstan, the principal function of the monitoring network could be proved. However, there were also limitations during the winter period. In order to address this issue, an additional technique will be added to the lysimeter station. The modification should hereafter avoid ice bridges and enable successful weighing.

## 6 A novel method for reliable lysimeter measurements under snow and ice conditions?

This chapter based on a manuscript submitted on 22/09/2020 to *European Journal of Soil Science*.

### 6.1 Abstract

Various studies have indicated the challenge to determine the soil water balance by weighable lysimeters during cold and snowy winter periods. It has been shown that low temperatures and high snow amounts affected lysimeter measurements. In the grass steppe of Kazakhstan, a monitoring network consisting, inter alia, of two weighable lysimeters were established where one lysimeter had been additionally equipped with a thermal technology that should prevent freezing effects. Since only one lysimeter was equipped by the technique (LYS-H), the efficiency and the effects can be evaluated compared to those of the non-equipped lysimeter (LYS-N). The results indicated the partly maintaining of the weighing at LYS-H, whereas the measurements of LYS-N became implausible with increasing snow heights. Precipitation was detected with up to 21.8 mm day<sup>-1</sup> (LYS-N) and 14.4 mm day<sup>-1</sup> (LYS-H). On the other side, an evapotranspiration rate of up to 0.6 mm day<sup>-1</sup> was measured at LYS-H, whereas an implausible high rate of 5 mm day<sup>-1</sup> at LYS-N showed the impact of snow and ice which resulted in falsified measurements. However, the technology showed an obvious influence on soil parameters. The thermal function led to an increase in soil temperature and supported the melting process. As a result, a high increase in soil moisture was observed at LYS-H. Finally, the technology falsified the water balance and consequently, the solution had proved to be unsuccessful.

### 6.2 Introduction

The availability of water is particularly important for regions that rely on agriculture. Agriculture in semiarid environments is nowadays affected by high temperatures and low precipitation rates which lead more and more to crop losses. Water as a limited resource has to preserve in soils to make it available for plant production. However, semiarid environments usually have a negative water balance. The water which fills up the water storage of the soil cannot be stored for as long as necessary for effective agriculture. Evapotranspiration as part of the soil water balance is usually the reason for water losses which affects crop growth.

Knowledge of precipitation and evapotranspiration amounts are essential to estimate crop water requirements and therefore for the management of regional water resources. A popular method to determine the soil water balance is lysimetry (Wegehenkel et al., 2008; Meissner et al., 2010; Schrader et al., 2013; Gebler et al., 2015; Mauder et al., 2017). Through weighable lysimeters, the determination of actual evapotranspiration will be enabled by high accuracy compared to methods such as soil water balance, residual energy balance, or Bowen ratio energy balance (Shi et al., 2008; Allen et al., 2011). Furthermore, the balance calculations require information about meteorological parameters. Many regions are not even covered by weather stations, like Russia and Kazakhstan, for instance. However, these regions have a large resource of agricultural land and therefore the potential to become the 'bread basket' of the world (Bagley et al., 2012; Swinnen et al., 2017). Large parts of Siberia were previously investigated regarding evapotranspiration, but preferably by indirect measuring methods (Yamazaki et al., 2004, Park et al., 2008; Fleischer et al., 2015). On the other hand, studies on soil water balance and its parameters conducted in Kazakhstan do not exist, even though it may also be necessary.

Within the study described in Chapter 5, the soil water balance of the local steppe soils should be optimised for a climate-adapted agriculture. For this purpose, the water balance will be determined by a monitoring network established in the semiarid grass steppe of Kazakhstan. The network consisted, inter alia, of two weighable lysimeters which enable the measurement of precipitation, actual evapotranspiration, soil moisture, and outflow. Lysimeter measurements during winter periods are usually assessed as unreliable and highly inaccurate, even though this assessment is dependent on the study site. In general, weighable lysimeters could be used for the determination of snow, dew, and hoar frost (Groh et al., 2018) or sublimation (Herndl et al., 2017). However, for regions that are characterised by low temperatures and high snow amounts, it is difficult to get information about soil water balance parameters since the lysimeter weighing could be affected under cold and snowy conditions. Previous studies showed the effect of snow on the lysimeter weighing (Tarboton, 1994; Seyfried et al., 2001; Gebler et al., 2015; Herndl et al., 2017). Within a study conducted in the southwestern Siberian Kulunda steppe (Bondarovich et al., 2020), it was assumed that as soon as the temperature dropped down below the freezing point and a higher snow amount occurred, ice and snow bridges have developed between the lysimeter vessel and the collar. Thus, the free alignment above the load cells were no longer given, which resulted in unreliable measurements. In this case, the lysimeters were equipped by a circular mechanically driven snow cutter, which should separate the snow on the lysimeter from the adjacent layer of the surrounding. However, the technique failed due to the crusted snow and the ball coupling which popped out when strong crusts of snow were hit. Gebler et

al. (2015) tackled the problem by using a vibration plate that was activated between two measurements. Herndl et al. (2017), on the other hand, developed a method that used interval deflection of the lysimeter vessel to break the snow bridges. The procedure directs the vessel in one direction, whereby a rotationally symmetrical deflection will be achieved due to the 3-point suspension.

As the previous technologies have been based on mechanical separation, the solution of the issue relies on thermal technology in this study. One of two lysimeters was modified to provide flawless functioning and therefore to enable reliable measurements during cold and snowy conditions. The objective of this study is to present the first data for winter measurements in the Kazakh steppe. Moreover, the efficiency of the lysimeter modification and its effects on the determination of the soil water balance parameters precipitation, evapotranspiration, drainage, and soil moisture will be evaluated compared to the results of the non-equipped lysimeter.

## **6.3 Material and methods**

### **6.3.1 Site description and experimental set-up**

This study based on the same lysimeter experiment in the Kazakh steppe described in the chapters 5.3.1 and 5.3.2.

### **6.3.2 Data processing**

Overall, the data of the lysimeter and weather station was tested on outliers and all data during system maintenance was removed. If the resulting gaps did not exceed one hour, the values were estimated by linear interpolation. Data on soil moisture, soil temperature, air temperature, and wind speed was converted to daily mean values. The processing of the lysimeter data was conducted by using R software in the following steps. First, within the time series duplicates of time steps were removed. Additionally, a corrected time series was created for the case of lost time steps. Second, the original time series was compared to the corrected time series and the values were transferred to the new time series. The resulting data gaps were also interpolated when they did not exceed one hour. Third, the data was filtered and smoothed by the method Empirical Mode Decomposition (EMD; Huang et al., 1998). Fourth, within the corrected time series the difference between each pair of consecutive time steps were calculated. Finally, precipitation ( $P$ ) and actual evapotranspiration ( $ET_a$ ) was calculated according to Eq. 2. Due to the geometry of the

vessel mentioned above, a change of mass is equal to a water storage change in millimetres ( $1 \text{ kg} \approx 1 \text{ l m}^{-2} = 1 \text{ mm}$ ). Therefore, all changes in mass are given in millimetres henceforth.

### **6.3.3 Study preparatory to experimental development**

Based on the knowledge gained from the study in the Siberian Kulunda steppe (Bondarovich et al., 2020), a solution has to be developed to prevent the freezing effects at weighable lysimeters and to enable reliable measurements. To get an understanding of these effects, a lysimeter experiment was conducted in a ski hall (Senftenberg, Germany) where the cold and snowy conditions could be imitated. Three scenarios have to be considered and tested. First, snow bridges develop within the snow cover. Its adhesion leads to a measurement of the overall snow cover and not only the snow cover above the lysimeter. Second, the snow bridges develop vertical above the lysimeter collar. Thus, the force will be absorbed by the collar, whereby the weighing should be paused. Third, the space between the lysimeter vessel and collar iced-up. The weighing will be overlapped by the tensions, which would lead to chaotic measurements and possibly large measuring values. For the first assumption, the cutting of the snow around the lysimeter collar should restore the weighing, but it was shown that this procedure had no impact on the weighing. There was only a weak to none response to the test load. In the second scenario, the snow was removed until the collar was no longer covered by it. It could be observed as a correct and immediate response to the test load. Concerning scenario 3, no freezing between the lysimeter vessel and collar was observed. This knowledge gained was subsequently included in the development of technology.

### **6.3.4 Applied technology**

On 20 November 2019, the steppe lysimeter was equipped with a fence that was wrapped by several heating wires (Fig. 20). The fence was implemented above the soil surface, directly adjacent to the lysimeter collar. The total height of the fence was 24 cm and there were four heating wire windings at the heights of 0, 4, 8, and 16 cm. The fence automatically starts to heat at an air temperature of +3 °C. This should keep free the space between the collar and the vessel and separate additionally the snow cover on the lysimeter from those of the surrounding.

For the sake of simplicity, the lysimeter equipped by the heating fence is hereinafter referred to as LYS-H and the non-equipped lysimeter as LYS-N.

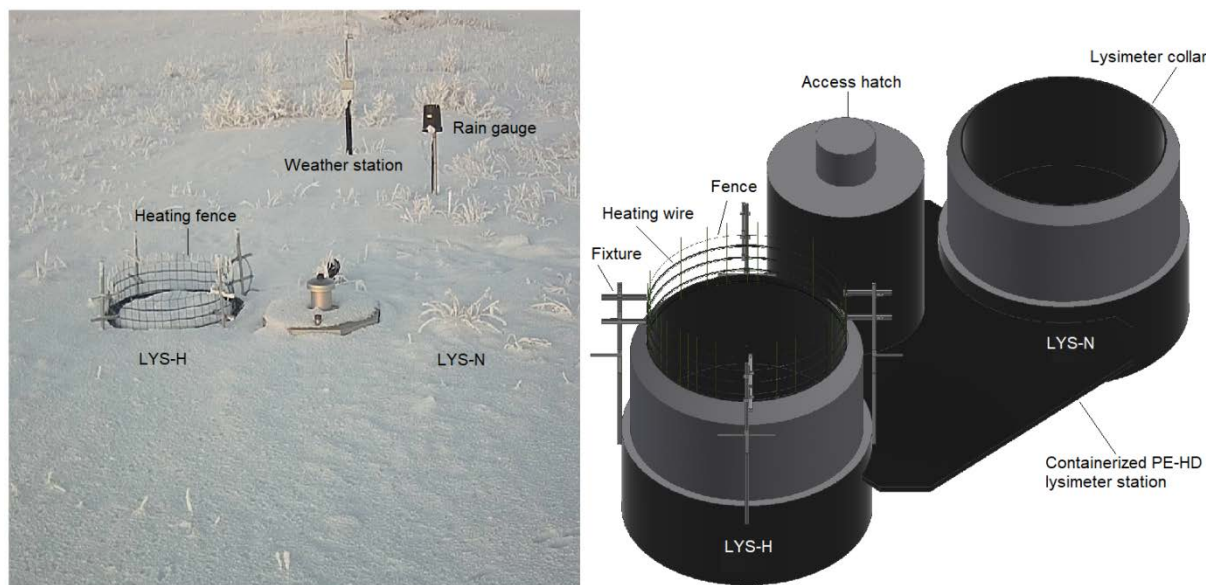


**Figure 20:** Photo of the top view of the installed double lysimeter station (left) in winter season 2019/2020 in Pervomayka, Kazakhstan, and an illustration of the non-equipped lysimeter collar (LYS-N) as well as the lysimeter collar equipped with a heating wire system (LYS-H) (right).

## 6.4 Results

### 6.4.1 Precipitation and actual evapotranspiration

The evaluation of the winter measurements was done using the period 01/11/2019 – 31/03/2020, in total 152 observation days. Figure 21 shows the course of the lysimeter mass. On 09 November, the first snowfall could be observed with an increase in weight which should correlate with a P amount of 21.8 mm (LYS-N) and 14.4 mm (LYS-H), respectively. On the contrary, the rain gauges showed considerably lower daily totals. The tipping bucket at a height of 1 m indicated a sum of 8 mm, whereas the mean of the rain gauges at ground level were at 5.7 mm. As P fell in the form of snow, a stable snow cover developed above the lysimeters. On 12 November, both lysimeters measured a mass increase again with 14.6 mm at LYS-N and 4.6 mm at LYS-H. However, according to the images of the camera, no new snowfall occurred. Instead, there were snowdrifts caused by wind speeds up to  $14 \text{ m s}^{-1}$  (Fig. 22). From the end of November, the weighing at LYS-N became affected until the end of the observation period, whereas the measurements at LYS-H seemed to be reliable due to the heating fence. The function of the technique was becoming apparent during 09–12 December. Meanwhile, no wind and P were measured which led us to assume that  $ET_a$  occurred. Indeed, within three days sublimation (as part of  $ET_a$ ) of 1.3 mm was measured at LYS-H. In contrast, LYS-N showed an increase of 6.5 mm, which would indicate

a P event that could be excluded. From 21 December, however, strong snowfall occurred and the snow height increased up to 20 cm confirmed by a measuring pole and the camera images. Therefore, the last heating wire of the fence was exceeded. From then onwards, the measuring errors within the data of LYS-H became stronger. A notable event was the period 26-27 February where a respective increase of 53.5 mm and 33.3 mm was observed, but without any indication of P. From March, however, the apparent measuring errors became slowly lower since the snow on LYS-H started to melt despite further closed snow cover at the surrounding. From 20 March, LYS-H is free of snow, while the surrounding snow cover was still at a height of 20 cm. Within the last 11 days, no P was observed, but a total  $ET_a$  of 34 mm with a decreasing daily rate was measured. On 21 March, the  $ET_a$  rate was  $5.4 \text{ mm day}^{-1}$ , whereas a value of  $1.1 \text{ mm day}^{-1}$  was detected on 31 March.

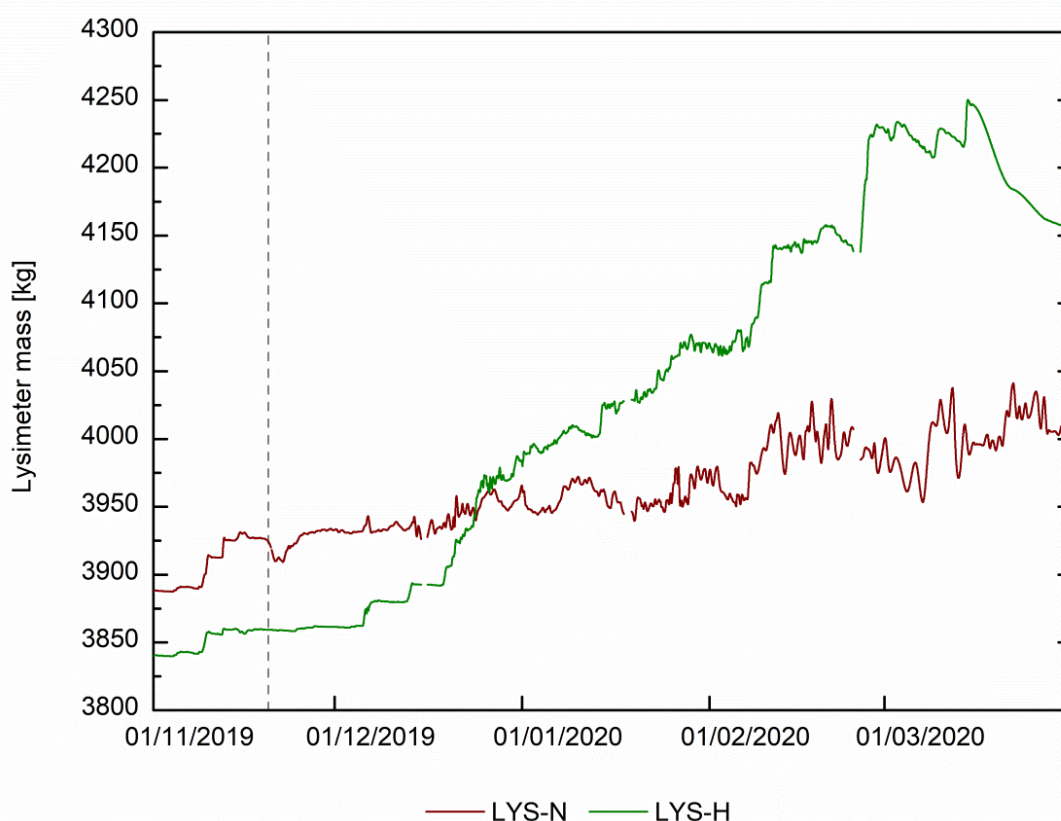


**Figure 21:** Mass of the lysimeter with a heating fence (LYS-H) and the non-equipped lysimeter (LYS-N) from 01/11/2019 to 31/03/2020. The dashed line represents the time of installation of the heating fence.

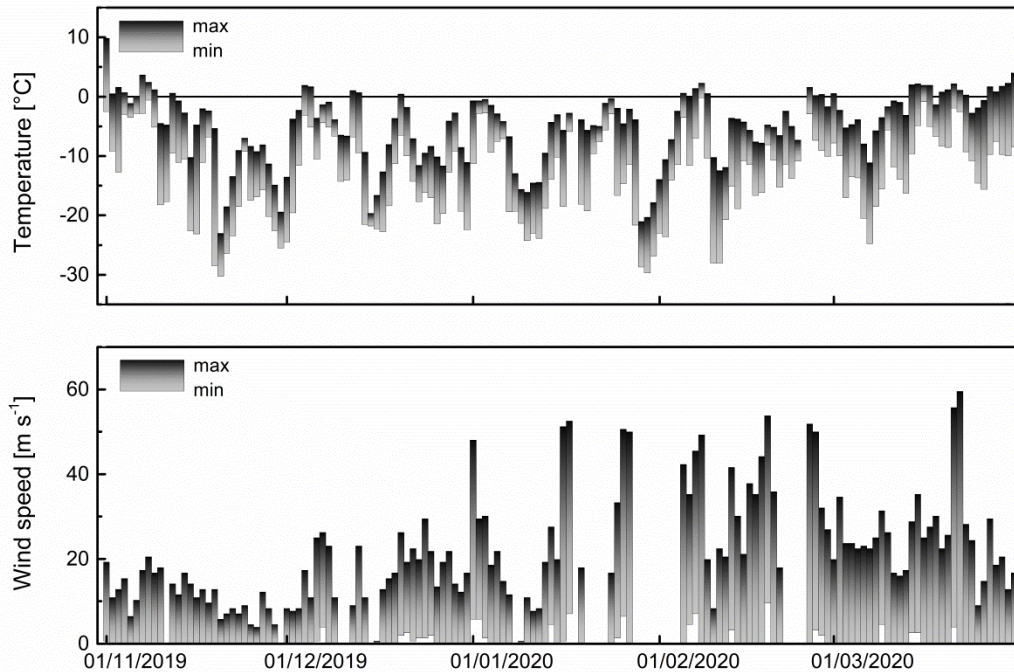


**Figure 22:** Daily minima and maxima of air temperature and wind speed from 01/11/2019 to 31/03/2020.

#### 6.4.2 Soil parameters

Within the observation period, it could be observed anomalies in soil temperature of LYS-H (Fig. 23). It was shown that the pristine steppe soil (LYS-H) froze faster compared to the arable soil (LYS-N). This effect starts with the first snowfall at the beginning of November. However, after the installation of the heating fence, the soil temperature of LYS-H increased. On 20 November, the temperature at the depth of 30 cm was by +1.7 °C (LYS-N) and -2.4 °C (LYS-H), respectively. The soil temperature of LYS-H increased and reached the same level as LYS-N with +0.9 °C on 09 December. From then, both lysimeters showed the same soil temperatures until 20 December. The same pattern was also observed in the depth of 50 cm and 120 cm. Later, a continuous increase in the temperature of LYS-H followed (up to 2.6 °C at 30 cm and 2.8 °C at 50 cm). Generally, LYS-H indicated a relatively constant temperature level, whereas the soil temperature of LYS-N considerably fluctuated until the end of the period. Accordingly, a difference up to 4.3 °C (at 30 cm) could be observed between LYS-N and LYS-H. However, this effect was less pronounced at the depth of 50 and 120 cm. Finally, as March progressed, the soil temperature of LYS-N increased with increasing air temperatures.

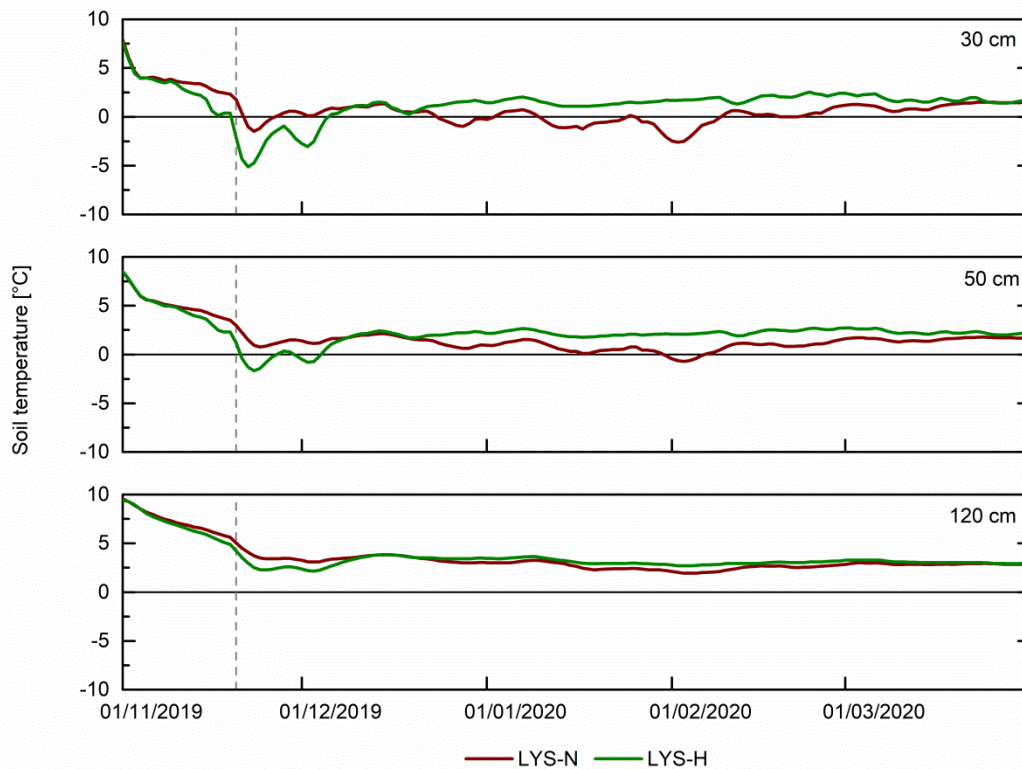


**Figure 23:** Soil temperatures in the depths of 30, 50, and 120 cm within the lysimeter with a heating fence (LYS-H) and the non-equipped lysimeter (LYS-N) from 01/11/2019 to 31/03/2020. On 20 November 2019 (dashed line) the heating fence was added to LYS-H.

On 12 December, there was an increase up to +1 °C in air temperature. Using images from the camera mounted near the lysimeter station, it could be observed how the majority of the previous snow cover was melting throughout the day, but there was neither surface runoff nor an increase in soil moisture (Fig. 24). However, the soil moisture indicated a sudden increase in 30 and 50 cm depth of LYS-H at the end of December. Within two days, there was an increase from 11 Vol.-% to 28 Vol.-% in 30 cm on 20 December and from 12 Vol.-% to 27 Vol.-% in 50 cm on 31 December. At the depth of 120 cm, the soil moisture began to rise from 14 Vol.-% on 31 January to 30 Vol.-% on 10 February. On the other side, an increase in soil moisture at LYS-N was only observed at the end of March where the natural snow melting period was starting. In this case, there was an increase from 10 Vol.-% on 21 March to 25 Vol.-% on 25 March at 30 cm and from 11 Vol.-% on 30 March to 29 Vol.-% on 31 March. The infiltration at LYS-H even led to drainage. The first seepage water was measured on 29 February. Until the end of the observation period, a total outflow of 162.4 mm could be determined.

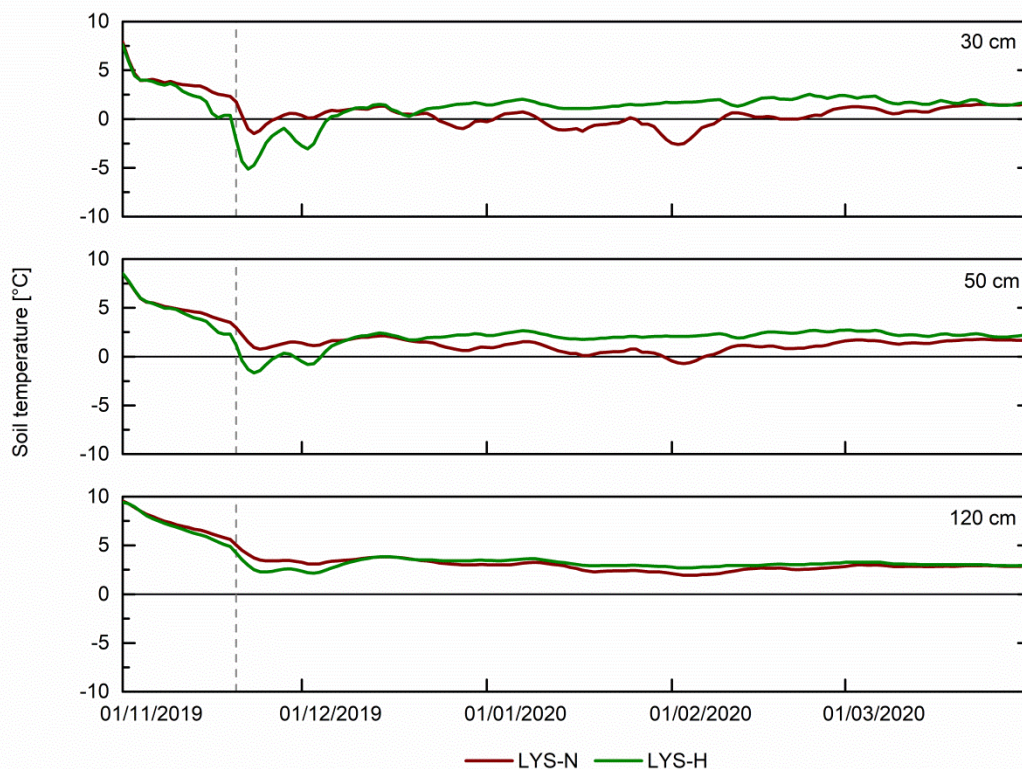


**Figure 24:** Soil moisture in the depths of 30, 50, and 120 cm within the lysimeter with heating fence (LYS-H) and the non-equipped lysimeter (LYS-N) from 01/11/2019 to 31/03/2020.

## 6.5 Discussion

### 6.5.1 Lysimeter weighing, precipitation, and actual evapotranspiration

The results showed considerable differences in P measurements which are caused by several reasons. First of all, the measuring devices of the monitoring network are characterised by different resolutions and measurement accuracies. Furthermore, they also had a different collecting area. The main differences, however, resulted from the wind impact. It was noted that the rain gauges only measured P when the wind speed was lower than  $3 \text{ m s}^{-1}$ . During 09 November, the wind velocities were up to  $16 \text{ m s}^{-1}$ . Therefore, the rain gauges were not able to record the snow, which led to a systematic underestimation (Sevruk, 1982; Richter, 1995; Goodison et al., 1998). The differences between the rain gauges themselves were questionable. Usually, P rates decreased with increasing measuring heights (Gebler et al., 2015; Hoffmann et al., 2016). Furthermore, the wind-induced error decreased at P measurements at ground level (Mekonnen et al., 2015). Thus, the rain gauges at ground level should have shown a higher total sum compared to the heightened rain gauge. An explanation could be their restricted function from time to time. It was observed that the tipping buckets were sometimes filled by eolian sediments from the

surrounding. The large difference of 7.4 mm between the lysimeters was particularly caused by the different vegetation cover. LYS-H showed only a short grass cover, whereas LYS-N was cultivated by summer wheat. The vegetation height was still around 25 cm. Due to the stalks of wheat, more snow was intercepted.

The snow cover reached heights up to 28 cm between December and March and the weighing data indicated its impact on the reliability. Due to the heating fence, data records were produced which cannot be unambiguously assessed. It cannot be stated clearly, whether the fence was functioning consistently efficient and it was also unclear to which effects the fence led while the snow exceeded the fence. Obvious mass increases which should be a result of P could not be confirmed by visual comparison as shown by the example of 26-27 February. It could be observed how the snow cover above LYS-H was melting, probably caused by the increased air temperature up to +1 °C on 26 February. It is assumed that the heat of the fence led to the melting of ice bridges, whereby the already existing mass of the snow was eventually added to the again working weighing. The increase of 30.3 mm the next day, however, was snow deposited by the wind. With wind velocities up to 50 m s<sup>-1</sup> the hole within the snow cover was filled. Just two days later, the snow height on LYS-H was at the level of the surrounding again. Nevertheless, reliable measurements of P and ET<sub>a</sub> only began from the point where LYS-H was completely free of snow; in this case from 20 March. However, the high ET<sub>a</sub> rates at the end of March cannot be plausible for the natural cold conditions. The fence led to an additional supply of heat which supports the evaporation process of the soil. It was only with increasing air temperatures that the ET<sub>a</sub> rates became more plausible. From 27 March, the air temperatures started to rise above 0 °C during the day. At a temperature of +3 °C, the fence will automatically turn off. Therefore, the daily ET<sub>a</sub> rates decreased since the soil was no longer subjected to the artificially heated ambient air.

In general, the weighing of LYS-N seemed to be more affected compared to those of LYS-H. The considerable weight gains and losses were also observed in the previous study in Siberia. Therefore, the experiment described above was conducted to identify potential error sources, but the results do not agree with the observations in this study. According to the detected error source (scenario 2), the weighing has to be paused which is not the case. However, the experiment was conducted by using a small shallow lysimeter (dimensions 40 x 40 x 11.5 cm) where the total load of the snow can be supported on the collar. In this study, a lysimeter with a diameter of 1 m<sup>2</sup> was used. Due to the rounded collar, the snow will not extend the whole area since the snow cover will sag, whereby only a part of it will be measured. Processes such as material slide onto or down from the lysimeter would maybe explain the strong weight fluctuations. Finally, the experiment should disprove the previous

assumption that the main error source is the development of snow and ice bridges between the lysimeter vessel and the collar. As the gap of the shallow lysimeter was only 2 mm and no freezing effects were observed, it is highly probable that this effect does also not occur at larger lysimeters. Nevertheless, it is to mention that the snow of the ski hall is artificial snow that consists of small ice balls, whereby the informative value of this assumption is restricted.

### **6.5.2 Soil parameters**

One of the more notable instances of a possible impact of the heating fence indicated the soil temperature. Before its installation, differences could be already observed between LYS-N and LYS-H. The low decrease in soil temperature at LYS-N could be explained by the higher snow accumulation due to the stalks of wheat. Since snow is a poor conductor of heat, the soil has been kept isolated from frost (Zhang, 2005; Zhang et al., 2008; Roznovsky and Brzezina, 2017). Furthermore, due to the soil heat flux, it may occur considerable differences in temperature between soil and snow cover at the beginning of winter. In contrast, the lower snow heights and the absence of a closed snow cover led to a quick cooling down of the steppe soil (LYS-H). A further remarkable aspect was the reduction of the differences in soil temperature between LYS-N and LYS-H with increasing depth. As the heat source (equivalent to radiation) occurred at the soil surface, there is amplitude insulation. The heat flux has to heat more and more soil volume with increasing depth, whereby its intensity will be decreased. In general, there is a decrease in soil temperature with increasing depth at higher radiation (e.g. in summer), whereas the successive cooling-down of the soil dominates during winter. Thus, there is an increase in soil temperature with increasing depth as observed in this study.

The most impact on soil temperature seemed to be caused by soil water in this study. It is assumed that the melting water of 12 December needed time to infiltrate due to the nearly frozen soil and the high percentage of silt (up to 58% of the soil volume). Considering that no increase in soil moisture at LYS-N was observed, it is to be expected that the heating fence additionally contributed to the snow melting. The increase in soil temperature proved that this water warmed up the soil, which led to a higher infiltration rate. It is noteworthy that the soil temperature at 50 cm increased before the water reached the depth. This is probably caused by the thermal properties of the soil. The thermal conductivity depends on soil texture, bulk density, and soil moisture (Abu-Hamdeh and Reeder, 2000). The dependency is highest at low soil moisture content. It is proved that thermal conductivity and thermal diffusivity increased with increasing soil density and moisture content, whereby the thermal diffusivity exhibit a maximum at water contents between 10 and 25 Vol.-% (Arkhangelskaya and Lukyashchenko, 2018).

### 6.5.3 Soil water balance

The lysimeter technology enables the measurement of all components of the soil water balance in a nearly direct way. With the focus on P and  $ET_a$ , its determination depends on the ability of the weighable lysimeters. Although the detection of P could be done by standard tipping buckets, meanwhile it became also popular to measure P by weighable lysimeters (Meissner et al., 2010; Schrader et al., 2013; Gebler et al., 2015) due to the higher accuracy (Hoffmann et al., 2016). Within this context, the way of its determination was necessary since the tipping buckets were not equipped by a heating function. Thus, the snow amount could not have been recorded. On the other side, there are only a few direct methods to measure  $ET_a$ . Furthermore, this parameter will often neglect during winter periods, but it plays a crucial role in semiarid environments, particularly since snow is an additional water resource. The sublimation of snow presents a loss of water that would fill up the soil water during the melting period in spring. The study demonstrated how difficult it is to get reliable measurements of sublimation. Regardless of the restricted lysimeter weighing, the wind impact and the nature of snow make it virtually impossible to get long-term measuring periods at this site. There was already the consideration of a snow fence, but the natural wind field would be disturbed. Moreover, there is the possibility that more snow may be deposited above the lysimeters, dependent on wind direction.

Usually, the change in soil water would play a subordinate role during winter in this environment. Experience to date clearly shows that the soil can freeze down to 2 m (Meissner et al., 2017). Accordingly, the same principle applies to drainage. Nevertheless, the technology showed a substantial impact on almost all soil water balance parameters. P was influenced since a snow gap was induced through the melting process. This gap was refilled repeatedly by intercepted snow, amounting to an increase in P. As mentioned above, the major issue in  $ET_a$  measurements was the wind impact, but the last days of the observation period let assume that the heat supported the water loss. Thus, the  $ET_a$  rate was increased. The most impact, however, was on soil moisture and drainage. Through the heating fence, artificial snowmelt was initiated and led to an increase in soil moisture. This meltwater is the source for  $ET_a$  during spring and summer, whereas drainage rarely occurs since the water does not infiltrate often into the deeper soil layers in these environments. Finally, it can be noted that the current soil water balance is no longer under natural conditions.

#### **6.5.4 Technology to prevent freezing effects**

As the applied technology did not provide the desired effect, an optimisation or alternative would be necessary to solve the continuing issue. For the current technique, there is first of all the opportunity to increase the height of the heating fence. The weighing data let assume that the impairments began as the snow height exceeds the heating wires. However, a more effective solution would be a temperature control of the fence. Currently, it heats with a temperature that seems to be inappropriate. A continuous power control based on the air temperature and the temperature in the snowpack would provide just the heat that is necessary to separate the snow cover on the lysimeter from those of the surrounding. For an effective adaption, it could be beneficial when the temperature will be measured directly above the surface ground, within the snow cover, and directly above the snow cover. As differences in temperature exist between soil and snow cover, several references would form the basis for a correct setting. A further correction may be a change in place of the heating wires. The first heating wire is positioned directly above the soil. With a slight increase, the impact on soil temperature could be reduced.

Nevertheless, as a purely thermal solution still bears the danger of influencing the soil water balance, an alternative could be the preferred option. In light of the gained knowledge and experience of previous studies, a combination of mechanics and thermal could be a solution for this lysimeter type. The snow cutter mentioned above has failed due to the crusted snow. This challenge may be met when the snow cutter will be heated. Thus, the resistance of the snow can be overcome. Moreover, the snow cutter cut the snow outside of the collar. If this will be changed to cutting inside the collar, the identified source of the measuring error would also be eliminated. By cutting the snow cover inside the collar, the snow load resting vertically above the collar will be separated from the part above the lysimeters soil surface. The inner part can rest freely on the lysimeter and will be then the only mass that will be measured. However, it must be noted that the experience of the snow cutter has been made in Siberia, but the properties of snow may vary from site to site. In the case of powder snow, the snow cutter might not exert any effect.

#### **6.6 Conclusions**

Frost effects caused by low temperatures and high snow amounts led usually to an impairment of lysimeter measurements. Therefore, it is difficult to get reliable data for the determination of the soil water balance. The set-up of a monitoring network consisting of two weighable lysimeters allows year-round measurements in the semiarid grass steppe of Kazakhstan. Utilising thermal technology, an attempt in the form of a heating fence has been

made to enable the maintenance of lysimeter weighing, whereby the technique should prevent the lysimeters from freezing. It has been shown that the technique sustained the weighing to a certain extent, but only so far as the snow height did not exceed the fence. It was detected a considerable influence on the soil water balance. The thermal impact has significantly contributed to soil heating and snow melting. As a result, water infiltrated into the soil and filled up the soil water storage. This effect represents under no circumstances natural conditions. The water balance has been falsified. As a solution, an optimised version of the fence is already in planning which will be implemented in autumn 2020 and will be tested during the next winter.

## **7 Measured and simulated water fluxes in dry steppe soils: A comparison between pristine grassland and agricultural land**

This chapter based on the manuscript submitted on 21/09/2020 to *Water*.

### **7.1 Abstract**

Kazakhstan stands as a part of the grain belt for high grain production and large land reserves in the form of grass steppes. A transformation of unused grassland to agricultural land would lead to an increase in yields and could contribute to the global food crisis. However, to meet this challenge an understanding of the local water dynamics is necessary. For this purpose, measurements by two weighable lysimeters with monolithically extracted soil columns stemming from arable land and grassland were conducted in the steppe of Kazakhstan. The records of precipitation, actual evapotranspiration, and water content will be compared to estimations calculated by HYDRUS-1D. The results indicated more water lost by the grassland and a high negative soil water balance. The slight moister conditions of the arable soil were also been proved by the simulations, where the water fluxes agreed with the observations. The drier conditions of the steppe soil, however, could not be captured by the model. Overall, this study provides the first step toward a consideration of an increase in cropland through the current development of climate-adapted and sustainable agriculture.

### **7.2 Introduction**

The hydrological cycle in arid and semiarid environments is dominated by soil evaporation or evapotranspiration. As part of the water regime, it can exceed the overall water availability due to high temperatures and low precipitation. If the water demand of sparse vegetation cannot meet, land degradation, desertification, and biodiversity losses could be the result (Foley et al., 2005). These processes are closely related to increasing soil evaporation/evapotranspiration as a result of inappropriate land management (Meyer et al., 2008; Smits et al., 2012; Fruehauf et al., 2020b). The latter is one of the reasons for yield losses, which finally intensify the global food crisis. To stabilise agricultural yields and minimise ongoing degradation and desertification processes, sustainable land management practices will be developed (Belyaev et al., 2020; Grunwald et al., 2020). Further consideration could be the transformation of unused land to agricultural land to increase

yields. There are 'transition countries' in Eastern Europe and Central Asia, which indicate an important contributing role in the global food security debate due to its large land reserves (Swinnen et al., 2017). Moreover, they have the potential to become a 'bread basket' for the world because of the already large wheat production. One of the major wheat-producing countries is Kazakhstan. In the 1950s, approximately 23 million hectares of steppe grassland were converted into cropland (Kraemer et al., 2015). However, after the collapse of the Soviet Union in 1991 most of this land was abandoned and partly reverted to grassland. After 2000, grain production increased again, but rather in yield than in cropland. Thus, there is a large potential to put back this land in use for food production. Nevertheless, doubts have arisen since the idle cropland is mainly located in areas that are hardly appropriate for crop production due to the soils (Kraemer et al., 2015). Despite the knowledge of the regional soil distribution and its assessment of suitability for crop production, little is known about the water dynamics at these sites. However, the water balance of the soil is essential for agricultural purposes. To the knowledge of the authors, there are no studies on soil water balance in Kazakhstan, neither for cropland nor for grassland.

Our aim is to get a deeper understanding of the water dynamics in this environment with a special interest in regional land management. For this purpose, two weighable lysimeters were established in the steppe of Kazakhstan to obtain in situ measurements of the following soil water balance components: actual evapotranspiration, precipitation, surface runoff, soil moisture at various depths, and outflow. The lysimeters include undisturbed soil monoliths extracted from a pristine steppe site and an agricultural used land site. The respective land management of steppe grassland and summer wheat has been maintained. The lysimeter measurements were also being used for numerical simulations using a process-based soil physical model implemented in HYDRUS-1D (Simunek et al., 2016). This software package was used, among other reasons, because its application is controversial discussed for arid and semiarid soils (Assouline et al., 2013; Balugani et al., 2018; Du et al., 2018; Kanzari et al., 2018). It will be tested to what extent the model is able to reflect the water dynamics in semiarid soils.

The activities set out above aim at:

- i. the quantification of the soil water balance components for the vegetation period 2019 as a function of the respective land management,
- ii. the simulation of surface fluxes and water content for the pristine steppe soil and arable soil; the estimations will be compared with the observations,
- iii. the evaluation of the model in respect of its performance under dry conditions.

## **7.3 Material and methods**

### **7.3.1 Study site and experimental set-up**

This study based on the lysimeter experiment in the Kazakh steppe described in the chapters 5.3.1 and 5.3.2. As in the chapters before, the arable lysimeter is referred to as LYS 1 and the pristine steppe as LYS 2.

### **7.3.2 Data availability**

For reliable determination of the soil water balance, one year of data at least is needed. Although lysimeter measurements are available for the full year 2019 (Fig. 25), the data could not be used for the entire period. The measurements were impaired due to the cold and snowy conditions at this site. It was shown that low temperatures and high snow heights led to implausible measurements resulting from an impact on the weighing. Thus, data gained between November and March is non-applicable for analysis and have to be excluded from the calculation of the soil water balance. Nevertheless, the soil was frozen during winter and it is assumed that the sublimation of snow (as part of actual evapotranspiration) is low, whereby the change in soil water storage is negligible. The amount of snow as part of precipitation could be calculated from the change in water content and the surface runoff during the snowmelt in spring.

Finally, only the data between 01 April and 31 October 2019 (in total 214 days) were suitable for the study.

### **7.3.3 Model set-up**

The simulation of water flow in soils was done by using HYDRUS-1D (Simunek et al., 2016). The one-dimensional vertical movement of water in unsaturated soils is described by the Richard's equation (Richards, 1931). The model simulates water flow through soil, estimates, inter alia, water content and pressure head by depth, and provides water fluxes as a function of climate, soil, and plant characteristics. To determine the water regime and identify the impact of land management, two models were performed according to the lysimeter properties. The soil profiles were defined with a depth of 185 cm since the filter layer was excluded. Moreover, the profiles were divided into four sublayers due to the different soil properties (Tab. 10). Due to the similar bulk density of the subsoil layers of LYS 2, they were merged to one layer to minimise the model domain layer number since the set-up of multiple layers would result in a high number of parameters (Dijkema et al., 2017). Both soil columns

were vertically discretised into 370 finite elements with a thickness of 0.5 cm. The van Genuchten-Mualem hydraulic model with no hysteresis was used for both models. The unsaturated soil hydraulic properties according to van Genuchten (1980) were derived from laboratory analyses of soil samples taken at several depths at the extraction sites. However, the parameters were optimised by using the inverse solution. The parameter optimisation was done as follows:

1. By using the Rosetta software (Schaap et al., 2001) initial values were obtained by the data of soil texture and bulk density for each soil layer (Tab. 10).
2. The resulting values were used as input for the RetC software (van Genuchten et al., 1991) to determine the van Genuchten retention curve by using the measured water retention data.
3. These values were used as initial values for the inverse simulation in HYDRUS-1D. As RetC does not optimise the saturated hydraulic conductivity ( $K_s$ ), values obtained from laboratory analyses were used as initial values.

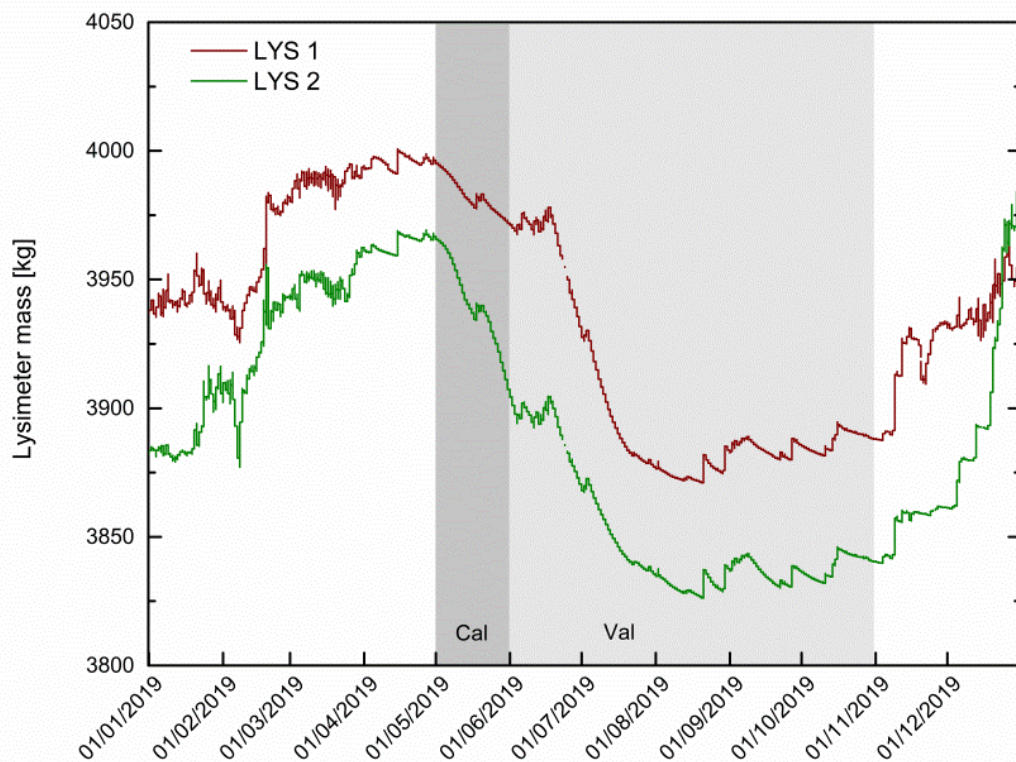


**Figure 25:** Mass of the lysimeters with an arable soil (LYS 1) and pristine steppe soil (LYS 2) between 01/01/2019 and 31/12/2019. The shaded parts represent the calibration period (Cal) and the validation period (Val) for HYDRUS-1D.

**Table 10:** Particle size distribution and bulk density of the lysimeter soil layers.

LYS 1					LYS 2				
Layer	Silt	Clay	Sand	$\rho_b$	Layer	Silt	Clay	Sand	$\rho_b$
cm	%	%	%	$\text{g cm}^{-3}$	cm	%	%	%	$\text{g cm}^{-3}$
0-42	56.3	39.7	4.0	1.22	0-50	57.9	37.6	4.5	1.40
42-75	51.2	45.6	3.2	1.43	50-64	55.7	40.2	4.1	1.45
75-140	49.7	46.4	3.9	1.35	64-98	53.5	42.6	3.9	1.61
140-200	53.0	43.5	3.5	1.57	98-122	57.7	38.3	4.0	1.55
					122-200	53.8	42.6	3.6	1.53

The upper boundary was defined as the atmospheric boundary condition with surface runoff, where the maximum height at soil surface was set by 5 cm for the model of LYS 1 and by 10 cm for the model of LYS 2. As input for precipitation and evaporation, the measured data of the lysimeters (calculated according to Eq. 2) was used in a daily resolution. The lower boundary was determined as seepage face with  $h = 0$ , i.e. a water-saturated layer has to be formed at the bottom before water can drain out. The data provided by the Tensiomark sensors in the depths of 30, 50, and 120 cm were used as initial pressure head values. As input data for the inverse solution daily values for water content were given for every instrumented depth. The van Genuchten parameters optimised by HYDRUS-1D are listed in Table 11.

To calibrate and validate, the models were divided into two subsets (cf. Fig. 25). For inverse simulation, a drying period was selected which should reflect typical site conditions. Thus, the models were calibrated for the period from 01 May to 31 May. The validation period lasted from 01 May to 30 September, a total of 153 days.

**Table 11:** The soil hydraulic van Genuchten parameters and saturated hydraulic conductivity ( $K_s$ ) optimised for each layer of the soil profile by HYDRUS-1D.

LYS 1					LYS 2						
Layer	$\theta_r$	$\theta_s$	$\alpha$	n	$K_s$	Layer	$\theta_r$	$\theta_s$	$\alpha$	n	$K_s$
cm	$\text{cm}^3 \text{cm}^{-3}$	$\text{cm}^3 \text{cm}^{-3}$	$\text{cm}^{-1}$	-	$\text{cm d}^{-1}$	cm	$\text{cm}^3 \text{cm}^{-3}$	$\text{cm}^3 \text{cm}^{-3}$	$\text{cm}^{-1}$	-	$\text{cm d}^{-1}$
0-42	0.006	0.293	0.004	1.257	216.0	0-50	0.009	0.275	0.003	1.224	81.2
42-75	0.040	0.254	0.0005	1.533	284.3	50-64	0.066	0.252	0.0005	1.586	24.7
75-140	0.183	0.236	0.046	1.172	6.4	64-98	0.004	0.248	0.041	1.097	43.9
140-185	0.151	0.170	0.002	1.330	7.1	98-185	0.028	0.153	0.005	1.133	10.9

$\theta_r$  – residual water content;  $\theta_s$  – saturated water content;  $\alpha$  - is related to the inverse of the air entry suction; n - is a measure of the pore-size distribution;  $K_s$  – saturated hydraulic conductivity

### 7.3.4 Analysis of model performance

The measured data of surface fluxes and water content obtained from the lysimeters should be compared with those simulated by HYDRUS-1D. The quality of the model performance was evaluated by RMSE (Eq. 6) and the Nash-Sutcliffe efficiency (NSE, Eq. 9) coefficient.

$$\text{NSE} = 1 - \frac{\sum_{i=1}^n (X_i - Y_i)^2}{\sum_{i=1}^n (Y_i - \bar{Y})^2} \quad (9)$$

where the variables  $X_i$  and  $Y_i$  are the  $i$ th estimated values and observed references,  $\bar{X}$  and  $\bar{Y}$  the mean of all estimated and observed values, respectively;  $n$  is the total number of data for the observation period. NSE ranges between  $-\infty$  and 1, where an efficiency of 1 corresponds to the best fit of simulated and observed value, while a RMSE value of 0 indicates a perfect match.

## 7.4 Results

### 7.4.1 Lysimeter measurements

#### *Precipitation and actual evapotranspiration*

The lysimeter data offers an overview of changes in water storage, whereby the difference between precipitation ( $P$ ), actual evapotranspiration ( $ET_a$ ), outflow, and surface runoff determines the soil water balance. It has been shown that the soil water balance was negative with -57.4 mm at LYS 1 and -88.3 mm at LYS 2, respectively. In detail, the arable soil (LYS 1) lost 269.1 mm water, while 211.7 mm was provided by  $P$ . At LYS 2 (steppe soil) it was an  $ET_a$  of 283.6 mm and  $P$  of 195.4 mm. In addition, surface runoff with an amount of 0.1 mm was measured at LYS 2 during snowmelt in April. No outflow was measured at both lysimeters during the whole observation period.

With a view on monthly  $ET_a$  and  $P$  rates, striking patterns exist (Tab. 12). There is not much difference in  $P$  between the lysimeters. The major difference was in April due to the input of meltwater; otherwise only up to 2 mm severed the measurements. With only 5% of the total  $P$ , May and July were characterised by a dry period. In contrast, there were considerable differences in  $ET_a$  rates, particularly during these dry periods. LYS 1 showed more than three times the monthly  $P$  rate in May, while LYS 2 measured six times more  $ET_a$  than  $P$ . In July, a similar pattern could be observed, just vice versa. From August, both lysimeters have lost the same amount of water by  $ET_a$ , albeit it is to note that only the share evaporated which was provided by  $P$ .

**Table 12:** Monthly  $ET_a$  and  $P$  rates for the lysimeters, monthly mean temperatures, and mean maximum temperatures (in parantheses) measured by the weather station.

	Apr	May	Jun	Jul	Aug	Sep	Oct
LYS 1 – $ET_a$ (mm)	27.0	36.2	73.5	64.3	24.2	25.3	18.6
P (mm)	77.3 <sup>1</sup>	10.7	39.9	9.2	28.7	26.6	19.3
LYS 2 – $ET_a$ (mm)	23.1	67.1	69.5	46.8	27.8	27.6	17.8
P (mm)	61.4 <sup>1</sup>	10.6	37.3	11.1	28.3	26.3	20.1
Mean temperature (°C)	5.0 (11.8)	12.9 (21.4)	16.4 (23.3)	21.3 (29.5)	18.7 (26.4)	10.8 (17.5)	6.3 (13.3)

<sup>1</sup> The water equivalent of snow is included.

### Soil moisture

At both lysimeters, the snowmelt was visible at the beginning of the observation period (Fig. 26). There was a distinct increase in soil moisture in the topsoil with 16 Vol.-% (from 14 to 30 Vol.-%) at LYS 1 and 13 Vol.-% (from 15 to 28 Vol.-%) at LYS 2. With similar initial values, the change in water content could be observed during the vegetation period. From June, a strong decline could be identified at LYS 1, which resulted in low soil moisture down to 10 Vol.-% from mid-July. In contrast, LYS 2 showed a decrease at the beginning of May and already reached the initial state of 15 Vol.-% in June. Until the end of the observation period, the soil moisture at LYS 2 decreased down to 11 Vol.-%. A similar pattern with a minimal time displacement was observed in the depth of 50 cm. In the subsoil, however, there was only a slight increase apparent with a change of 7 Vol.-% (from 15 to 22 Vol.-%) at LYS 1 and 2 Vol.-% (from 12 to 14 Vol.-%) at LYS 2, respectively. Furthermore, it was noticeable that only an  $ET_a$  rate of  $>2 \text{ mm day}^{-1}$  caused a continuous decrease in soil moisture at a depth of 30 cm.

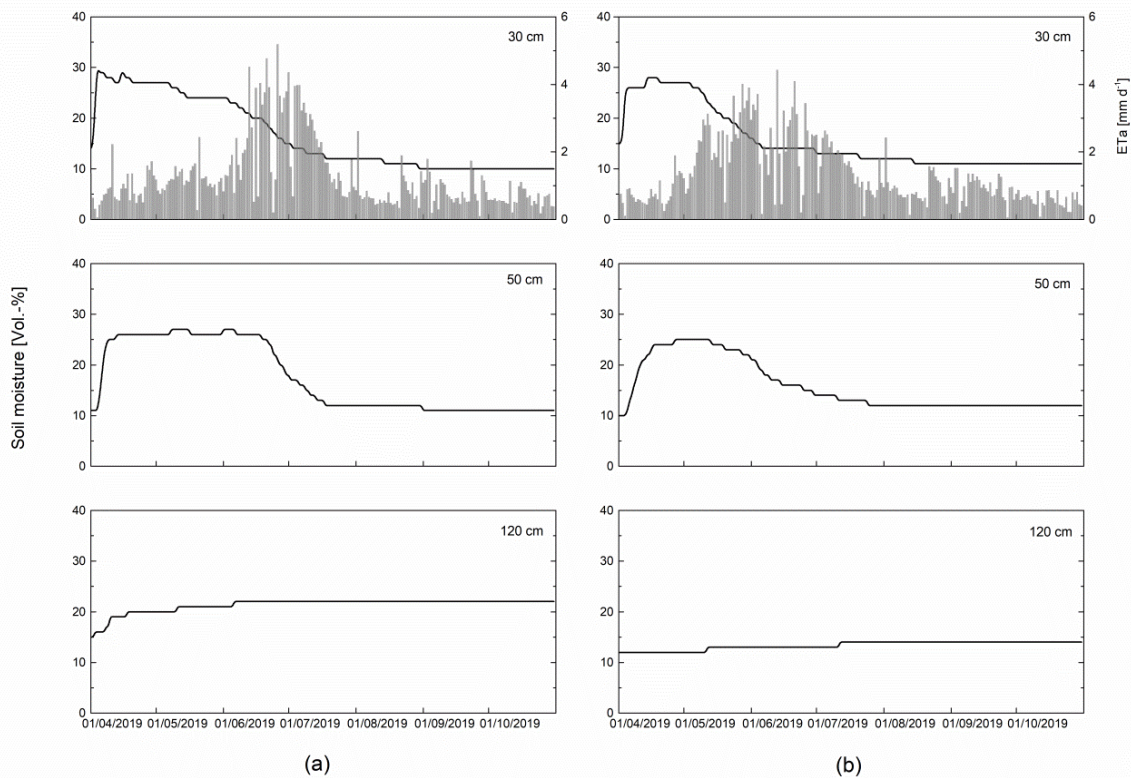


**Figure 26:** Soil moisture in the depths of 30, 50, and 120 cm inside of (a) LYS 1 and (b) LYS 2 between 01/04/2019 and 31/10/2019. The upper bars represent the daily  $ET_a$  measured by the respective lysimeter.

## 7.4.2 Hydrological simulations

### *Surface fluxes*

As the daily measured  $ET_a$  and P rates were used as input data for the models, estimations and observations should be identical. This was the case for LYS 1, which was also reflected in the RMSE and NSE values of 0.0001 and 1, respectively; while the simulated surface fluxes at LYS 2 did not agree with the observations (Fig. 27). The model underestimated the fluxes from Day 59 caused by the dry period identified above. It seemed that HYDRUS-1D simulated the dry period much slower than observed. Therefore, it came to discrepancies in  $ET_a$  that increase over time. It is obvious that this circumstance was depending on the surface pressure head. The simulated surface pressure head at LYS 1 ranged between  $-10^2$  and  $-10^5$  cm, while the pressure head at LYS 2 reached the value of  $-10^6$  cm which is the default setting in HYDRUS-1D. The model was apparently not able to simulate  $ET_a$  as soon as the limit was reached. Due to these discrepancies, the model performance was lower with a RMSE value of 0.45 and a NSE value of 0.95.

With a view on the cumulative surface fluxes (Fig. 28), it can be stated that the observations and the simulation of LYS 1 resulted in a water balance of -108.3 mm for 153 days. A total of -128.9 mm was measured by LYS 2, while the model estimated the value of -97.4 mm. That is a difference of 31.5 mm and it shows the overall underestimation of the soil water balance.

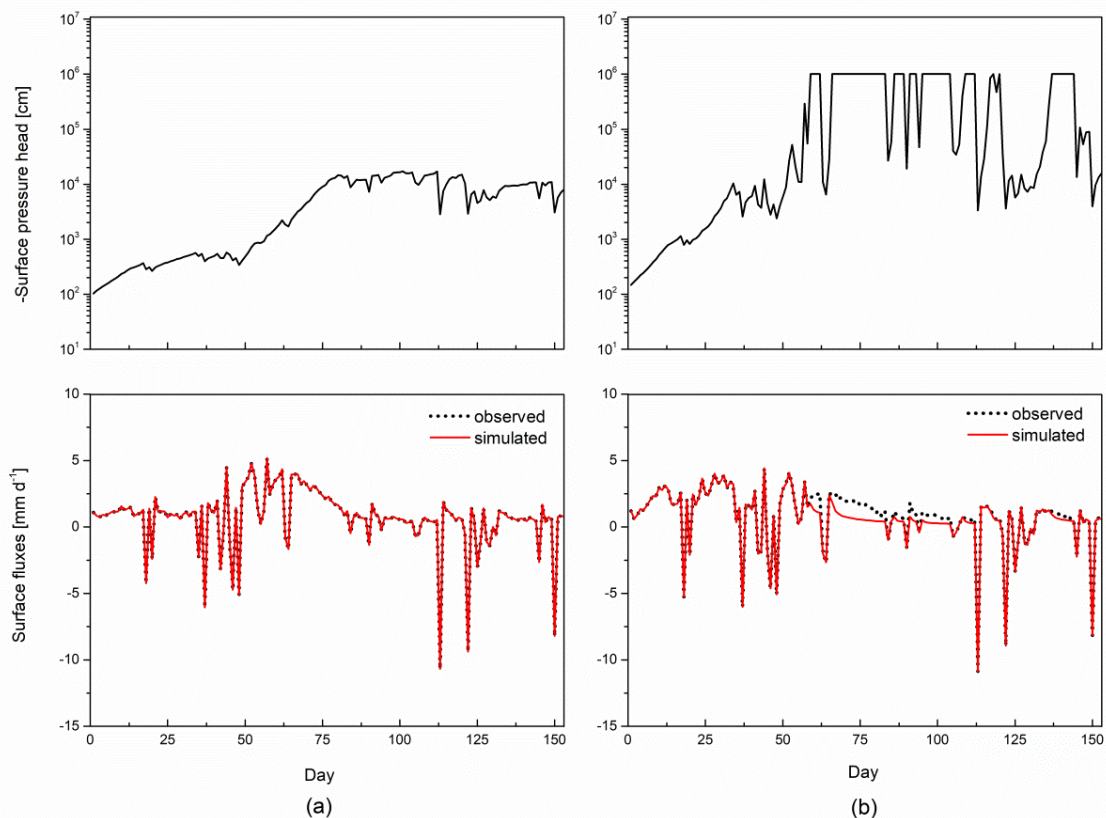


**Figure 27:** The surface pressure head (upper) and surface fluxes (lower) of (a) LYS 1 and (b) LYS 2.

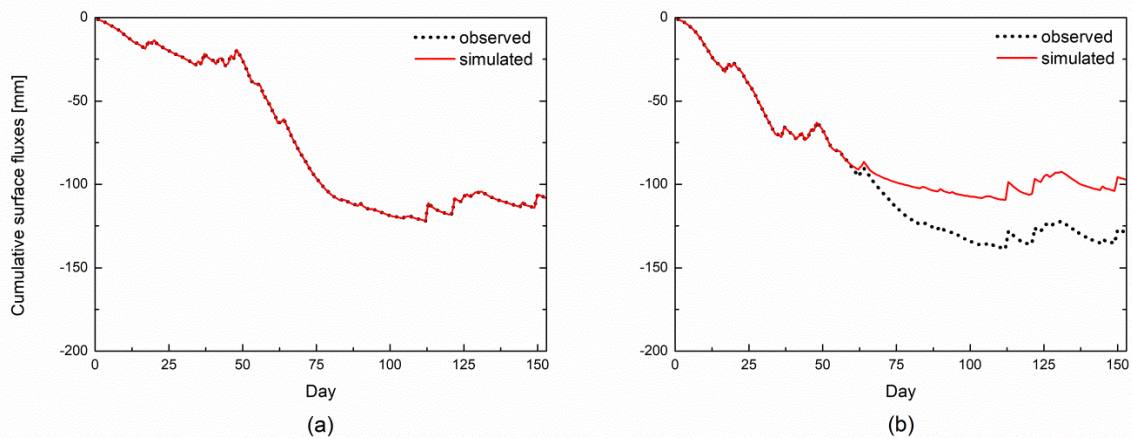


**Figure 28:** Cumulative surface fluxes simulated by HYDRUS-1D and calculated by mass changes of (a) LYS 1 and (b) LYS 2 for the 153 observation days.

### Soil moisture

In general, the simulations agreed well with the observations, whereby the model of LYS 2 simulated the soil moisture better according to the statistic analyses (Tab. 13). At LYS 1, the best match was for the depth of 30 cm (Fig. 29). However, the model was not able to catch the impact of P which resulted in an overestimation. This issue led to an overall overestimation during dry periods. The same pattern also appeared in the depth of 50 cm, whereby the error rate was higher. In the depth of 120 cm, the model was not able to catch the increase in soil moisture between Day 0 and 37 which was also reflected in the NSE value of -1.26. In contrast, the water content was simulated very well in the depth of 50 cm in LYS 2, although the P event around Day 46 was also overestimated. On the other hand, the dry period between Day 25 and 41 was underestimated. In the topsoil, the overestimation was lower than in the topsoil of LYS 1 resulting in a higher NSE value. As in the subsoil of LYS 1, the model did not catch the slight changes in water content.

**Table 13:** Values of the model performance indices RMSE and NSE for the soil moisture.

Depth	LYS 1		LYS 2	
	RMSE	NSE	RMSE	NSE
30 cm	0.018	0.90	0.011	0.94
50 cm	0.022	0.88	0.008	0.96
120 cm	0.008	-1.26	0.011	-2.11

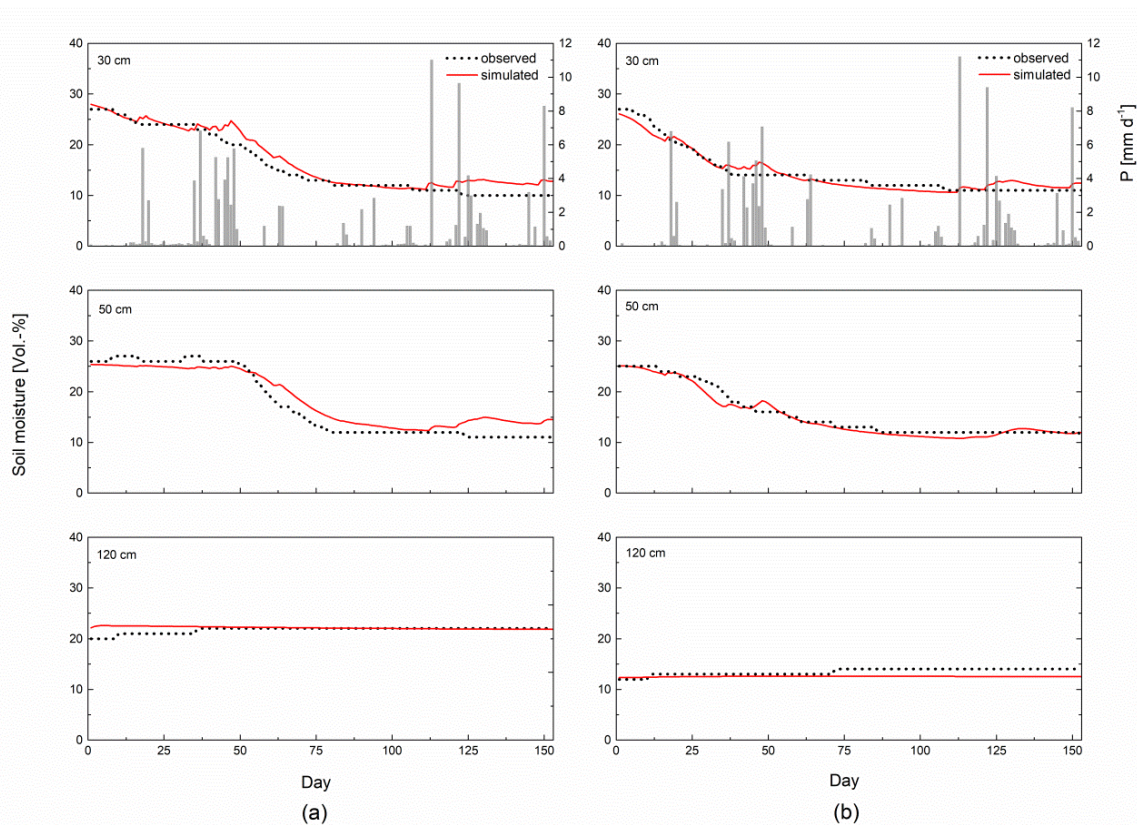


**Figure 29:** Soil moisture measured by (a) LYS 1 and (b) LYS 2, and simulated by HYDRUS-1D for the depths 30, 50, and 120 cm. The upper bars represent the daily P measured by the respective lysimeter.

## 7.5 Discussion

### 7.5.1 Impacts on field measurements

The differences in P and  $ET_a$  are probably due to the vegetation of the lysimeters. In particular, the  $ET_a$  rates during May represent the first growth stages of the vegetation. After snow melting in March, both lysimeters were only covered by ruderal vegetation. The pristine steppe grass at LYS 2 was in its initial stage and covered approximately 10% of the ground (Allen et al., 1998). During this stage, soil evaporation is predominant. As the arable soil was bare, the same process occurred at LYS 1, which explains the similar  $ET_a$  rates in April. However, the summer wheat was seeded on 18 May, while the steppe grass was already in the crop development stage (>10% ground cover) resulting in a higher transpiration rate and therefore in an  $ET_a$  amount nearly twice as high. According to Allen et al. (1998), wheat has an initial stage of 40 days, which would mean that the transpiration would exceed the evaporation from the end of June. The  $ET_a$  rates of the summer wheat considerably increased however from mid-June. According to our observation, the soil was already

covered by more than 10% of the crop and the  $ET_a$  rates exceeded  $>4 \text{ mm day}^{-1}$  from then on. The length of the crop development must differ from the values in the literature since spring wheat is assumed with a seeding date of April, while summer wheat was used in this study. In general, differences in the crop, planting date, and climate have an impact on the length of the initial period. The achievement of the mid-season stage was already observed in July, whereby the crop stage length is shorter compared to the spring wheat usually used in a temperate climate. In contrast, the steppe grass had reached its mid-season stage with an effective full vegetation cover in June, which is reflected in the highest monthly  $ET_a$  rate and daily maximum (4.4 mm). These growth stages also showed an impact on the soil moisture, and vice versa. Due to the low water content level in July,  $ET_a$  of both lysimeters decreased from then on resulting in an early observed late season stage with maturity indicated by yellowing of leaves.

The low  $ET_a$  rates from August may be caused due to the formation of a dry soil layer (DSL). In arid and semiarid regions it is not unusual that the water transport can occur as water vapour, since the liquid continuity through the soil is lost when the evaporation demand is higher than the water availability (Balugani et al., 2018). In such a case, a DSL is formed in the topsoil, which has an impact on the evaporation process. There are two to three evaporation stages. The first stage consists of the liquid continuity between the vadose zone and the soil surface where the evaporation of water occurs at a vaporisation plane at the soil surface. With increasing drying, the vaporisation plane decreased. The force of the capillary flow which moves the liquid water upward becomes smaller and is eventually no longer able to ensure the liquid continuity. Therefore the hydraulic connectivity to the water table is lost (Lehmann et al., 2008). Now the evaporation of the vaporisation plane below the soil surface is the second stage. In this stage, water evaporates mainly by vapour diffusion. A potential third stage differs only in the respect of evaporation rates. In unsaturated soil profiles like in this study, the process is similar, only that the very dry topsoil is caused by the depletion of water near the soil surface (Balugani et al., 2018). The depth of a DSL is controversial. Balugani et al. (2018) stated generally the first decimeters of the soil, Pedram et al. (2017) find the existence of a DSL up to  $>10 \text{ cm}$ , while Assouline et al. (2013) observed a DSL between 1 and 5 cm. It is assumed that the depth depends on soil texture with lower values at the coarse texture and higher values at a very fine texture (Shokri and Or, 2011). Nevertheless, the depth of a DSL determines the evaporation rate. With decreasing of the drying front, the path for the water vapour to the soil surface increases leading to a decrease in the evaporation rate (Dijkema et al., 2017). During the second stage of the evaporation, the rates may account for  $<1 \text{ mm day}^{-1}$  (Balugani et al., 2018), which was mainly detected at the end of the period. Assouline et al. (2013) observed a completely dry soil layer at the

surface after 5 days of only evaporation. Such a period was also often observed where  $ET_a$  rates decreased down to  $<0.7 \text{ mm day}^{-1}$ . In the study of Balugani et al. (2018) the presence of a DSL is defined as a soil layer with a pressure head of  $< -15,000 \text{ cm}$ . As the pressure head was not measured at the soil surface in this study, the results of the simulation could be given an overview (cf. Fig. 27). The limit was exceeded on 06 August (Day 98) at LYS 1 and on 21 June (Day 52) at LYS 2 for the first time. The simulated pressure head of LYS 1 matched well with the beginning low  $ET_a$  rates ( $<1 \text{ mm day}^{-1}$ ) and therefore agree with the definition by Balugani et al. (2018), while the surface pressure head of LYS 2 indicated a DSL formation at a transition of a wet period to a dry period, where the  $ET_a$  rates were still comparatively high. This is more likely due to the model performance (more on that later). Nevertheless, it is always possible that as soon as P occurs the evaporation stages can switch back to the first stage due to the new water supply (Wang, 2015). This may be a reason for the increasing  $ET_a$  rates after P.

The different land management was even visible in the measurement of P. The difference in April was mainly due to the infiltration of snow which was added as water equivalent to P. The higher value at LYS 1 could be explained by the lower bulk density in the topsoil (cf. Tab. 10) leading to a higher infiltration rate. The difference of approximately 2 mm in June and July could have resulted from i) interception where P does not reach the soil surface as it will be intercepted by vegetation and evaporate immediately, or ii) dew formation which is more pronounced between spring and summer (Groh et al., 2018). Interception is influenced by many factors such as rainfall and canopy characteristics. It occurs mainly at light P intensity and the amount of the intercepted P is also dependent on the leaf surface of the canopy (Holder and Gibbes, 2017; Pedram et al., 2018). The higher the leaf area is, the higher the rainfall interception will be. There is a very strong argument for saying that P intercepted or evaporated before it infiltrated into the soil because no increase in soil moisture was observed after P. On the other side, dew formation will be initiated by radiative cooling and high air humidity at night. This process of condensation at the soil surface can be measured by weighable lysimeters (Xiao et al., 2009; Groh et al., 2018). As it is accompanied by a mass increase, it will be recorded as P. Groh et al. (2018) indicated that dew can contribute between 4.5% and 6.9% of the annual P for grassland and is, therefore, an effective water source during droughts, particularly in semiarid environments.

The change in soil moisture and its course in the first two observation depths (30 and 50 cm) are mainly dependent on  $ET_a$  and the impact of the land management described above. However, the observation in the depth of 120 cm was interesting. Although wheat shows maximum effective root depths down to 150 cm (Allen et al., 1998), no impact of the land management in the form of root water uptake could be observed. Nyéki et al. (2017) stated

that the root development of a crop is also dependent on soil bulk density. Root growth is affected in silty clay soils at bulk densities of  $1.49 \text{ g cm}^{-3}$  and  $1.39 \text{ g cm}^{-3}$  at soil layers with >45% clay content, which is the case in the depths of 42 to 140 cm in LYS 1. Instead, it is assumed that the bulk densities are the reason for the increase in water content in both subsoil profiles. The arable soil (LYS 1) showed generally lower bulk densities compared to the steppe soil (LYS 2) (cf. Tab. 10). The higher potential infiltration rate led to a faster record of soil moisture increase resulting from the snow melting in this case. Due to this aspect and the higher amount of infiltrated meltwater, the water content of LYS 1 was on a higher level compared to those of LYS 2. The latter however indicates a high compaction degree in the subsoil resulting in a lower infiltration rate and less water reaching that depth.

### 7.5.2 Impacts on model simulations

The relative considerable differences between observed and simulated water content can be a result of the inverse modelling. The parameters  $K_s$ ,  $\alpha$ , and  $n$  are a challenge for the inverse solution when the soil is almost saturated (Isch et al., 2019). Indeed, this issue should be avoided by using the calibration period of May where the impact of the snowmelt should be lower. However, the pressure heads in the depth of 30 and 50 cm in LYS 1 and 50 cm in LYS 2 still indicated a near saturation. As a result, the optimised  $K_s$  values of both soil profiles are overestimated. In the lysimeter study of Wegehenkel and Gerke (2015) the  $K_s$  values of its silty clay soils with comparable soil textures are substantially lower compared to those in this study. The high  $K_s$  values lead to highly permeable soil layers where the rainwater could quickly infiltrate into the soil. This would cause an increase in soil moisture which was however not observed and led finally to an overestimation by the model. Similar results were indicated by Pedram et al. (2017). In particular, the changes in water content in the subsoil (120 cm) could not be captured by the model. Small variations in water content are difficult to simulate properly, which was also detected in depths <40 cm by Isch et al. (2019).

Considering a DSL at the soil surface the simulation of  $ET_a$  must have been impaired. HYDRUS-1D bases on the numerical solution of the Richard's equation, which assumes a liquid continuity. However, the model is not able to simulate properly an air-dry DSL due to the present liquid discontinuity (Dijkema et al., 2017). Therefore, recent studies used modified approaches to model a DSL, albeit the dimension of the DSL seems to be essential. Assouline et al. (2013) also used the standard van Genuchten (1980) model with DSL depths between 1 and 5 cm and obtained good evaporation estimates, but water content simulations were deviating considerably from the observations. Dijkema et al. (2017), however, used the

bimodal Durner model (Durner, 1994) in its lysimeter study in Nevada, USA. They were not able to simulate neither the low water content in the topsoil nor the evaporation during dry periods, even though a DSL was not directly observed, but rather assumed due to the very dry conditions down to a depth of 0.25 m. Their results are similar to those of LYS 2. The modelling of drying periods caused an underestimation of evaporation leading to a widening gap between simulations and observations. If the soil reached air-dry conditions with a pressure head of  $-10^6$  cm, the strong gradient in pressure head cannot overcome the steep drop in the hydraulic conductivity (Dijkema et al., 2017). As a result, the model failed to catch the drying process. In other words, if the simulated water content at the soil surface is lower than the residual value ( $\theta_r$ ), hydraulic continuity is lost and HYDRUS-1D is unable to describe water fluxes (Assouline et al., 2013). Just the modelled surface pressure heads of LYS 2 indicated this case and most probably the temporal presence of a DSL, while the arable soil of LYS 1 seemed to be moister at the topsoil, which results in identical simulated and observed surface fluxes.

### 7.5.3 Model limitations

The results of this study proved the limitations in the application of HYDRUS-1D for simulations of water fluxes in semiarid soils. As stated above, the underlying equations do not allow discontinuity in the liquid phase. Although HYDRUS-1D avoid thermodynamically pressure heads and thus numerical instability by setting a minimum pressure head value ( $h_{crit} = -10^6$  cm), hydraulic discontinuity and the high vapour water transfer from a subsurface drying front to the soil surface leads to a pressure head that tends toward infinity at the soil surface during a drying process (Dijkema et al., 2017). Moreover, according to the assumption behind Mualem's model the water flow is not sufficiently described in a very dry regime.

There are further reasons for the underestimation of evaporation related to possible processes not included in HYDRUS-1D. According to Balugani et al. (2018), these processes could be:

1. mechanical dispersion,
2. air advection in the dry unsaturated zone,
3. natural convection in a sloping, dry unsaturated zone,
4. preferential evaporation flow,
5. abrupt pressure and temperature changes because of strong eddies formation on the soil surface,

6. a constitutive liquid hydraulic conductivity function which is incorrect in dry conditions.

While the latter was already identified as a major error source, the first and third points can be excluded due to the lack of a 'Stefan flow' (Balugani et al., 2018) and the sloping soil profile. Abrupt pressure and temperature changes could also be excluded because these effects occur mainly at bare soils. The only period with a bare soil was the first thirty days at LYS 1 before summer wheat was seeded. The model, however, had captured the surface fluxes during this period. Air advection plays a subordinate role in the evaporation process. Nevertheless, in dry unsaturated soil layers where water will be transported only as water vapour, gas can move by advection; in case of a strong gas pressure gradient and well connected pores filled with gas. The preferential evaporation flow could be induced by heterogeneities in the soil texture, structure, and compaction. As this is the case in this study, it could be a further reason for underestimated evaporation rates. Although perhaps not decisive in itself, these unaccounted processes are noteworthy due to its role in field conditions, particularly in arid and semiarid environments.

## 7.6 Conclusions

A comparative lysimeter study of water fluxes in silty clay soils as a function of land management, pristine grassland and agricultural use, allows the following conclusions:

- i. At both sites, a negative water balance could be determined, whereby the pristine grassland lost more water by  $ET_a$  than the arable soil. More water infiltrated into the arable soil due to a higher amount of infiltrating meltwater as well as a lower bulk density in the topsoil. Surface runoff only occurred on the grassland during snowmelt, and no outflow was generally measured. Overall, the arable soil indicated slightly higher water content, particularly in the subsoil. The development of  $ET_a$  and soil moisture was largely dependent on the growth stages of the respective crop. However, the water content of both sites reached the same low level down to 50 cm at the end of the observation period. Nevertheless, agricultural land showed a higher soil water budget compared to those of the pristine grassland.
- ii. The simulations by HYDRUS-1D proved the general moisture conditions of the arable soil by identical estimated and observed surface fluxes. The simulation of the pristine grassland, however, was limited due to the dry conditions. The estimated  $ET_a$  rates were underestimated compared to those observed. The model performance showed a high agreement regarding water content, but it was shown that wet periods were overestimated.

- iii. The underestimation of  $ET_a$  was properly caused by the formation of a DSL at the soil surface, which led to surface pressure heads which tend toward infinity. The latter is a limitation of the model of why the evaporation cannot accurately be estimated. The overestimation of wet periods in water content let's assume too high  $K_s$  values. As the hydraulic soil parameters were inversely optimised by using water content data of a relatively wet period, the values of  $K_s$  have been overestimated.
- iv. Furthermore, it is assumed that a formation of a DSL at the soil surface was the reason for  $ET_a$  rates  $<1\text{mm day}^{-1}$  during mid-summer.
- v. Apart from the snowmelt period, only a few positive changes in water content could be observed. Thus,  $P$  must have been intercepted by the vegetation or the evaporation demand was so high that water evaporated before reaching the ground whereby less water remained for deeper infiltration.

Based on the available findings, it can be noticed that the soil water balance allows sustainable agricultural use as arable land. As the observation period included a dry period common for this climate, the water regime could be also observed under these extreme conditions. However, it must be kept in mind that this study is only the first step in the direction to a consideration of the transformation of unused grassland to crop land with sustainable agriculture. For significant statements it will need long-term measurements, and – not to be forgotten – lysimeter measurements are point measurements. For this reason, the simulation of the soil water balance should provide an opportunity to transfer lysimeter measurements to the field. It has been clearly shown that the process-based soil physical model of HYDRUS-1D is able to reflect the unsaturated flow in semiarid soils but unable to estimate  $ET_a$  during dry periods. However,  $ET_a$  is the most important component within the hydrological cycle in arid and semiarid environments and thus its accurate quantification is indispensable for soil water balance analyses.

## **8 Synthesis and conclusions**

### **8.1 Precipitation and evapotranspiration under semiarid conditions**

The studies conducted in southwest Siberia and Kazakhstan do not lead to a determination of an annual soil water balance. In despite of partly long-term measurements, only information on seasonal scale could be collected. Nevertheless, practical and important knowledge has been gained regarding P and ET in semiarid environments. It was proved that P is lower as ET on timescales of seasons, but it has to be noted that this fact is only valid for summer seasons at the study sites. Although no reliable data could be obtained over a winter season, the observations led to assume that winter precipitation – in these cases in form of snow – is higher as sublimation as part of ET. Moreover, as an exception to early spring where the water storage of the soils has been filled up with meltwater, the soil moisture was usually low. In southwest Siberia, it could be observed that  $ET_a$  was controlled by P and vegetation instead. The  $ET_a$  rates have increased after P occurred, whereas  $ET_a$  was lower in total under the wheat stocks compared to the pristine steppe grass at both sites. Furthermore, the higher water loss by transpiration became apparent in the Kazakh steppe. It was only after seeding that  $ET_a$  has increased with crop development, while soil moisture has decreased from that point on. From the investigations presented, it emerged that ET is the dominating factor within the hydrological cycle in semiarid environments. However, it requires long-term data of all components to allow reliable conclusions on the water budget, especially since P and ET are under a high variability. If these parameters will not be precisely determined, it is virtually impossible to get an accurate and robust soil water balance.

### **8.2 Measuring methods for determining soil water balance parameters**

There are numerous methods to determine the components of the soil water balance, which can be basically divided in direct and indirect methods. Through a measuring network consisted of a lysimeter and weather station, it was possible to measure the soil water balance parameters under direct conditions. Due to two different rain gauges and weighable lysimeters, there was the opportunity to detect the parameter P on different ways. As the methods indicated different measuring techniques, the determination of P could be evaluated regarding practicability. It has been shown that weighable lysimeters provide precise data compared to standard rain gauges. Based on the detection at ground level, the major systematic error sources of rain gauges are excluded. Moreover, the current weighable lysimeters are able to measure with an accuracy of 20 g, which correspond to 0.02 mm.

However, the method has certain disadvantages. Although lysimeters reflect natural conditions, the vegetation cover has an impact not to be neglected. Aspects such as interception or dewfall which still are part of the precipitation term affect the reliable detection of rainfall. Furthermore, high intensity rainfall can lead to surface runoff, which may not be measured as P. In contrast, standard rain gauges are usually installed at increasing heights, whereby the P amount will be decreased, mainly due to the wind impact. In the recent years, the application of acoustic precipitation sensors became more popular. Besides the detection of rainfall amount, they are also capable to provide information about rainfall intensity. Nevertheless, the case study presented, has indicated that this type of rain gauge shows quite different error sources. As the method bases on the detection of individual raindrop impacts, the shape and velocity of raindrops may be potential influencing factors.

While the determination of P is relatively simple, measuring  $ET_a$  is more complex. For this issue, model applications became common practice. The decision on a respective model approach depends on the availability of data. The more input data that is available, the more accurate the results will be. Generally, modelling is a simple and cost-effective alternative to direct measurements. However, there are also limitations and it should take into consideration that modelling results are only estimations. Two widely used model approaches were chosen to compare ET estimations with direct measurements by weighable lysimeters. It can be noted that the models were not able to reflect the side conditions, especially the impact of the low water availability. As the models have mainly reached their limits due to high water demand and vegetation properties, ET was improperly estimated. In the case of the PM FAO model, ET was underestimated during sufficient water supply provided by P. It is assumed that the part of transpiration was underestimated since the steppe grass showed different properties to those presumed from the model. Independent of the climate taken into account, the steppe vegetation and therefore its demand on soil water requires a more plant-specific approach. The soil physical model implemented in HYDRUS-1D partly failed to the dryness which resulted also in an underestimation of ET.

It has become apparent that lysimeters are a sufficient tool to get reliable measuring data of soil water balance parameters. Through the weighing system it is possible to record P and  $ET_a$  with high accuracy. Error sources of lysimeters are limited. Continuous maintenance services ensured the functioning of the technique and small disturbances within the weighing data could be eliminated by data processing. However, the lysimeter experiments have also shown that the vegetation cover of a lysimeter has a significant impact on measurements. Besides the mentioned effects of interception and dewfall, there is also the possibility of the occurrence of edge effects such as oasis or bloom effect. Nevertheless, if potential influential

factors will be considered and are reduced to a minimum, lysimeters are and shall remain an attractive method within this research field.

### **8.3 Potential and challenges in the determination of soil water balance parameters**

This thesis shows the wide range of opportunities to determine the components of the soil water balance. It has also shown how the technique has been developed over time. It was a challenge to determine the parameter of  $ET_a$  in a direct way for a long time. Nowadays, though, it is possible to measure various parameters by only one method. Furthermore, the resolution and accuracy of measurements become higher, which also give data more expressiveness. Due to the high technical degree in the form of data transfer or automatic measuring systems, long-term measurements campaigned at remote locations are today a common practice. These in situ measurements enable to fill data gaps which still continue to exist due to non-equipped regions – including the steppes of southwest Siberia and Kazakhstan. As the regions are considered partly unused, scientific interest is still rather low.

With respect to the quantification of the water budget, it is difficult to determine all components by direct methods due to the climate. However, the hardly determined parameter drainage can be excluded from the balance equation since seepage water is usually non-existent or negligible in semiarid areas. Thus, the balancing will be simplified. As the determination of  $ET_a$  is of particular interest for these environments, the application of a direct method is recommended. Although there are also sufficient model approaches, which consider the dry conditions, they provide, however, only estimations.

On the other site, it is to note that there is rarely the opportunity to determine all components of the soil water balance with the same method at the same time. As the usage of several methods is common, the range of results and error sources will be increased. Furthermore, direct methods are often associated with high costs and efforts. In regards of data record, the mentioned high resolution involves simultaneously higher effort and uncertainties within the data processing. It is also important to remember that the measurements are only point measurements and have therefore a low validity for entire regional areas. All studies presented have shown that the methods have to be adapted to site conditions. In the case of lysimeters, edge effects have to be considered. The vegetation cover on the lysimeter should correspond to the surrounding or advection caused by the wind should not be neglected since this effect will be favoured by the flat plain of the steppe. Besides these effects occurred usually in summer, the studies have also indicated that the measurement of  $ET_a$  is

very difficult to determine during winter. In general, the term sublimation will often neglect, but it is also of particular importance. At the study sites, snow is a large water resource which fills up the soil reserves in spring. Thus, it is also necessary to quantify the loss of water in form of sublimation. However, it was observed that frost, ice, and snow affect the lysimeter weighing, whereby no reliable data for  $ET_a$  could be gained. Until now, there is no solution for the lysimeter type used in these studies, whereby the long-term determination of the soil water balance is furthermore not possible for these regions.

#### **8.4 Outlook and recommendations**

As has been shown, some methods for the quantification of soil water balance parameters are more suitable, while others only are less promising. The successful determination depends on many factors, albeit direct methods are favoured for an accurate determination. The method should generally consider the natural conditions of the study site and the minimum of interfering influences. Nevertheless, indirect methods and model applications still remain popular due to the lower costs and efforts as well as the increased availability. Moreover, in the case of the selection of a model approach, the results could close the currently existing data gaps. Additionally, its estimations can be extrapolated from point measurements to a wider area.

In the light of the recent years, the rising popularity of weighable lysimeters as tool for the determination of soil water balance parameters indicates its further increased application, especially also outside Europe. The monitoring networks in southwest Siberia und Kazakhstan pursue the objective of receiving long-term data for its steppe soils which provide potential agricultural land. However, the determination of the soil water balance by weighable lysimeters includes ensuring to drive the development of a winter solution forward. Without a technique which enables a reliable lysimeter weighing despite frost, ice, and snow, a determination of the parameter  $ET_a$  during winter will not be possible. It is necessary to investigate more in detail which opportunities are available for the consisting lysimeter type. It is only once the necessary foundations have been created there is a possibility to determine the soil water balance.

Until now, the agricultural land of the Siberian and Kazakh steppes are mainly used for the cultivation of wheat. Through the comparative analyses by the two lysimeters, the different land use systems can be evaluated, particularly in regard of water consumption. With a deeper understanding of the local water usage of wheat, the available water resources can be used more efficient in future. It is important to identify how the large water resources provided by the winter precipitation can be hold and stored into the soil in the long term. If

successful, crop losses could be decreased and yields could be increased by an increase of cropland with adapted land management. It would not just assure the agriculture of the region, but also finally positive effects on its socio-economy.

## Bibliography

- Abu-Hamdeh, N. H., Reeder, R. C., 2000. Soil thermal conductivity: Effects of density, moisture, salt concentration, and organic matter. *Soil Sci. Soc. Am. J.* 64, 1285-1290.
- Allen, R.G., Pereira, L.S., Raes, D., Smith, M., 1998. *Crop Evapotranspiration. Guidelines for computing crop water requirements*. FAO – Food and Agriculture Organization of the United Nations, Rome, Italy, 300 pp.
- Allen, R.G., Pereira, L.S., Howell, T.A., Jensen, M.E., 2011. Evapotranspiration information reporting: I. Factors governing measurement accuracy. *Agric. Water Manag.* 98, 899-920.
- Amatya, D.M., Irmak, S., Gowda, P., Sun, G., Nettles, J.E., Douglas-Mankin, K.R., 2016. Ecosystem evapotranspiration: challenges in measurements, estimates, and modeling. *Trans. ASABE* 59, 555-560.
- Arkhangelskaya, T. A., Lukiashchenko, K. I., 2018. Estimating soil thermal diffusivity at different water contents from easily available data on soil texture, bulk density, and organic carbon content. *Biosyst. Eng.* 168, 83-95.
- Armstrong, R.N., Pomeroy, J.W., Martz, L.W., 2008. Evaluation of three evaporation estimation methods in a Canadian prairie landscape. *Hydrol. Process.* 22, 2801-2815.
- Assouline, S., Tyler, S.W., Selker, J.S., Lunati, I., Higgins, C.W., Parlange, M.B., 2013. Evaporation from a shallow water table: Diurnal dynamics of water and heat at the surface of drying sand. *Water Resour. Res.* 49, 4022-4034.
- Bagley, J.E., Desai, A.R., Dirmeyer, P.A., Foley, J.A., 2012. Effects of land cover change on moisture availability and potential crop yield in the world's breadbaskets. *Environ. Res. Lett.* 7, 014009.
- Balugani, E., Lubczynski, M.W., van der Tol, C., Metselaar, K., 2018. Testing three approaches to estimate soil evaporation through a dry soil layer in a semi-arid area. *J. Hydrol.* 567, 405-419.
- Balykin, D., Puzanov, A., Stephan, E., Meissner, R., 2016. Using the innovative lysimeter technology in the German-Russian research project "KULUNDA". In: Mueller, L., Sheudshen, A.K., Eulenstein, F. (Eds.), *Novel Methods for Monitoring and Managing Land and Water Resources in Siberia*. Springer Water, Switzerland, pp. 387-399.

- Belyaev, V.I., Grunwald, L.-C., Akshalov, K.A., Meinel, T., Sokolova, L.V., 2020. Modernization of current agricultural technologies of grain production under the conditions of a steppe zone of the Altai region. In: Fruehauf, M., Guggenberger, G., Meinel, T., Theesfeld, I., Lentz, S. (Eds.), KULUNDA: Climate Smart Agriculture, Innovations in Landscape Research. Springer Nature, Switzerland, pp. 341-354.
- Bethge-Steffens, D., Meissner, R., Rupp, H., 2004. Development and practical test of a weighable groundwater lysimeter for floodplain sites. *J. Plant Nutr. Soil Sci.* 167, 516-524.
- Bondarovich, A. A., Scherbinin, V., Ponkina, E. V., Matsyur, A., Puzanov, A., Stephan, E., Balykin, D., Rupp, H., Meissner, R., 2020. Soil moisture and Evapotranspiration. In: Fruehauf, M., Guggenberger, G., Meinel, T., Theesfeld, I., Lenz, S. (Eds.), KULUNDA: Climate Smart Agriculture. South Siberian Agro-steppe as Pioneering Region for Sustainable Land Use. Springer Nature, Switzerland, pp. 167-181.
- Changhai, S., Baodi, D., Yunzhou, Q., Yuxin, L., Lei, S., Mengyu, L., Haipei, L., 2010. Physiological regulation of high transpiration efficiency in winter wheat under drought conditions. *Plant Soil Environ.* 56, 340-347.
- Degefie, D. T., Fleischer, E., Klemm, O., Soromotin, A.V., Soromotin, O. V., Tolstikov, A. V., Abramov, N. V., 2014. Climate extremes in South Western Siberia: past and future. *Stoch. Environ. Res. Risk Assess.* 28, 2161-2173.
- DehghaniSanij, H., Yamamoto, T., Rasiah, V., 2004. Assessment of evapotranspiration estimation models for use in semi-arid environments. *Agric. Water Manag.* 64, 91-106.
- Dijkema, J., Koonce, J. E., Shillito, R. M., Ghezzehei, T. A., Berli, M., van der Ploeg, M. J., van Genuchten, M. T., 2017. Water distribution in an arid zone soil: Numerical analysis of data from a large weighing lysimeter. *Vadose Zone J.* 17, 1-17.
- Du, C., Yu, J., Wang, P., Zhang, Y., 2018. Analysing the mechanisms of soil water and vapor transport in the desert vadose zone of the extremely arid region of northern China. *J. Hydrol.* 558, 592-606.
- Duncan, M. J., Srinivasan, M. S., McMillan, 2016. Field measurement of groundwater recharge under irrigation in Canterbury, New Zealand, using drainage lysimeters. *Agric. Water Manag.* 166, 17-32.
- Durner, W., 1994. Hydraulic conductivity estimation for soil with heterogeneous pore structure. *Water Resour. Res.* 30, 211-223.

- El Bably, A.Z., 2003. Estimation of evapotranspiration using statistical mode. In: Camarda, D., Grassini, L. (Eds.), *Local Resources and Global Trades: Environments and Agriculture in the Mediterranean region*. Bari: CIHEAM, pp. 441-449.
- Fang, G.H., Yang, J., Chen, Y.N., Zammit, C., 2015. Comparing bias correction methods in downscaling meteorological variables for a hydrologic impact study in an arid area in China. *Hydrol. Earth Syst. Sc.* 19, 2547-2559.
- Fank, J., Klammler, G., 2013. Measurement of precipitation using lysimeters. *Geophys. Res. Abstr.* 15., EGU2013-10703.
- Field, C. B., Barros, V., Stocker, T. F., Qin, D., Dokken, D. J., Ebi, K. L., Mastrandrea, M. D., Mach, K. J., Plattner, G-K., Allen, S. K., Tignor, M., Midgley, P. M. 2012. *Managing the risks of extreme events and disasters to advance climate change adaptation. A Special Report of Working Groups I and II of the Intergovernmental Panel on Climate Change*. Cambridge University Press, Cambridge.
- Fleischer, E., Bölter, J., Klemm, O., 2015. Summer evapotranspiration in western Siberia: a comparison between eddy covariance and Penman method formulations. *Hydrol. Process.* 29, 4498-4513.
- Foley, J.A., DeFries, R., Asner, G.P., Barford, C., Bonan, G., Carpenter, S.R., Chapin, F.S., Coe, M.T., Daily, G.C., Gibbs, H.K., Helkowski, J.H., Holloway, T., Howard, E.A., Kucharik, C.J., Monfreda, C., Patz, J.A., Prentice, I.C., Ramankutty, N., Snyder, P.K., 2005. Global consequences of land use. *Science* 309, 570-574.
- Førland, E.J., Allerup, P., Dahlström, B., Elomaa, E., Jonsson, T., Madsen, H., Perälä, J., Rissanen, P., Vedin, H., Vejen, F., 1996. *Manual for operational correction of Nordic precipitation data*. DNMI-report 24/96, Norwegian Meteorological Institute, Oslo.
- Fraser, E.D.G., Simelton, E., Termansen, M., Gosling, S.N., South, A., 2013. "Vulnerability hotspots": integrating socio-economic and hydrological models to identify where cereal production may decline in the future due to climate change induced drought. *Agric. For. Meteorol.* 170, 195-205.
- Frey, K. E., Smith, L. C., 2003. Recent temperature and precipitation increases in West Siberia and their association with the Arctic Oscillation. *Polar Res.* 22, 287-300.
- Fruehauf, M., Guggenberger, G., Meinel, T., Theesfeld, I., Lentz, S., 2020a. *KULUNDA: Climate Smart Agriculture, Innovations in Landscape Research*. Springer Nature, Switzerland.
- Fruehauf, M., Schmidt, G., Illiger, P., Meinel, T., 2020b. Types, occurrence and tendencies of soil degradation in the Altai Krai and the KULUNDA research region. In: Fruehauf, M., Guggenberger, G., Meinel, T., Theesfeld, I., Lentz, S. (Eds.), *KULUNDA: Climate*

- Smart Agriculture, Innovations in Landscape Research. Springer Nature, Switzerland, pp. 201-222.
- Gebler, S., Hendricks Franssen, H.-J., Pütz, T., Post, H., Schmidt, M., Vereecken, H., 2015. Actual evapotranspiration and precipitation measured by lysimeters: a comparison with eddy covariance and tipping bucket. *Hydrol. Earth Syst. Sci.* 19, 2145-2161.
- Goodison, B.E., Louie, P.Y.T., Yang, D., 1998. WMO solid precipitation measurement intercomparison. Final report. Instruments and Observing Methods Report 67, World Meteorological Organization, Geneva, pp. 212.
- Groh, J., Slawitsch, V., Herndl, M., Graf, A., Vereecken, H., Pütz, T., 2018. Determining dew and hoar frost formation for a low mountain range and alpine grassland site by weighable lysimeter. *J. Hydrol.* 563, 372-381.
- Grunwald, L.-C., Meinel, T., Kozhanov, N.A., Rudev, N.V., Belyaev, V.I., 2020. Perspectives for a sustainable production of row crops in systems of minimised tillage – A special focus on sunflower cropping in Western Siberia. In: Fruehauf, M., Guggenberger, G., Meinel, T., Theesfeld, I., Lentz, S. (Eds.), *KULUNDA: Climate Smart Agriculture, Innovations in Landscape Research*. Springer Nature, Switzerland, pp. 367-392.
- Guo, D., Westra, S., Maier, H.R., 2016. An R package for modelling actual, potential and reference evapotranspiration. *Environ. Model. Softw.* 78, 216-224.
- Hagenau, J., Meissner, R., Borg, H., 2015. Effect of exposure on the water balance of two identical lysimeters. *J. Hydrol.* 520, 69-74.
- Hannes, M., Wollschläger, U., Schrader, F., Durner, W., Gebler, S., Pütz, T., Fank, J., von Unold, G., Vogel, H.-J., 2015. High-resolution estimation of the water balance components from high-precision lysimeters. *Hydrol. Earth Syst. Sci. Discuss.* 12, 569-608.
- Herbrich, M., Gerke, H.H., 2016. Autocorrelation analysis of high resolution weighing lysimeter time series as a basis for determination of precipitation. *J. Plant Nutr. Soil Sci.* 179, 784-798.
- Herndl, M., Slawitsch, V., von Unold, G., 2017. Eine Methode zur Quantifizierung von Niederschlag und Verdunstung im Winter unter Klimawandelbedingungen. 17. Gumpensteiner Lysimetertagung 2017, HBLFA Raumberg-Gumpenstein, 131-136. (in German)
- Hoffmann, M., Schwartengraber, R., Wessolek, G., Peters, A., 2016. Comparison of simple rain gauge measurements with precision lysimeter data. *Atmos. Res.* 174, 120-123.
- Holder, C.D., Gibbes, C., 2017. Influence of leaf and canopy characteristics on rainfall interception and urban hydrology. *Hydrolog. Sci. J.* 62, 182-190.
- Huang, N., Shen, Z., Long, S. R., Wu, M. L. C., Shih, H. H., Zheng, Q., Yen, N. C., Tung, C.-C., Liu, H. H., 1998. The empirical mode decomposition and the Hilbert spectrum

- for nonlinear and non-stationary time series analysis. *Proc. R. Soc. Lond. A.* 454, 903-995.
- Isch, A., Montenach, D., Hammel, F., Ackerer, P., Coquet, Y., 2019. A comparative study of water and bromide transport in a bare loam soil using lysimeters and field plots. *Water* 11, 1199.
- Jennings, K. S., Winchell, T. S., Livneh, B., Molotch, N. P., 2018. Spatial variation of the rain-snow temperature threshold across the Northern Hemisphere. *Nat. Commun.* 9, 1-9.
- Jensen, M. E., Burman, R. D., Allen, R. G., 1990. *Evapotranspiration and irrigation water requirements*. American Society of Civil Engineers, New York.
- Kanzari, S., Nouna, B.B., Mariem S.B., Rezig, M., 2018. Hydrus-1D model calibration and validation in various field conditions for simulating water flow and salts transport in a semi-arid region of Tunisia. *Sustain. Environ. Res.* 28, 350-356.
- Kraemer, R., Prishchepov, A.V., Mueller, D., Kuemmerle, T., Radeloff, V.C., Dara, A., Terekhov, A., Fruehauf, M., 2015. Long-term agricultural land-cover change and potential for cropland expansion in the former Virgin Lands area of Kazakhstan. *Environ. Res. Lett.* 10, 054012.
- Kohfahl, C., Molano-Leno, L., Martínez, G., Vanderlinden, K., Guardiola-Albert, C., Moreno, L., 2019. Determining groundwater recharge and vapor flow in dune sediments using a weighable precision meteo lysimeter. *Sci. Total Environ.* 656, 550-557.
- Kurc, S. A., Small, E. E., 2004. Dynamics of evapotranspiration in semiarid grassland and shrubland ecosystems during the summer monsoon season, central New Mexico. *Water Resour. Res.* 40, W09305.
- Lambers, H., Chapin III, F. S., Pons, T. L., 2008. *Plant Physiological Ecology*, 2nd Edition. Springer Science + Business Media, New York.
- Legates, D.R., DeLiberty, T.L., 1993. Precipitation measurement biases in the United States. *Am. Water Resour. Assoc.* 29, 855-861.
- Lehmann, P., Assouline, S., Or, D., 2008. Characteristic lengths affecting evaporative drying of porous media. *Phys. Rev. E* 77, 056309.
- Lhomme, J.-P., 1997. Towards a definition of potential evaporation. *Hydrol. Earth Sys.* 1, 257-267.
- López-Urrea, R., Marin de Santa Olalla, F., Fabeiro, C., Moratalla, A., 2006. Testing evapotranspiration equations using lysimeter observations in a semiarid climate. *Agr. Water Manage.* 95, 553-565.
- Louzada, F.I.R. de O., Xavier, A.C., Pezzopane, J.E.M., 2018. Climatological water balance with data estimated by tropical rainfall measuring mission for the Doce river basin. *Eng. Agricola* 38, 376-386.

- Lukanu, G., Savage, M. J., 2006. Calibration of a frequency-domain reflectometer for determining soil-water content in a clay loam soil. *Water S.A.* 32, 37-42.
- Makkink, G.F., 1957. Testing the Penman formula by means of lysimeters. *Journal of the Institution of Water Engineers and Scientist* 11, 277-288.
- Martel, M., Glenn, A., Wilson, H., Kröbel, R., 2018. Simulation of actual evapotranspiration from agricultural landscapes in the Canadian Prairies. *J. Hydrol. Reg. Stud.* 15, 105-118.
- Mashtayeva, S., Dai, L., Che, T., Sagintayev, Z., Sadvakasova, S., Kussainova, M., Alimbayeva, D., Akynbekkyzy, M., 2016. Spatial and temporal variability of snow depth derived from passive microwave remote sensing data in Kazakhstan. *J. Meteor. Res.* 30, 1033-1043.
- Mauder, M., Genzel, S., Fu, J., Kiese, R., Soltani, M., Steinbrecher, R., Zeeman, M., Banerjee, T., De Roo, F., Kunstmann, H., 2017. Evaluation of energy balance closure adjustment methods by independent evapotranspiration estimates from lysimeters and hydrological simulations. *Hydrol. Process.* 32, 1-18.
- Meissner, R., Rupp, H., Schubert, M., 2000. Novel lysimeter techniques - a basis for the improved investigation of water, gas, and solute transport in soils. *J. Plant Nutr. Soil Sci.* 163, 603-608.
- Meissner, R., Seeger, J., Rupp, H., Seyfarth, M., Borg, H., 2007. Measurement of dew, fog, and rime with a high-precision gravitation lysimeter. *J. Plant Nutr. Soil Sci.* 170, 335-344.
- Meissner, R., Rupp, H., Seyfarth, M., 2008. Advances in out door lysimeter techniques. *Water Air Soil Pollut: Focus* 8, 217-225.
- Meissner, R., Prasad, M.N.V., Du Laing, G., Rinklebe, J., 2010. Lysimeter application for measuring the water and solute fluxes with high precision. *Curr. Sci. India.* 99, 601-607.
- Meissner, R., Bondarovich, A.A., Scherbinin, V.V., Ponkina, E.V., Matsyura, A.V., Puzanov, A.V., Rupp, H., Schmidt, G., Stephan, E., Illiger, P., Fruhauf, M., Harlamova, N.F., Galahov, V.P., Balykin, D.V., Rudev, N.V., 2016. Calculation of water balance for the south desert area of Western Siberiaby international monitoring network data. *Biological Bulletin of Bogdan Chmelnitskiy Melitopol State Pedagogical University* 6, 223-238.
- Meissner, R., Rupp, H., Bondarovich, A.A., Rinklebe, J., 2017. Soil water management in the Siberian Kulunda-dry steppe. *Mech. Agric. Conserv. Resour.* 5, 87-91.

- Mekonnen, G., Matula, S., Dolezal, F., Fisak, J., 2015. Adjustment to rainfall measurement undercatch with a tipping-bucket rain gauge using ground-level manual gauges. *Meteorol. Atmos. Phys.* 127, 241-256.
- Meyer, B.C., Schreiner, V., Smolentseva, E.N., Smolentsev, B.A., 2008. Indicators of desertification in the Kulunda Steppe in the south of Western Siberia. *Arch. Agron. Soil Sci.* 54, 585-603.
- Monteith, J.L., 1965. Evaporation and environment. 19<sup>th</sup> Symposia of the Society for Experimental Biology 19, 205-234.
- Moorhead, J. E., Marek, G. W., Gowda, P. H., Lin, Y., Colaizzi, P. D., Evett, S. R., Kutikoff, S., 2019. Evaluation of evapotranspiration from eddy covariance using large weighing lysimeters. *Agronomy* 9, 99.
- Mueller, L., Suleimenov, M., Karimov, A., Qadir, M., 2014. Land and water resources of Central Asia, their utilisation and ecological status. In: Mueller, L., Saparov, A., Lischeid, G. (Eds.), *Novel measurement and assessment tools for monitoring and management of land and water resources in agricultural landscapes of Central Asia*. Springer International Publishing, Switzerland, pp. 3-59.
- Neff, E., 1978. How much rain does a rain gage gage. *Agric. Res.* 27, 213-220.
- Nolz, R., Cepuder, P., Kammerer, G., 2014. Determining soil water-balance components using an irrigated grass lysimeter in NE Austria. *J. Plant Nutr. Soil Sci.* 177, 237-244.
- Noy-Meir, I., 1973. Desert ecosystems: Environment and producers. *Annu. Rev. Ecol. Syst.* 4, 25-51.
- Nyéki, A., Milics, G., Kovács, A.J., Neményi, M., 2017. Effects of soil compaction on cereal yield. A review. *Cereal Res. Commun.* 45, 1-22.
- Oberholzer, S., Prasuhn, V., Hund, A., 2017. Crop water use under Swiss pedoclimatic conditions - Evaluation of lysimeter data covering a seven-year period. *Field Crops Res.* 211, 48-65.
- Park, H., Yamazaki, T., Yamamoto, K., Ohta, T., 2008. Tempo-spatial characteristics of energy budget and evapotranspiration in the eastern Siberia. *Agr. Forest Meteorol.* 148, 1990-2005.
- Pedram, S., Wang, X., Liu, T., Duan, L., 2018. Simulated dynamics of soil water and pore vapor in a semiarid sandy ecosystem. *J. Arid Environ.* 151, 58-82.
- Peters, A., Nehls, T., Schonsky, H., Wessolek, G., 2014. Separating precipitation and evapotranspiration from noise - a new filter routine for high-resolution lysimeter data. *Hydrol. Earth Syst. Sci. Discuss.* 18, 1189-1198.

- Phillips, F. M., 1994. Environmental tracers for water movement in desert soils of the American Southwest. *Soil Sci. Soc. Am. J.* 58, 15-24.
- Pilifosova, O., Eserkepova, I., Dolgih, S., 1997. Regional climate change scenarios under global warming in Kazakhstan. *Clim. Change* 36, 23-40.
- Priestley, C.H.B., Taylor, R.J., 1972. On the assessment of surface heat flux and evaporation using large-scale parameters. *Mon. Weather Rev.* 100, 81-92.
- Rana, G., Katerji, N., 2000. Measurement and estimation of actual evapotranspiration in the field under Mediterranean climate: a review. *Eur. J. Agron.* 13, 125-153.
- Reynolds, J., Kemp, P., Tenhunen, J., 2000. Effects of long-term rainfall variability on evapotranspiration and soil water distribution in the Chihuahuan desert: A modeling analysis. *Plant Ecol.* 150, 145-159.
- Richards, L.A., 1931. Capillary conduction of liquids through porous mediums. *J. Appl. Phys.* 1, 318-333.
- Richter, D., 1995. Ergebnisse methodischer Untersuchungen zur Korrektur des systematischen Messfehlers des Hellmann-Niederschlagsmessers. *Berichte des Deutschen Wetterdienstes* 194. Offenbach am Main. (in German)
- Rodriguez-Iturbe, I., 2000. Ecohydrology: A hydrologic perspective of climate-soil-vegetation dynamics. *Water Resour. Res.* 36, 3-9.
- Roth, D., Günther, R., Knoblauch, S., Michel, H., 2005. Wasserhaushaltsgrößen von Kulturpflanzen unter Feldbedingungen. Thüringer Landesanstalt für Landwirtschaft. Schriftenreihe Heft 1, Jena. (in German)
- Roznovsky, J., Brzezina, J., 2017. Effect of snow cover on soil frost penetration. *Contrib. to Geophys. Geodesy* 47, 287-297.
- Sabziparvar, A.-A., Tabari, H., 2010. Regional Estimation of Reference Evapotranspiration in Arid and Semiarid Regions. *J. Irrig. Drain. E. - ASCE* 136, 724-731.
- Sala, O., Lauenroth, W., Parton, W., 1992. Long-term soil water dynamics in the shortgrass steppe. *Ecology* 73, 1175-1181.
- Salmi, A., Ikonen, J., 2005. Piezoelectric precipitation sensor from Vaisala. Vaisala Oyj, Helsinki.
- Savitzky, A., Golay, M., 1964. Smoothing and differentiation of data by simplified least squares procedures. *Anal. Chem.* 36, 1627-1639.
- Schaap, M., Leij, F.J., Genuchten, M.T.V., 2001. Rosetta: A computer program for estimating soil hydraulic parameters with hierarchical pedotransfer functions. *J. Hydrol.* 251, 163-176.
- Schrader, F., Durner, W., Fank, J., Gebler, S., Pütz, T., Hannes, M., Wollschläger, U., 2013. Estimating precipitation and actual evapotranspiration from precision lysimeter measurements. *Procedia Environ. Sci.* 19, 543-552.

- Sevruk, B., 1981. Methodische Untersuchungen des systematischen Messfehlers der Hellmann-Regenmesser im Sommerhalbjahr in der Schweiz. Technische Hochschule Zürich, Switzerland. (in German)
- Sevruk, B., 1982. Methods of correction for systematic error in point precipitation measurement for operational use. Operational Hydrology Report No. 21, World Meteorological Organization, Geneva.
- Seyfried, M. S., Hanson, C. L., Murdock, M. D., Van Vactor, S., 2001. Long-term lysimeter database, Reynolds Creek Experimental Watershed, Idaho, United States. *Water Resour. Res.* 37, 2853-2856.
- Shi, T., Guan, D., Wu, J., Wang, A., Jin, C., Han, S., 2008. Comparison of methods for estimating evapotranspiration rate of dry forest canopy: eddy covariance, Bowen ratio energy balance, and Penman-Monteith equation. *J. Geophys. Res.* 113, D19116.
- Shokri, N., Or, D., 2011. What determines drying rates at the onset of diffusion controlled stage-2 evaporation from porous media? *Water Resour. Res.* 47, W09513.
- Shrestha, M., Acharya, S.C., Shrestha, P.K., 2017. Bias correction of climate models for hydrological modelling - are simple methods still useful? *Meteorol. Appl.* 24, 531-539.
- Shuttleworth, W. J., 1991. Evaporation models in hydrology. In: Schmugge, T. J., André, J. (Eds.), *Land Surface Evaporation*. Springer, New York, pp. 93-120.
- Simunek, J., van Genuchten, M.T., Sejna, M., 2016. Recent developments and applications of the HYDRUS computer software packages. *Vadose Zone J.* 15, 1-25.
- Smits, K.M., Ngo, V.V., Cihan, A., Sakaki, T., Illangasekare, T.H., 2012. An evaluation of models of bare soil evaporation formulated with different land surface boundary condition and assumptions. *Water Resour. Res.* 48, W12526.
- Sungmin, O., Foelsche, U., Kirchengast, G., Fuchsberger, J., 2018. Validation and correction of rainfall data from the WegenerNet high density network in southeast Austria. *J. Hydrol.* 556, 1110-1122.
- Swinnen, J., Burkitbayeva, S., Schierhorn, F., Prishchepov, A.V., Müller, D., 2017. Production potential in the "bread baskets" of Eastern Europe and Central Asia. *Glob. Food Sec.* 14, 38-53.
- Tarboton, D., 1994. Measurements and Modeling of Snow Energy Balance and Sublimation from Snow. Utah Water Research Laboratory Reports. Paper 61.
- Teutschbein, C., Seibert, J., 2012. Bias correction of regional climate model simulations for hydrological climate-change impact studies: Review and evaluation of different methods. *J. Hydrol.* 456-457, 12-29.
- Thies Clima, 2008. User's Guide - Precipitation Transmitter. Thies Clima, Göttingen.

- Topp, G., Davis, J., Annan, A., 1980. Electromagnetic determination of soil water content: Measurement in coaxial transmission lines. *Water Resour. Res.* 16, 574-582.
- Vaisala, 2012. User's Guide - Vaisala Weather Transmitter WXT520. Vaisala Oyj, Helsinki.
- van Genuchten, M.T., 1980. A closed-form equation for predicting the hydraulic conductivity of unsaturated soils. *Soil Sci. Soc. Am. J.* 44, 892-898.
- van Genuchten, M.T., Leij, F.J., Yates, S.R., 1991. The RETC Code for Quantifying Hydraulic Functions of Unsaturated Soils. US Department of Agriculture, USA.
- von Unold, G., Fank, J., 2008. Modular design of field lysimeters for specific application needs. *Water Air Soil Pollut.* 8, 233-242.
- Wang, X., 2015. Vapor flow resistance of dry soil layer to soil water evaporation in arid environments: An overview. *Water* 7, 4552-4574.
- Wegehenkel, M., Zhang, Y., Zenker, T., Diestel, H., 2008. The use of lysimeter data for the test of two soil-water balance models: A case study. *J. Plant Nutr. Soil Sci.* 171, 762-776.
- Wegehenkel, M., Gerke, H.H., 2013. Comparison of real evapotranspiration measured by weighing lysimeters with simulations based on the Penman formula and a crop growth model. *J. Hydrol. Hydromech.* 61, 161-172.
- Wegehenkel, M., Gerke, H.H., 2015. Water table effects on measured and simulated fluxes in weighing lysimeters for differently-textured soils. *J. Hydrol. Hydromech.* 63, 82-92.
- Wever, L.A., Flanagan, L.B., Carlson, P.J., 2002. Seasonal and interannual variation in evapotranspiration, energy balance and surface conductance in a northern temperate grassland. *Agric. For. Meteorol.* 112, 31-49.
- WMO, 2008. Guide to Meteorological Instruments and Methods of Observation. WMO-No. 8. 8th Edition. World Meteorological Organization, Geneva.
- WMO, 2014. Guide to Meteorological Instruments and Methods of Observation. WMO-No. 8. 8th Edition. World Meteorological Organization, Geneva.
- Wohlfahrt, G., Ischick, C., Thalinger, B., Hörtnagl, L., Obojes, N., Hammerle, A., 2010. Insights from independent evapotranspiration estimates for closing the energy balance: A grassland study. *Vadose Zone J.* 9, 1025-1033.
- Xiao, H., Meissner, R., Seeger, J., Rupp, H., Borg, H., 2009. Testing the precision of a weighable gravitation lysimeter. *J. Plant Nutr. Soil Sci.* 172, 194-200.
- Yamazaki, T., Yabuki, H., Ishii, Y., Ohta, T., Ohata, T., 2004. Water and energy exchanges at forests and a grassland in eastern Siberia evaluated using a one-dimensional land surface model. *J. Hydrometeorol.* 5, 504-515.

- Yang, F., Zhang, Q., Wang, R., Zhou, J., 2014. Evapotranspiration measurement and crop coefficient estimation over a spring wheat farmland ecosystem in the Loess Plateau. *PLoS One* 9, e100031.
- Zhang, T., 2005. Influence of the seasonal snow cover on the ground thermal regime: An overview. *Rev. Geophys.* 43, RG4002.
- Zhang, Y., Whang, S., Barr, A. G., Black, T. A., 2008. Impact of snow cover on soil temperature and its simulation in a boreal aspen forest. *Cold Reg. Sci. Technol.* 52, 355-370.

## Curriculum vitae

**Name** Lisa Haselow

### Ausbildung

2014-2017 Master of Science in Geographische Wissenschaften mit dem  
Studienschwerpunkt Umwelthydrologie an der Freien Universität Berlin  
2011-2014 Bachelor of Science in Geographische Wissenschaften an der Freien  
Universität Berlin

### Beruflicher Werdegang

2017-2020 Doktorandin am Helmholtz-Zentrum für Umweltforschung – UFZ im  
Department Bodensystemforschung (Halle/Saale)  
seit 2020 wissenschaftliche Mitarbeiterin an der Universität Rostock in der Professur  
Hydrologie und Angewandte Meteorologie

## List of Publications

Haselow, L., Rupp, H., Akshalov, K., Meißner, R., 2020. Forschungsarbeiten zum Bodenwasserhaushalt in der kasachischen Steppe. *WasserWirtschaft* 110, 34-40.

Meissner, R., Rupp, H., Haselow, L., 2020. Use of lysimeters for monitoring soil water balance parameters and nutrient leaching. In: Prasad, M.N.V., Pietrzykowski, M. (Eds.), *Climate Change and Soil Interactions*. Elsevier, Amsterdam, pp. 171-205.

Haselow, L., Meissner, R., Rupp, H., Miegel, K., 2019. Evaluation of precipitation measurements methods under field conditions during a summer season: A comparison of the standard rain gauge with a weighable lysimeter and a piezoelectric precipitation sensor. *J. Hydrol.* 575, 537-543.

Haselow, L., Rupp, H., Bondarovich, A., Meissner, R., 2019. Measurement and estimation of evapotranspiration in semi-arid grassland during the summer season in southwest Siberia. *Eurasian J. Soil Sci.* 8, 257-266.

Haselow, L., Rupp, H., Meißner, R., 2019. Lysimeteruntersuchungen zum Bodenwasserhaushalt eines Steppenstandorts in Sibirien. In: Höhere Bundeslehr- und Forschungsanstalt für Landwirtschaft Raumberg-Gumpenstein (Ed.), *Lysimeter – ein geeignetes Instrument zur Quantifizierung von Wasser-, Nähr- und Schadstoffflüssen*. 18. Gumpensteiner Lysimetertagung, 21.-22.05.2019, Bericht HBLFA Raumberg-Gumpenstein, 29-32.

## Danksagung / Acknowledgement

Mein besonderer Dank gilt zu allererst Prof. Dr. Ralph Meißner, dem Helmholtz-Zentrum für Umweltforschung und dem Bundesministerium für Bildung und Forschung, die es mir überhaupt ermöglichten diese Arbeit innerhalb des spannenden Forschungsprojekts „Innovationen für nachhaltige landwirtschaftliche Ressourcennutzung und Klimaanpassung in Trockensteppen Kasachstans und Südwestsibiriens (ReKKS)“ (FKZ 01LZ1704C) zu erstellen.

Meinen Betreuern Ralph Meissner und Holger Rupp möchte ich besonders für ihre Unterstützung, ihr Vertrauen und der Motivation danken, die sie mir auch in den schwachen Momenten zukommen lassen haben. Vielen Dank auch für die Freiheiten, die sie mir gaben, womit diese Arbeit mit viel Leidenschaft und Freude angegangen werden konnte. Den Mitarbeitern des Departments Bodensystemforschung danke ich für die angenehme Arbeitsatmosphäre, den aufschlussreichen Fachdiskussionen und den unterhaltsamen Pausen. Hier möchte ich insbesondere Martina Stange für ihren Einsatz im Labor danken sowie René Zahl für seine unermüdliche Geduld bei dem stets nervenaufreibendem Thema HYDRUS. Ebenso gilt mein Dank mehreren Mitarbeitern der Firma UGT, die mit ihrer freundlichen und offenen Art eine harmonische Zusammenarbeit gestalteten. Einen herzlichen Dank möchte ich hier Lasse Pein widmen, der sich mit mir auf so manch abenteuerliche Einsätze in Kasachstan einließ. Lasse, ich danke dir für deinen Enthusiasmus und vor allem für deinen Optimismus, mit dem du mich dem ein oder anderen Mal wieder ermutigt hast, als ich bereits an meine Grenzen kam. Vielen Dank auch an Dr. Olga Shibistova, die für mich Herz und Seele des Projektes darstellte. Danke Olga für dein grenzenloses Engagement und den Aufwand, den du betreiben musstest, wenn ich dich mal wieder um die Organisation eines sehr spontanen Trips nach Kasachstan bat; und nicht zu vergessen für deine Gelassenheit bezüglich der Aufrechterhaltung der Datenübertragung meiner Sorgenkinder – den Lysimetern.

Mein größter Dank gilt meiner Familie und dem Mann an meiner Seite, die mir in den letzten drei Jahren den Rücken freihielten und dafür sorgten, dass ich meiner Arbeit jederzeit entspannt nachgehen konnte. Phil, ich danke dir für alles und in diesem Zusammenhang vor allem für dein stets offenes Ohr, obwohl du in der Regel noch nicht mal wusstest über was ich überhaupt rede.

Last but not least, I would like to thank my hardworking proofreaders Kliti Bousi and Jade Kilty.

## **Eidesstattliche Erklärung / *Declaration under oath***

Ich erkläre an Eides statt, dass ich die Arbeit selbstständig und ohne fremde Hilfe verfasst, keine anderen als die von mir angegebenen Quellen und Hilfsmittel benutzt und die den benutzten Werken wörtlich oder inhaltlich entnommenen Stellen als solche kenntlich gemacht habe.

*I declare under penalty of perjury that this thesis is my own work entirely and has been written without any help from other people. I used only the sources mentioned and included all the citations correctly both in word or content.*

25 September 2020

.....

ISSN 1860-0387

Helmholtz Centre for  
Environmental Research – UFZ  
Permoserstraße 15  
04318 Leipzig | Germany  
[www.ufz.de](http://www.ufz.de)

NOT FOR SALE.